Space Science Reviews

Establishing the analogy between quasi-periodic pulsations in solar and stellar flares

--Manuscript Draft--

Manuscript Number:	
Full Title:	Establishing the analogy between quasi-periodic pulsations in solar and stellar flares
Article Type:	Vol xxx: Oscillatory Processes in Solar and Stellar Coronae
Keywords:	Solar flares; Stellar flares; Quasi-periodic pulsations (QPPs); MHD oscillations; MHD waves; Magnetic reconnection
Corresponding Author:	Ivan ZIMOVETS, Ph.D. FSBSI Space Research Institute of the Russian Academy of Sciences: FGBUN Institut kosmiceskih issledovanij Rossijskoj akademii nauk Moscow, RUSSIAN FEDERATION
Corresponding Author Secondary Information:	
Corresponding Author's Institution:	FSBSI Space Research Institute of the Russian Academy of Sciences: FGBUN Institut kosmiceskih issledovanij Rossijskoj akademii nauk
Corresponding Author's Secondary Institution:	
First Author:	Ivan ZIMOVETS, Ph.D.
First Author Secondary Information:	
Order of Authors:	Ivan ZIMOVETS, Ph.D.
	James A. McLaughlin, Ph.D.
	Abhishek K. Srivastava, Ph.D.
	Dmitrii Y. Kolotkov, Ph.D.
	Alexei A. Kuznetsov, Ph.D.
	Elena G. Kupriyanova, Ph.D.
	Il-Hyun Cho, Ph.D.
	Andrew R. Inglis, Ph.D.
	Fabio Reale, Ph.D.
	David J. Pascoe, Ph.D.
	Hui Tian, Ph.D.
	Ding Yuan, Ph.D.
	Dong Li, Ph.D.
	Qingmin Zhang, Ph.D.
Order of Authors Secondary Information:	
Funding Information:	budgetary funding of Basic Research program (``PLASMA'') — Dr Ivan ZIMOVETS
	UK Science and Technology Facilities Council (STFC) (ST/T000384/1) — James A. McLaughlin
	budgetary funding of Basic Research program II.16 — Dmitrii Y. Kolotkov Alexei A. Kuznetsov
	UK Science and Technology Facilities Council (STFC) (ST/T000252/1) — Dmitrii Y. Kolotkov

National Natural Science Foundation of China (11825301)	Hui Tian
National Natural Science Foundation of China (11790304(11790300))	Hui Tian
National Natural Science Foundation of China (11803005)	Ding Yuan
National Natural Science Foundation of China (11911530690)	Ding Yuan
Shenzhen Technology Project (JCYJ20180306172239618)	Ding Yuan
National Research Foundation of Korea (NRF-2019R1C1C1006033)	Il-Hyun Cho
Korea Astronomy and Space Science Institute (2020-1-850-07)	Il-Hyun Cho
European Research Council (ERC) under the European Union's Horizon 2020 research and innovation programme (724326)	David J. Pascoe
Internal Funds KU Leuven (C1 grant TRACEspace)	David J. Pascoe
Российский Фонд Фундаментальных Исследований (РФФИ) (18-02-00856)	Elena G. Kupriyanova
Russian Basic Research programs (0041-2019-0019)	Elena G. Kupriyanova

Abstract:

The phenomenon of quasi-periodic pulsations (QPPs) in solar and stellar flares has been known for over 50 years and significant progress has been made in this research area. It has become clear that QPPs are not rare -- they are found in many flares and, therefore, robust flare models should reproduce their properties in a natural way. At least fifteen mechanisms/models have been developed to explain QPPs in solar flares, which mainly assume the presence of magnetohydrodynamic (MHD) oscillations in coronal structures (magnetic loops and current sheets) or quasi-periodic regimes of magnetic reconnection. We review the most important and interesting results on flare QPPs, with an emphasis on the results of recent years, and we present the predicted and prominent observational signatures of each of the fifteen mechanisms. However, it is not yet possible to draw an unambiguous conclusion as to the correct underlying QPP mechanism because of the qualitative, rather than quantitative, nature of most of the models and also due to insufficient observational information on the physical properties of the flare region, in particular the spatial structure of the QPP source. We also review QPPs in stellar flares, where progress is largely based on solar-stellar analogies, suggesting similarities in the physical processes in flare regions on the Sun and magnetoactive stars. The presence of QPPs with similar properties in solar and stellar flares is, in itself, a strong additional argument in favor of the likelihood of solar-stellar analogies. Hence, advancing our understanding of QPPs in solar flares provides an important additional channel of information about stellar flares. However, further work in both theory/simulations and in observations is needed.

Space Sci. Rev. manuscript No.
(will be inserted by the editor)

Establishing the analogy between quasi-periodic pulsations in solar and stellar flares

I.V. Zimovets · J.A. McLaughlin · A.K. Srivastava · D.Y. Kolotkov · A.A. Kuznetsov · E.G. Kupriyanova · I.-H. Cho · A.R. Inglis · F. Reale · D.J. Pascoe · H. Tian · D. Yuan · D. Li · Q.M. Zhang

Received: date / Accepted: date

I.V. Zimovets [0000-0001-6995-3684]
Space Research Institute of the Russian Academy of Sciences (IKI), 84/32 Profsoyuznaya Str, Moscow 117997, Russia
E-mail: ivanzim@iki.rssi.ru

James A. McLaughlin [0000-0002-7863-624X]
Northumbria University, Newcastle upon Tyne, NE1 8ST, UK E-mail: james.a.mclaughlin@northumbria.ac.uk

A.K. Srivastava [0000-0002-1641-1539]
Department of Physics, Indian Institute of Technology (BHU), Varanasi-221005, India E-mail: asrivastava.app@itbhu.ac.in

D.Y. Kolotkov [0000-0002-0687-6172]
Centre for Fusion, Space and Astrophysics, Physics Department, University of Warwick, Coventry CV4 7AL, United Kingdom E-mail: d.kolotkov.1@warwick.ac.uk
Institute of Solar-Terrestrial Physics SB RAS, Irkutsk 664033, Russia

A.A. Kuznetsov [0000-0001-8644-8372]
Institute of Solar-Terrestrial Physics, Irkutsk 664033, Russia E-mail: a_kuzn@iszf.irk.ru

E.G. Kupriyanova [0000-0001-9664-0552]
Central Astronomical Observatory at Pulkovo of the RAS, Pulkovskoe shosse 65, Saint-Petersburg, 196140 Russia E-mail: elenku@bk.ru

I.-H. Cho [0000-0001-7514-8171]
Kyung Hee University, South Korea E-mail: ihjo@khu.ac.kr

A.R. Inglis [0000-0003-0656-2437]
Solar Physics Laboratory, Code 671, Heliophysics Science Division, NASA Goddard Space Flight Center, Greenbelt, MD 20771, USA E-mail: andrew.inglis@nasa.gov

F. Reale [0000-0002-1820-4824]
Dipartimento di Fisica & Chimica, Università di Palermo, Piazza del Parlamento 1, I-90134 Palermo, Italy E-mail: fabio.reale@unipa.it
INAF-Osservatorio Astronomico di Palermo, Piazza del Parlamento 1, I-90134 Palermo, Italy

D.J. Pascoe [0000-0002-0338-3962]
Centre for mathematical Plasma Astrophysics, Mathematics Department, KU Leuven, Celestijnenlaan 200B bus 2400, B-3001 Leuven, Belgium E-mail: david.pascoe@kuleuven.be

H. Tian
School of Earth and Space Sciences, Peking University, Beijing 100871, China E-mail: huitian@pku.edu.cn
Key Laboratory of Solar Activity, National Astronomical Observatories, Chinese Academy of

Abstract The phenomenon of quasi-periodic pulsations (QPPs) in solar and stellar flares has been known for over 50 years and significant progress has been made in this research area. It has become clear that QPPs are not rare – they are found in many flares and, therefore, robust flare models should reproduce their properties in a natural way. At least fifteen mechanisms/models have been developed to explain QPPs in solar flares, which mainly assume the presence of magnetohydrodynamic (MHD) oscillations in coronal structures (magnetic loops and current sheets) or quasi-periodic regimes of magnetic reconnection. We review the most important and interesting results on flare QPPs, with an emphasis on the results of recent years, and we present the predicted and prominent observational signatures of each of the fifteen mechanisms. However, it is not yet possible to draw an unambiguous conclusion as to the correct underlying QPP mechanism because of the qualitative, rather than quantitative, nature of most of the models and also due to insufficient observational information on the physical properties of the flare region, in particular the spatial structure of the QPP source. We also review QPPs in stellar flares, where progress is largely based on solar-stellar analogies, suggesting similarities in the physical processes in flare regions on the Sun and magnetoactive stars. The presence of QPPs with similar properties in solar and stellar flares is, in itself, a strong additional argument in favor of the likelihood of solar-stellar analogies. Hence, advancing our understanding of QPPs in solar flares provides an important additional channel of information about stellar flares. However, further work in both theory/simulations and in observations is needed.

Keywords Solar flares · Stellar flares · Quasi-periodic pulsations (QPPs) · MHD oscillations · MHD waves · Magnetic reconnection

Contents

1 Introduction . . . 3
2 Recent progress in solar flare QPPs . . . 8
2.1 Brief introduction to the QPP-detection techniques . . . 8
2.2 Key instruments driving progress in recent observations of QPPs in solar flares 9
2.3 Summary of the main solar flare QPP models . . . 11
2.4 Properties of the QPP models and supporting observations . . . 16
2.4.1 Group (i): direct modulation by MHD and electrodynamic oscillations of all types . . . 16
2.4.2 Group (ii): modulation of the efficiency of energy release processes by MHD oscillations . . . 26

Sciences, Beijing 100012, China

D. Yuan [0000-0002-9514-6402]
Institute of Space Science and Applied Technology, Harbin Institute of Technology, Shenzhen, Guangdong 518055, China E-mail: yuanding@hit.edu.cn
Key Laboratory of Solar Activity, National Astronomical Observatories, Chinese Academy of Sciences, Beijing 100012, People's Republic of China

D. Li [0000-0002-4538-9350]
Key Laboratory for Dark Matter and Space Science, Purple Mountain Observatory, Chinese Academy of Sciences, Nanjing 210034, People's Republic of China E-mail: lidong@pmo.ac.cn

Q.M. Zhang
Key Laboratory for Dark Matter and Space Science, Purple Mountain Observatory, Chinese Academy of Sciences, Nanjing 210034, People's Republic of China E-mail: zhangqm@pmo.ac.cn

2.4.3 Group (iii): spontaneous quasi-periodic energy release (DC-to-AC models) 35
2.5 Review of recent statistical studies on QPPs in solar flares 42
3 Review of observations of stellar flare QPPs 45
3.1 Observations of stellar flare QPPs in optical bands 46
3.1.1 Optical stellar QPPs and their association with possible MHD modes . 47
3.1.2 Optical stellar QPPs and their association with transient energetic processes 50
3.2 Observations of stellar flare QPPs in radio 51
3.3 Observations of stellar flare QPPs in X-rays 53
3.3.1 X-ray QPPs and their association with MHD modes 53
3.3.2 X-ray QPPs and their association with other energetic plasma processes 55
3.3.3 Observations and modelling of QPPs in X-ray flares of star forming regions 56
3.4 Observations of stellar flare QPPs in UV/EUV: a possible clue to MHD wave activities 59
3.5 On multiwavelength observations of stellar flare QPPs 59
3.6 Statistical Studies of QPPs in stellar flares 60
4 Summary and prospects 63
A Appendix: Model-Property Table 66

1 Introduction

The Sun is a magnetically-active yellow dwarf of spectral class G2V. Solar activity is associated with the processes of generation and emergence of magnetic fields from the depths of the star, the formation and evolution of active regions at and above the visible surface (photosphere), and the dissipation of magnetic energy in the atmosphere. Active regions are formed due to the emergence of toroidal magnetic flux tubes from the depths of the convective zone. The convective zone of the Sun has a thickness of about 1/3 of the solar radius. In the framework of traditional dynamo models, toroidal flows are generated and amplified in the tachocline, a thin layer at the bottom of the convection zone. On the surface of the Sun, magnetic fields in the active regions are concentrated in the form of sunspot groups with magnetic induction in the sunspot umbra in the range of $\approx 2-3$ kG, sometimes reaching $5-6$ kG (Livingston et al., 2006; Anfinogentov et al., 2019). Typical total areas of sunspot groups in active regions are of the order of $S \sim 10^3$ MHS [1]; for the largest regions, the value can reach $S \sim 10^4$ MHS. In active regions above the surface of the Sun, magnetic tubes are predominantly in the form of magnetic loops of various sizes filled with plasma, connecting sections of opposite magnetic polarity on the surface. Typical coronal loops in active regions have lengths of $L \sim 10-100$ Mm, temperatures $T \approx 1-3$ MK (in the absence of flares), and plasma density $n \sim 10^8 - 10^{10}$ cm^{-3}. In flaring loops, $T \approx 10-30$ MK and $n \sim 10^{10} - 10^{12}$ cm^{-3}. The values of average magnetic field in coronal parts of the loops are usually of the order of $B \sim 10-100$ G (see a review by Reale, 2014). The characteristic values of the total magnetic energy in the active regions of the Sun are estimated roughly as $E \sim \left(B^2/8\pi\right) L^3 \sim 10^{28} - 10^{33}$ erg.

As a result of the explosive release of free (non-potential) magnetic energy in the active regions, extreme events such as solar flares and coronal mass ejections (CMEs) occur. They are the most powerful phenomena in the solar system releasing up to $\sim 10^{32} - 10^{33}$ erg of energy, which is comparable with the upper estimate of magnetic energy in the active regions given above (e.g. Emslie et al.,

[1] Millionths of the solar hemisphere; 1MHS $\approx 3 \times 10^6$ km^2.

2012; Aschwanden et al., 2017). In the framework of the 'standard' theory of solar flares, the process of energy release occurs due to magnetic reconnection during the interaction of oppositely-directed magnetic fluxes in the solar corona. As a result of reconnection, free magnetic energy is transformed into kinetic energy of plasma and non-thermal particles accelerated to sub-relativistic and relativistic energies (e.g. Priest and Forbes, 2002; Somov, 2013).

Magnetic reconnection occurs in almost every rotating object in the universe, for example, planetary magnetospheres, solar and stellar atmospheres, and compact objects (e.g. Zweibel and Yamada, 2009). These can have wide ranges of magnetic field strengths and plasma densities as well as a variety of field geometry. Among these, the Sun is a unique object whose corona can be observed in high-resolution, thus the detailed evolution of magnetic energy release can be explored with imaging observations (Benz and Güdel, 2010).

During typical solar flares, accelerated particles first collide with a thin coronal loop-top source and then with a thick chromospheric footpoints of flare loops, both producing non-thermal hard X-ray (and γ-rays) and radio emission. Collisional interaction of non-thermal particles in the loop footpoints heats up the plasma. This causes evaporation of the chromospheric plasma into coronal volumes of flare loops producing enhanced fluxes of thermal soft X-ray and EUV emissions, evolving first ionization potential (FIP) biases (Baker et al., 2019) and spectral line asymmetries. The chromospheric evaporation is associated with the Neupert effect (valid for about half of solar flares), according to which the time integral of the profile of non-thermal emissions approximately repeats the temporal behavior of thermal emissions (Veronig et al., 2002). In terms of duration in different spectral ranges (in particular, in soft X-rays), flares are divided into impulsive and gradual (or long-decay events, LDEs). Impulsive flares are typically observed with a soft-hard-soft behavior in their hard X-ray spectrum, while gradual flares are typically observed with a progressive hardening associated with continued heating (Grigis and Benz, 2008).

The aforementioned observational properties of solar flares (see, e.g., Fletcher et al., 2011; Benz, 2017, for reviews) were identically observed in stellar flares. In particular, stellar flares could be generally classified into two groups (Dal and Evren, 2010), and show spectral hardening (Preibisch and Zinnecker, 2002), line asymmetries (Fuhrmeister et al., 2008), the Neupert effect (Preibisch and Zinnecker, 2002), and FIP biases (Laming, 2015), which are signatures of the chromospheric evaporation by accelerated particles. An aperiodic variation on time-resolved stellar light curves accompanying the above signatures could be approximated by cooling of plasmas heated by impulsive energy releases and confined in a magnetic loop (Imanishi et al., 2001; Tsang et al., 2012). The loop lengths could be modeled by flare decay times (Reale et al., 1997; Reale, 2014), and exhibit both short (Doyle et al., 1991; Brasseur et al., 2019) and long loops (Guenther et al., 2000; Tsuboi et al., 2016) comparing to their stellar radii.

It seems that both partially and fully convective stars, including young stellar objects (YSOs), can produce flares in different bands. Flare activity has been detected in many stars that have a corona with a magnetic field generated by a dynamo mechanism in the convective zone (Benz and Güdel, 2010). The main-sequence stars of spectral classes F-M are the most active among other stars. Special attention is traditionally given to the UV Ceti variables (see the monography by Gershberg, 2005, and references therein). Powerful flares have also been

detected on several A class stars (Balona, 2012, 2013), despite the absence of strong convection inside them. Flares are also detected in cold giants, giants and supergiants in the cold part of the Hertzsprung-Russell diagram. Pre-main sequence (PMS) stars — T Tauri stars (TTS) and protostars — as well as young massive stars, are highly active. Powerful X-ray flares were detected in class I and more developed young stellar objects (YSO) with X-ray transparent environment. It is found that even young brown dwarfs exhibit powerful superflare activity (e.g. Gizis et al., 2017; Paudel et al., 2018).

Flares in massive stars could be originated from cool companions (Feigelson et al., 2002; Pedersen et al., 2017). However, studies revealed that massive stars seem to have magnetic fields (Pillitteri et al., 2014; Cantiello and Braithwaite, 2019) and bare flares (Kohno et al., 2002; Pillitteri et al., 2017). Fast rotating main-sequence stars are X-ray saturated (Tsikoudi and Kellett, 2000) or supersaturated (Jeffries et al., 2011). It was found that X-ray activities at weak-line TTS (wTTS) are saturated or supersaturated (Feigelson et al., 2003) as in main-sequence stars, while those at classical TTS (cTTS) show less clear saturation influenced by accretion (Preibisch et al., 2005; Telleschi et al., 2007; Briggs et al., 2007). The PMS stars which are mostly fast rotating are X-ray supersaturated (Argiroffi et al., 2016) and radio over-luminous relative to the conventional relation between microwave and X-ray emissions of solar-like stars (Guedel and Benz, 1993; Benz and Guedel, 1994). It was also found that fast-rotating ultracool stars are X-ray suppressed and radio enhanced (Williams et al., 2014), while emission properties of slowly-rotating ultracool stars including brown dwarfs are identical to that of solar-like partially convective stars (Güdel et al., 1997; Wright and Drake, 2016). A dichotomy in both quiescent and flare activities, between fast ($P_{rotation} < 10$ days) and slow ($P_{rotation} > 10$ days) rotators was reported (Stelzer et al., 2016; Pizzocaro et al., 2019). It was shown that the flare activity is influenced by binarity, e.g. Stelzer et al. (1999); Gao et al. (2016). Argiroffi et al. (2008) suggested that quiescent and flare components should follow different scaling laws for increasing stellar activity. It was found that confined plasma in a long loop with a strong magnetic field can explain the radio over-luminousity of PMS stars (Waterfall et al., 2019). The relationship between peak emission measure and temperature on PMS stars is different from that on the Sun, but could be explained by hot confined plasma in a longer loop (Shibata and Yokoyama, 1999; Getman et al., 2008).

For details on solar and stellar flares see the specific reviews. Observational and theoretical aspects of solar flares are reviewed in, e.g. Aschwanden (2002); Fletcher et al. (2011); Benz (2017) and Priest and Forbes (2002); Shibata and Magara (2011); Zharkova et al. (2011), respectively. The reviews of stellar flares are provided by Pettersen (1989); Haisch et al. (1991); Bastian (1994); Güdel (2004); Güdel and Nazé (2009); Benz and Güdel (2010); Testa et al. (2015).

Flares are short-term (from several minutes to several hours on the Sun and up to several days on some active stars) increases in the brightness of a star in a wide spectral range from radio to X-rays and γ-rays (unlike solar flares, no stellar flares were detected in γ-rays yet, probably because of insufficient sensitivity of available γ-ray detectors). The flare duration may differ in different spectral ranges. Typically, the intensity of thermal emissions has a shorter abrupt growth phase (to the maximum) and a much longer gradual decay phase (e.g. Fletcher et al., 2011; Davenport et al., 2014). Non-thermal emissions are usually observed

in the impulsive phase of a flare (up to the peak of thermal emissions, although events with pronounced, prolonged, non-thermal emissions are also detected, e.g. Zimovets and Struminsky 2012) and often manifest as a sequence of peaks (or bursts) of different duration and intensity (e.g. Aschwanden, 2002; Fletcher et al., 2011). Light curves of both thermal and non-thermal emissions can contain *quasi-periodic pulsations* (QPPs; see Section 2.1 for the definitions)[2]. Attention to solar flare QPPs was drawn by Parks and Winckler (1969). Solar radio pulsations had been reported several years earlier (e.g. Thompson and Maxwell, 1962; Dröoge, 1967) but the spectral (Fourier) analysis of the emission light curves was not done for identification of the quasi-periodic component, and those works attracted less attention. The first detection of QPPs in stellar flares was reported several years later by Rodono (1974).

Over the past half century, significant progress has been made in QPP research. It has been found that QPPs can appear in all phases of a solar flare: before the flare impulsive phase, in the impulsive phase, and in the decay phase. Typical periods of QPPs are in the range from a few seconds to a few minutes. Shorter and longer periods are also detected (e.g. Takakura et al., 1983; Karlický et al., 2010; Zaqarashvili et al., 2013) but less often, probably because of observational limitations. Recently, on the basis of a number of statistical studies, it has been shown that QPPs are a frequent and widespread phenomenon that occur in a large number of solar flares. Moreover, the probability of detecting QPPs increases with the flare class (see Section 2.5). This suggests that solar flare models should naturally explain the appearance of QPPs and their properties. More than a dozen different QPPs mechanisms/models in solar flares have been proposed. To a large extent, the models assume the presence of certain magnetohydrodynamic (MHD) oscillations or waves in flare magnetoplasma structures (magnetic loops, current sheets), quasi-periodic regimes of magnetic reconnection or repetitive reconnection (see Section 2.3). Nevertheless, we still do not know which of the proposed theoretical mechanisms is closest to reality. It is possible that different mechanisms may work in different flares, leading to different types of QPPs. The problem largely boils down to the fact that the proposed models of the QPPs are still qualitative, but not quantitative. This makes it difficult to determine all possible observational properties of each mechanism and their direct comparison with observations (see Section 2.4). Moreover, until now the capabilities of observational instruments are not enough to reliably determine all the necessary physical properties of QPP sources in flare regions on the Sun (see Section 2.2). As a result, the interpretation of QPPs in certain flares is usually not very confident and reliable.

Understanding of stellar flares are based on the notion that their mechanisms are close to those of solar flares, and on the progress made in understanding the latter. Accordingly, to interpret the QPPs in stellar flares, the models of QPPs developed for solar flares are very often used. However, due to the relative remoteness of stars, observations of QPPs in stellar flares are even more limited than observations of QPPs in solar flares. Usually, only the light curves of flare emissions are detected against the background of the star's radiation in one of the spectral ranges (see Sections 3.1, 3.2, 3.3, 3.4). Up to now, there are no examples of observations

[2] Some papers on solar and stellar flares use the term *quasi-periodic oscillations* (QPOs), but we will mainly use the abbreviation QPPs to avoid confusion with other high-energy astrophysical QPOs (e.g. van der Klis, 2006) not associated with "classical" stellar flares under discussion.

of stellar flare QPPs in principally different spectral ranges, e.g. simultaneously in optical and radio emissions, or radio and X-ray emissions (see Section 3.5), and there is no reliable information on the geometry of the QPP-emitting sources (by analogy with the Sun, almost all works assume a loop structure that is not proven). These circumstances greatly complicate the understanding of QPPs in stellar flares.

However, studies of stellar flare QPPs have also made significant progress in recent years. First, it is associated with several statistical studies that have multiplied the number of known stellar flares accompanied by QPPs (see Section 3.6). A great deal of progress has been made here thanks to precision observations in the optical range using the *Kepler* space observatory (Borucki et al., 2010). Interest in these observations was largely fueled by the discovery of a large number of superflares (with energy $> 10^{33}$ erg) in solar-type stars, which raised the urgent question of whether such superflares are possible on the Sun and what their probability is (Maehara et al., 2012; Shibata et al., 2013). Second, several observational signs of the similarity of QPPs in stellar and solar flares were obtained, such as the presence of oscillation harmonics and similar scaling of the ratio of the decay time and QPP period (see Sections 3.3 and 3.6). Third, we can note the good applicability of the hydrodynamic model (originally developed for the Sun) of the energy release in a magnetic tube for interpreting X-ray oscillations in flares of star-forming regions (see Section 3.3.3). Thus, more and more arguments appear in favor of the similarity of the QPP mechanisms in stellar and solar flares, and the validity of using the same mechanisms for their interpretation (of course, taking into account the peculiarities of the atmospheres of parent stars) is increasing.

There are a number of older reviews about QPPs in solar flares (Aschwanden, 1987, 2003; Nindos and Aurass, 2007; Nakariakov and Melnikov, 2009; Nakariakov et al., 2010b, 2016b). The methodology of diagnosing the physical parameters of stellar flare regions based on the interpretation of the QPPs as MHD oscillations of coronal loops – coronal seismology – is discussed in (e.g. Nakariakov, 2007; Stepanov et al., 2010, 2012; Srivastava and Lalitha, 2013). Recently, there have been three more relevant reviews (Van Doorsselaere et al., 2016; McLaughlin et al., 2018; Kupriyanova et al., 2020). However, the main emphasis in these reviews is placed on QPPs in solar flares and QPPs in stellar flares are mentioned only in passing.

The purpose of the present work is to give a more complete overview of the main observations of QPPs in stellar flares that are known to us at the present time, as well as the mechanisms that are used for their interpretation (Section 3). For this, before proceeding to the review of QPPs in stellar flares, we will briefly describe the main mechanisms/models of QPPs in solar flares (Section 2.3), review their characteristic observational properties and also some recent observations that could testify in favor of these mechanisms (Section 2.4). We do not pursue the goal of reviewing all the papers on QPPs in solar flares, of which there are now several hundred. The selection of referenced works is subjective. At the end of the review (Section 4), we summarize the current status of studies of QPPs in solar and stellar flares and outline (in our opinion) the main directions for further research. On the whole, we are of the opinion that QPPs in solar and stellar flares may be the result of similar physical mechanisms occurring in the atmospheres of various flare-active stars. However, this hypothesis is not yet conclusively proven and must be applied with caution.

2 Recent progress in solar flare QPPs

2.1 Brief introduction to the QPP-detection techniques

Intuitively, we could define flare QPPs as a sequence of bursts (or pulses, or cycles) of flare emission with similar time intervals between the successive peaks. However, in reality observations show a great variety of QPP temporal behaviour. Furthermore, different types of the low-frequency or aperiodic flare trend, apparent modulation of the amplitude and period, fast damping and low oscillation quality of QPPs, anharmonic shape of the individual pulses, superposition with noise, including both the high-frequency white noise and power-law distributed pink or red noise, all make QPPs difficult to recognize by eye. Therefore, a more advanced definition of the QPP phenomenon is based on the calculation of their significance relative to a noise level using rigorous mathematical techniques. Broomhall et al. (2019a) performed a blind test of eight different methods for detection of QPPs with different properties in simulated and observational flare light curves, addressing the effects of detrending and trimming data, colored noise, stationarity and drift of QPP periods. Among the detection techniques used in Broomhall et al. (2019a) are both standard methods (Fourier periodogram, wavelet analysis) and newly developed methods increasingly being applied to the analysis of solar observations, such as the Empirical Mode Decomposition (EMD) and Bayesian analysis. The future detailed analysis of the temporal properties of flare emission needs a thorough classification of QPP types, selection of the method (or methods) appropriate for the analysis of each type, and deliberate visual control of intermediate and final results. For example, the Fourier periodogram method is effective for the detection of high-quality harmonic oscillations with a stable period (periods) in a noisy time series. Wavelet analysis could be applied for searching for QPPs with a stationary or slowly drifting period. The EMD method is preferable for the analysis of more complicated signals of anharmonic form or with a highly non-stationary period. Bayesian methods allow for robust estimation of the QPP parameters and their uncertainties, provided the model function is prescribed adequately. Also, a combination of several independent techniques was found beneficial for improving the reliability of detection of QPPs in solar and stellar flares.

Estimation of the significance level, that is the power of noise exceeding which the QPPs are believed to have a non-noisy origin, is highly important. In particular, the question of the QPP significance in comparison with a power-law distributed background noise (or a combination of white and red noise) was addressed in Gruber et al. (2011); Inglis et al. (2015); Kolotkov et al. (2016a); Pugh et al. (2017a). However, the nature of the power-law shape of the Fourier spectra of solar flare emissions remains unclear, and varies with emission wavelength (e.g. McAteer et al., 2007). For example, Nakariakov et al. (2019a) demonstrated that a typical soft X-ray flare trend may be seen in the log-log Fourier spectrum as a power-law function with the slope identical to that of red noise. On the other hand, the bursty (or fractal) reconnection in the macroscopic current sheet (see Section 2.3) could also result in the power-law spectrum (Nishizuka et al., 2009; Bárta et al., 2011; Cheng et al., 2018).

More details on the novel techniques of the QPP analysis you can find in the review by Anfinogentov et al. in this volume.

2.2 Key instruments driving progress in recent observations of QPPs in solar flares

A solar flare is observed in a very broad wavelength range from radio to γ-ray bands. Thus, the understanding of QPPs, being an intrinsic feature of flares (see Section 2.5), requires comparative analysis of observations with different instruments in different bands. Temporally, spatially and spectrally resolved observations are necessary for progressing in the QPP problem. Hence, in this section we briefly overview the key past and existing solar observational instruments used for the analysis of QPPs.

Recent advances of solar flare QPP observations in the X-ray range are associated with several instruments:

1. the *Reuven Ramaty High-Energy Solar Spectroscopic Imager* (RHESSI; Lin et al., 2002), the big advantage of which is the ability to reconstruct images of flare sources with quite high spatial (up to $\approx 2.3''$) and temporal (typically $\approx 4 \times n$ s due to the instrument rotation period of ≈ 4 s) resolutions in a broad energy range from around 3 keV to several hundreds of keV, or even up to a few MeV in the most powerful flares. Another advantage of the instrument is the ability to perform precision spectral analysis, allowing the separation of thermal and non-thermal X-ray sources. However, due to the specifics of imaging, based on the use of nine rotating collimators, and also because of the moderate imaging dynamic range (≈ 10), RHESSI does not allow us to spatially resolve low-amplitude oscillations of flare loops. The satellite operated successfully from 2002 to 2018 and has detected over 1.2×10^5 X-ray events, some of which were accompanied by QPPs.
2. There are other instruments observing hard X-ray and γ-ray flare emission that do not supply spatial resolution but provide both spectral and different time resolutions depending on the waiting (or "background") and triggering (or "burst") observing mode. A key instrument is the *Gamma-ray Burst Monitor* (GBM) on board the *Fermi Gamma-ray Space Telescope* (former the *Gamma Ray Large Area Space Telescope* (GLAST) observatory; Meegan et al., 2009). Fermi/GBM's detectors cover the full sky and detect emission in a wide energy range from 10 keV to 30 MeV, with time cadence of 4.096 s in the waiting mode and up to 64 ms in the triggering mode. At any given time, some of these detectors are pointed near to the Sun and are sensitive to solar flares. Fermi/GBM data archive was used for a broad statistical study of the detection rate of QPPs in the non-thermal emission of solar flares (Inglis et al., 2016) (see Section 2.5). The *SOlar Neutrons and Gamma-rays* (SONG) instrument on board the *Complex ORbital Observations in Near-Earth space of the Activity of the Sun* (CORONAS-F) spacecraft observed (in 2001–2005) the emission with energies between 30 keV and 200 MeV with the time binning of 3.96 s (Myagkova et al., 2007). The Konus-W instrument on board the *Global Geospace Science Program* (GGS)-*Wind* spacecraft (launched in 1994) measures the count rate within 10 keV and 12 MeV with the cadence time 2.944 s in the waiting mode and up to 2 ms or 256 ms in the triggering mode (Pal'shin et al., 2014).
3. Another crucial data source is the upgraded *X-Ray Sensors* (XRS) installed on the *Geostationary Operational Environmental Satellites* (GOES) 13 (since 2015 to present), 14 (2009-2010) and 15 (since 2010 to present), which made it

possible to improve the temporal resolution of observations in the soft X-ray range (in two channels 1-8 and 0.5-4 Å) up to 2 s. Thanks to the upgrade, the signal-to-noise ratio is also increased, which contributes to the detection of small-amplitude oscillations in a solar soft X-ray flux. Although the XRS instruments do not have spatial resolution, they allow for almost continuous detection of solar X-ray radiation, due to which a large database of solar flares has been accumulated. This allows statistical studies of QPPs in solar flares to be carried out (see Section 2.5).

This set of instruments is not excessive but provides better data coverage in time filling the gaps when satellites are in the Earth's shadow and choosing the most full and the most qualitative data sets (Pugh et al., 2017b; Kashapova et al., 2020). Moreover, the approach comparing data from different instruments observing simultaneously the same event is in high demand for QPP-studies. It allows us to reveal and sift out instrumental artefacts, *e.g.,* caused by the rotation of spacecraft (Inglis et al., 2011). Additionally, finding similar QPP signatures in the light curves registered with different instruments enhances significantly their credibility (e.g. Nakariakov et al., 2010a).

Recent advances in observing solar flare QPPs in the UV and EUV ranges have been mainly associated with two space instruments:

1. the *Interface Region Imaging Spectrograph* (IRIS, De Pontieu et al., 2014);
2. the *Atmospheric Imaging Assembly* (AIA) onboard the *Solar Dynamics Observatory* (SDO, Lemen et al., 2012).

With the capability of performing simultaneous imaging and spectroscopic observations, IRIS has revealed new characteristics of QPPs (e.g., Brosius and Daw, 2015; Brosius et al., 2016; Li and Zhang, 2015; Li et al., 2015; Tian et al., 2016; Zhang et al., 2016; Li et al., 2017a). Launched around the solar maximum in 2013, IRIS has observed hundreds of solar flares so far. The three wavelength ranges of the IRIS spectrograph include several strong chromospheric and transition region (TR) lines such as Mg II 2796/2803 Å, C II 1334/1335 Å and Si IV 1394/1403 Å. These lines are usually very strong at flare ribbons. In addition, IRIS can observe the Fe XXI 1354 Å line formed at a temperature of about 11 MK under the situation of ionization equilibrium. This line is often entirely blueshifted at the ribbon in the impulsive phase, and could be very strong in flare loops in the gradual phase (Tian, 2017). IRIS can also take slit-jaw images (SJI) with four filters, 2832 Å, 2796 Å, 1330 Å and 1400 Å. Except the 2832 Å filter, the other three filters mainly sample plasma with typical chromospheric and TR temperatures, thus could provide context images of flare ribbons. Due to a high spatial resolution of $\approx 0.33''$ and a cadence as high as ≈ 2 s, IRIS allows to spatially resolve UV/EUV QPPs with periods down to a few seconds.

The advantage of SDO/AIA is the construction of images of the entire visible hemisphere of the Sun with a good angular resolution of $\approx 1.2''$ almost simultaneously in seven EUV channels (94, 131, 171, 193, 211, 304, and 335 Å) with a time step of 12 s and in two UV channels (1600 and 1700 Å) with a cadence of 24 s. This allows solar flares to be monitored almost continuously, 24/7 (since 2010). The combination of different channels makes it possible to detect radiation from sources at different altitudes in the solar atmosphere and to perform diagnostics of plasma with temperatures in the broad range from $\sim 10^4$ to $\sim 10^7$ K. One of

the disadvantages is the saturation of the CCD arrays of the instrument in the region of powerful solar flares, which often inhibits spatially resolved study.

A number of observational results on QPPs in solar flares have also recently been obtained using the *EUV SpectroPhotometer* (ESP) within the *Extreme Ultraviolet Variability Experiment* (EVE) onboard SDO, the *Large Yield Radiometer* (LYRA) onboard the *PRoject for Onboard Observatory* 2 (PROBA2, launched in 2009), and the *EUV Sensor* (EUVS) onboard GOES, capable of detecting solar UV and EUV fluxes without spatial resolution. The time resolution of ESP/EVE/SDO, LYRA/PROBA2 and EUVS/GOES is 0.25, up to 0.01, and 11 s, respectively (see, e.g., Dolla et al., 2012; Dominique et al., 2018; Li et al., 2020c, and references therein).

To date, the greatest advances in studying QPPs in solar microwave emission – both in flares and in quiet active regions – have been achieved using the instruments of the Nobeyama Radio Observatory. The Nobeyama Radioheliograph (NoRH, Nakajima et al., 1994), operating since 1992, provides two-dimensional images of the Sun at the frequencies of 17 and 34 GHz, with spatial resolutions of about $10''$ and $5''$, respectively, and temporal resolution of 1 s (down to 0.1 s during flares); it allows one to study the temporal characteristics of the QPPs and to resolve (for sufficiently long flaring loops) their spatial behaviour (e.g., Melnikov et al., 2005). The Nobeyama Radiopolarimeters (NoRP, Torii et al., 1979; Shibasaki et al., 1979; Nakajima et al., 1985) record the total (without spatial resolution) solar microwave flux at the frequencies of 1, 2, 3.75, 9.4, 17, 35 and 80 GHz, and with a time resolution of 0.1 s. Solar radio and microwave QPPs have been observed also with such radioheliographs as the Siberian Solar Radio Telescope (SSRT, Grechnev et al., 2003, 5.7 GHz), Owens Valley Solar Array (OVSA, Hurford et al., 1984; Gary and Hurford, 1994, $1 - 18$ GHz) and Nançay Radioheliograph (NRH, Kerdraon and Delouis, 1997, $150 - 450$ MHz), and with various single-dish spectrographs and spectropolarimeters. Currently, a new generation of solar radio instruments has been emerging, such as the Siberian Radioheliograph (SRH, Altyntsev et al., 2020), Expanded Owens Valley Solar Array (EOVSA, Gary et al., 2018) and Mingantu Ultrawide Spectral Radioheliograph (MUSER, Yan et al., 2009, 2016). These multiwavelength radioheliographs have been designed to provide simultaneous imaging observations at many frequencies in the microwave range with high (down to < 1 s) time resolution. Thus we expect new significant advances in studying the solar microwave QPPs in the emerging solar cycle 25.

2.3 Summary of the main solar flare QPP models

McLaughlin et al. (2018) provided a review of the physical mechanisms underpinning QPPs in solar and stellar flares, with an emphasis on the underlying physics that generates the resultant range of periodicities. Eleven mechanisms were reviewed and they were classified into three general groups: (A) *oscillatory* (which encompasses the physical mechanisms of MHD oscillations; QPPs triggered periodically by external waves; dispersive wave trains; the magnetic tuning fork; and the equivalent LCR contour), (B) *self-oscillatory* (which includes periodic or repetitive spontaneous reconnection, including oscillatory reconnection; thermal overstabil-

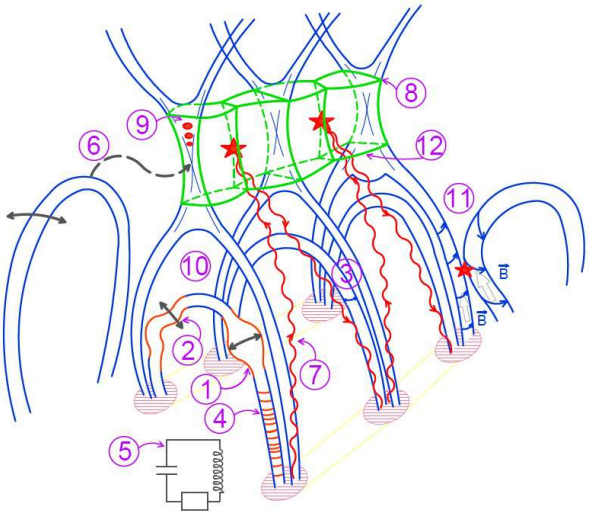

Fig. 1 Schematic illustration of the main models interpreting solar flare QPPs (from Kupriyanova et al. 2020). Numbers correspond to the following mechanisms: eigenmodes of a magnetic flux tube oscillations, including [1] sausage, [2] kink, [3] torsional Alfvén, and [4] slow magnetoacoustic modes; as well as [5] equivalent RLC circuit; [6] reconnection triggered periodically by external waves; [7] autowave processes; [8] flapping oscillations; [9] self-oscillatory processes; [10] thermal overstability; [11] periodic regime of coalescence of two twisted loops; and [12] magnetic tuning fork model.

ities; wave-flow overstabilities; wave-driven reconnection in the Taylor problem; and the coalescence of two magnetic flux tubes), and (C) *autowave processes*.

Figure 1 shows a schematic illustration of the main models interpreting solar flare QPPs (from Kupriyanova et al. 2020). Numbers correspond to the following mechanisms: eigenmodes of a magnetic flux tube oscillations, including [1] *sausage* (axisymmetrical oscillations of loop boundary, predominantly radial, 'peristaltic' flows, where mathematically the azimuthal wave number $m = 0$), [2] *kink* mode (transverse oscillations of loop axis, that displacement may be horizontal or vertical, but also circular or elliptical polarisation, where mathematically $m = 1$), [3] *torsional Alfvén* wave (twisting and untwisting of the cylinder and magnetic field), and [4] *slow magnetoacoustic* mode (longitudinal flows along magnetic field axis; as well as [5] *equivalent RLC circuit*; [6] *reconnection triggered periodically by external waves* (periodic modulation of the reconnection rate is induced by MHD oscillations located at a distance from the reconnection site); [7] *autowave* processes, e.g. slow magnetoacoustic wave pulses are generated above the arcade, these are reflected at the chromosphere, returning to the apex of the arcade, resulting in the next energy release, and the cycle repeats; another example is the older interacting loop model by Emslie (1981) (both these models could explain the observed progression of the quasi-periodic energy release site along the neutral line in a two-ribbon flare); [8] *flapping oscillations* (oscillations of the macroscopic current sheet above the flare arcade associated with the current sheet destabilization, and an alternative explanation for propagating of the quasi-periodic energy release site along the polarity inversion line – PIL); [9] *self-oscillatory* processes (the conversion of constant, non-periodic flow, e.g. direct current energy, into a periodic energy

release rate, e.g. alternating current energy); [10] *thermal overstability*; [11] periodic regime of *coalescence of two twisted loops*; and [12] *magnetic tuning fork model*.

In contrast to McLaughlin et al. (2018), Kupriyanova et al. (2020) groups the physical processes into three different classifications: (i) *direct emission modulation by MHD and electrodynamic oscillations of all types* (which collects together processes [1] sausage, [2] kink, [3] torsional Alfvén, [4] slow magnetoacoustic modes, and [5] equivalent RLC circuit from Figure 1); (ii) *periodic modulation, via MHD oscillations, of the efficiency of energy release processes such as magnetic reconnection* (which collects together processes [6] reconnection triggered periodically by external waves; [7] autowave processes; [8] flapping oscillations; and [12] magnetic tuning fork model); and (iii) *spontaneous quasi-periodic energy release* (covering [9] self-oscillatory regimes of magnetic reconnection; [10] thermal overstability; and [11] periodic regime of coalescence of two twisted loops). The mechanisms in group (iii) are based on transformation of a constant energy supply (e.g. a steady magnetic inflow or background heating) into oscillatory feedback, analogous to the transformation of a direct current to alternating current (DC-to-AC models). The creation of these three groupings is meant to help illuminate the underlying physical processes of each mechanism, but we note that a mechanism could be assigned to more than one grouping. E.g. mechanism [12], magnetic tuning fork model, has been assigned to group (ii) since it contains MHD oscillations which modulate the efficiency of energy transformation via the oscillating termination shock. However, it could also be classed into group (iii) since these oscillations are caused by an initially-steady driver – the regular plasma outflow (see Section 2.4.2). Another example is the *autowave* processes [7] (see Section 2.4.2). It belongs to the group (ii), since in the model of Nakariakov and Zimovets (2011), the slow mode waves trigger successive reconnection episodes in the current sheet above the loop arcade. However, this mechanism can also be attributed to group (iii), since, in fact, it can be viewed as a process of self-sustained oscillations (similar to *self-oscillatory* process [9], see Section 2.4.3) – each episode of reconnection initiated by a slow wave generates a new wave, thus, the wave is fed (impulsively) from the medium, and the process continues.

Of course, there is no core disagreement here: the (A) *oscillatory* mechanisms of McLaughlin et al. (2018) are refined further into classifications (i) and (ii) by Kupriyanova et al. (2020), who also adds the *autowave* mechanisms, (C), into group (ii), and *self-oscillatory mechanisms* (B) correspond to classification (iii) the *quasi-periodic regimes of reconnection*. Unlike McLaughlin et al. (2018), Kupriyanova et al. (2020) does not review *dispersive wave trains* as a QPP mechanism (we assign a number [13] to it), but this could be classified under (i), and likewise mechanism 'wave-driven reconnection in the Taylor problem' – see e.g. Fitzpatrick et al. (2003) – could be classified under (ii) under mechanism [6], and the 'wave-flow overstability' under (iii). In addition, McLaughlin et al. (2018) does not review the *flapping oscillation* mechanism [8] cited by Kupriyanova et al. (2020). Across both papers, a total of thirteen physical mechanisms are reviewed (note that McLaughlin et al. 2018 reviews MHD oscillations as one mechanism, whereas Kupriyanova et al. 2020 splits this into four separate modes).

In addition to the thirteen models detailed by McLaughlin et al. (2018) and Kupriyanova et al. (2020), there has been further development in modelling of potential mechanisms behind QPPs in solar flares in recent years. Here, we review briefly three additional models which are capable of producing QPPs in flares.

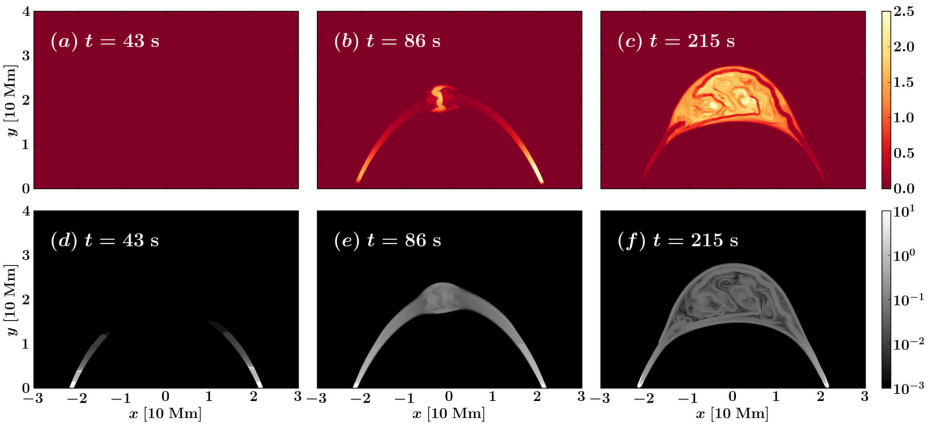

Fig. 2 Thermal Soft X-ray (top) and hard X-ray emissions (bottom) during turbulent magnetic reconnection driven by colliding plasma within a flare coronal loop. Adapted from Ruan et al. (2019) with permission.

Firstly, a model based on the Kelvin-Helmholtz Instability (KHI) in a flare loop-top caused by colliding evaporation flows, developed by Fang et al. (2016) and Ruan et al. (2018, 2019, 2020). Here, charged particles are accelerated smoothly (not periodic) at the loop top or above the loop top by magnetic reconnection and propagate to the footpoints along the magnetic field lines. As they precipitate on the chromosphere, the cooler and denser material is heated up and evaporates rapidly. Then plasma flows could be formed with speeds up to hundreds of km s^{-1}, and collide with each other at the loop top. This evaporated flow could distort the magnetic field lines and form a region with small magnetic islands, see Figures 2c and 2f. Then the highly-distorted magnetic fields are relaxed by turbulent magnetic reconnection, and release a significant amount of energy. Local plasma could be heated up to 20 MK and the fluid motion could overwhelm the constraint of the magnetic field (Fang et al., 2016). This bulk of hot and dense plasma, confined by the expanded magnetic field lines, oscillates back-and-forth and the integrated flux in soft X-ray exhibit a QPP effect, see Figure 3. Ruan et al. (2019) found that the oscillatory signal only originates from a very compact source (Figure 3a), and the oscillatory signal is highly correlated within this tiny region. This model (we assign a number [14] to it), based on the KHI in a flare loop-top, can be classified under [ii] periodic modulation, via MHD oscillations, of the efficiency of energy release processes such as magnetic reconnection.

Secondly, Jelínek and Karlický (2019) detailed a model in which sudden pulse-beam heating of deep atmospheric layers at the flare arcade footpoints generates two magnetohydrodynamic shocks, one propagating upwards and the second propagating downwards in the solar atmosphere. The downward-moving shock is reflected at the deep, dense atmospheric layers and triggers oscillations of these layers. These oscillations of the photospheric and sub-photospheric layers generate the upward-moving magnetohydrodynamic waves that can influence the flare magnetic reconnection (located at an X-point) in a quasi-periodic way. The model of Jelínek and Karlický (2019) is an example of [6] and thus can be categorised as (ii) *periodic modulation, via MHD oscillations, of the efficiency of energy release processes*

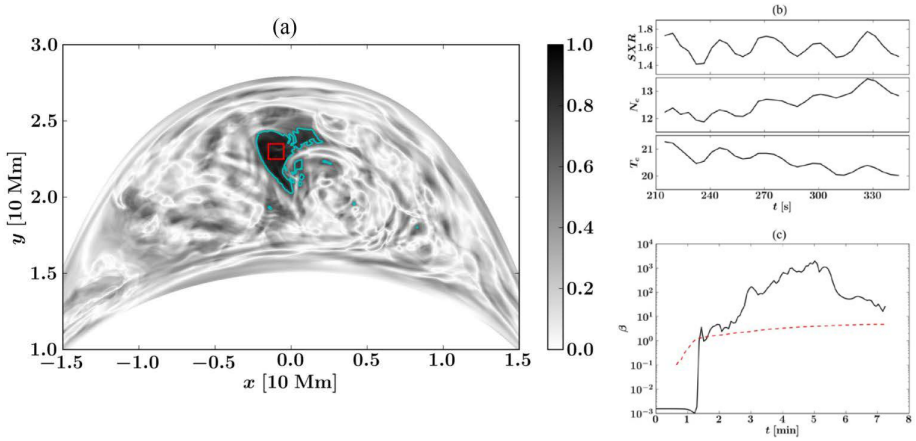

Fig. 3 (a) Correlation coefficient between the oscillatory signals within the turbulent region. The cyan contour label the value at 0.7. (b) Temporal evolution of SXR flux, average density, and temperature within the red box in panel (a). (c) Temporal evolution of average plasma beta in the red box (black solid line). Adapted from Ruan et al. (2019) with permission.

such as magnetic reconnection. It is a different model to that of Nakariakov et al. (2006), of which Figure 1 process [6] is based on, however the underlying physical process is the same, i.e. the reconnection rate is modulated quasi-periodically by external waves. Due to this, we do not assign a special number to this model.

Thirdly, Ledentsov and Somov (2016, 2017) proposed another model (we assign a number [15] to it). The authors solved the problem of the stability of small longitudinal perturbations of a reconnecting homogeneous neutral current layer within the dissipative one-fluid MHD approximation. The effects of Joule heating, heat-conducting redistribution of energy inside the current sheet and radiative cooling of the plasma in it are taken into account. It is shown that an efficient suppression of plasma heat conduction by a magnetic field perturbation inside the current layer serves as a thermal instability condition. The instability in the linear phase grows in the characteristic radiative plasma cooling time. A periodic structure of cold and hot filaments located across the direction of the electric current can be formed as a result of the instability in the current layer. The estimated spatial scale of the instability $\lambda \approx 10$ Mm is consistent with the observed distances between individual bright loops in flare arcades on the Sun. The proposed mechanism can be useful for explaining both the sequential brightening ("ignition") of flare loops along the PIL and QPPs of flare emission in a broad wavelength range. This model is similar to the model of the flapping oscillations proposed by Artemyev and Zimovets (2012) ([8] in Figure 1) in that both of these models consider disturbances propagating in the current sheets along the PIL, but different types of instabilities are considered. Since the solution found by Ledentsov and Somov (2016) corresponds to the surface magnetoacoustic waves, the considered mechanism, as well as the mechanism of flapping oscillations, belongs to group (ii) of Kupriyanova et al. (2020).

Naturally, the QPPs generated via these different underlying physical mechanisms manifest in different ways, giving clues to which could be the correct interpretation(s). For example, the advantage of the MHD-oscillation-related expla-

nation (that is, the underlying physical mechanisms based on the classifications of (i) *direct emission modulation by MHD oscillations of all known types*; and (ii) *periodic modulation, via MHD oscillations, of the efficiency of energy release processes such as magnetic reconnection*) is the observation of multiple periodicities in QPPs. A summary of the observational properties of the fifteen QPP models is given in Section 2.4. There we also cited some observational works supporting these models or mentioning these models as possible interpretations of the observations.

2.4 Properties of the QPP models and supporting observations

In this section we briefly describe the most expected and prominent observational properties (signatures) of the main QPPs mechanisms/models [1]–[15] summarized in Section 2.3. We do not provide a detailed description of the mechanisms themselves. Interested readers can find them in the original papers as well as in the recent reviews written by McLaughlin et al. (2018) and Kupriyanova et al. (2020). For the mechanisms for which this is available, we will provide references to some observations that could be interpreted using these mechanisms. Strong supporting observations are not yet available for all mechanisms. It can also be noted that (a) most of the models are still of a qualitative nature and (b) observational instruments are still far from being perfect and do not provide all the necessary information to unambiguously identify one mechanism over another. Because of this, most observations can be interpreted by several different mechanisms and it is not yet possible to make an unambiguous choice. In Appendix A we provide the 'Model-Property Table' (Table 1) with some possible (expected) observational properties of these mechanisms/models.

2.4.1 Group (i): direct modulation by MHD and electrodynamic oscillations of all types

– **Sausage mode – mechanism [1].**

The sausage mode is one of the eigenmodes of a coronal loop, which is approximated by a straight magnetic plasma cylinder (Edwin and Roberts, 1983). The sausage mode corresponds to $m = 0$ azimuthal wave number, and it means the radial oscillations of the magnetic loop cross-section implying variations of the local magnetic field strength. The phase speed of the sausage mode, C_p, lies between the Alfvén speeds inside (C_{A0}) and outside (C_{Ae}) the loop: $C_{A0} < C_p < C_{Ae}$. Depending on the wavelength, the sausage mode can exist in two regimes: trapped and leaky. In the short-wavelength limit, i.e. if the axial wavenumber is greater than the cutoff value, the sausage mode manifests in the trapped regime. In this regime, the oscillations experience total internal reflection at the cylinder boundaries and are evanescent outside the cylinder. The period of the global trapped sausage mode is defined by its phase speed C_p and length of the loop L: $P_{GSM} = 2L/C_p$. The leaky regime occurs in the long-wavelength limit, when the axial wavenumber is smaller than the cutoff value. The oscillatory energy transfers outside the cylinder, so that the magnetic loop acts as an antenna emitting MHD waves into the surrounding media, in the form of wave trains (see Nakariakov et al. (2012) for a description of this mechanism [13]). The principal parameter defining the period in this regime

is the loop cross-section radius a: $P_{saus} = 2\pi a/\eta_j \sqrt{C_{s0}^2 + C_{A0}^2}$, where C_{s0} is the sound speed inside the loop, $\eta_j \simeq 2.40, 5.52, 8.65$, are zeros of the Bessel function $J_0(\eta)$ (e.g., Zajtsev and Stepanov, 1975; Kopylova et al., 2007). This formula is also suitable for describing trapped modes at $j > 1$.

The quality factor (Q) of the oscillations depends on the ratio of the Alfvén speeds outside and inside the loop: $Q = \tau_{saus}/P_{saus} \propto (C_{Ae}/C_{A0})^2$, where τ_{saus} is the damping time. If the contrast is higher, the oscillations live longer. Lim et al. (2020) found that the damping times of higher radial harmonics could be significantly longer than the periods of oscillations even in the long-wavelength limit, meaning that they could in principle be observed. Moreover, this effect exists even if the contrast between the Alfvén speeds is low.

The particular effect of the sausage oscillations on the observables is highly dependent on the emission mechanism. On one hand, variations of the local magnetic field lead to variations of the local plasma density inside the loop and, therefore, the emissivity of local thermal plasma. This make the sausage oscillations potentially pronounced in those wave bands related to the thermal emission: in the infrared, optic, (E)UV, soft X-ray bands. In particular, forward modelling of the EUV lines emission reveals that both intensity and Doppler shift oscillates with the period P_{saus} and the phase shift differs from $\pi/2$ while the Doppler width oscillates with the periods P_{saus} and $P_{saus}/2$, where P_{saus} dominates over $P_{saus}/2$ in the flare plasma.

On the other hand, radial variations of the local magnetic field of the loop lead to variations of the magnetic mirror ratio and, thereby, modulate the number of accelerated electrons. These electrons gyrate around magnetic field lines, generating the gyrosynchrotron emission usually observed in microwaves. As these electrons precipitating into the dense chromospheric plasma they lose their energy via collisions and generate hard X-ray emission. Therefore, the sausage mode could be a source of variations of these emissions.

The spatial amplitude of variations of the loop parameters in the trapped regime is up to a few percent of the loop cross-section radius. Schrijver (2007), studying of the parameters of the coronal loops based on the data in EUV and soft X-ray bands, found that the loop cross-section radius could vary within the interval $1-10$ Mm, while Aschwanden and Peter (2017) found the broader interval, $0.1 - 40$ Mm. Thus, the amplitude of the sausage variations are expected to be from a few km to $\simeq 1000$ km. This complicates the spatial detection of these oscillations with modern instruments, which best spatial resolution corresponds to $\simeq 100 - 1000$ km at the solar surface.

Depending on the emission mechanism, such amplitudes of the radial oscillations could result in a higher modulation depth of the QPPs in flare emission light curves, which is found to be up to a few tens of percent both for thermal (Antolin and Van Doorsselaere, 2013) and non-thermal (Mossessian and Fleishman, 2012) emission. Therefore, the modulation depth of the QPPs could be considered as one of the observational signatures of the trapped sausage mode, allowing it to be distinguished from those mechanisms related to magnetic reconnection where the modulation depth could reach as high as 100%. On the other hand, the leaky sausage mode could be considered as one of the triggers for mechanism [6] and, thus, the amplitude of the resultant QPPs can be very high.

For typical coronal conditions, periods of the sausage mode vary from tenths of second to a few tens of seconds (e.g., Van Doorsselaere et al., 2016). Such periods could be observed with the instruments that have the highest temporal resolution. Therefore, either the short-period sausage oscillations or the higher radial harmonics could be detected in the radio band only, where a time resolution of tens of ms is achieved. The cadence in other wave bands is a few seconds or more and allows us to resolve periods from $\simeq 10$ s and longer.

Successful detections of the sausage oscillation in solar observations appear to exist, but remain very sporadic. In particular, Nakariakov et al. (2018) found pulsations with a period of both 1.4 s in the intensity channel and 0.7 s in polarisation channel in a solar microflare, using RATAN-600 data in the 3–4 GHz band. The authors interpret the double periodicity as a superposition of the fundamental and second harmonics of the standing sausage mode. Such short-period QPPs with periods 0.7 s and 2 s, associated with the sausage mode, have been detected in broadband microwave emission at 4–8 GHz (Mészárosová et al., 2016) and in the modulation of zebra-patterns in solar radio bursts (Kaneda et al., 2018). In the EUV band, sausage oscillations were observed by Tian et al. (2016) using IRIS data. The authors found high-quality oscillations with the period of ∼19–27 s in both the intensity and Doppler shift of the Fe XXI 1354 Å line in the hot post-flare loops. Similar QPPs were also found in the soft X-ray flux recorded by GOES (Figure 4). Additionally, the intensity and Doppler shift oscillations had a phase shift around $\pi/2$ (~ 5 s time delay). By estimating the phase speed and electron density, the authors interpreted the observations as the global fast sausage oscillations. The phase shift close to $\pi/2$ is consistent with the results of forward modelling of the standing sausage mode (Antolin and Van Doorsselaere, 2013; Shi et al., 2019).

A promising new avenue for the QPP-based coronal seismology is the detection of multi-modal QPPs (Chen et al., 2015b). As an illustrative example, Kolotkov et al. (2015) observed 15-s and 100-s QPPs simultaneously and interpreted them in terms of fundamental sausage and kink (see mechanism [2] below) modes of the flaring loop, respectively.

More details about theory of this mode is written in the review by Li et al. in this volume.

– **Kink mode – mechanism [2].**

The kink mode corresponds to the azimuthal wave number $m = 1$ and means the mechanical displacements of the coronal loops from their equilibrium states. In the most cases, the kink mode are observed in the trapped regime, and its period, $P_{kink} = 2L/jC_k$, depends on the loop length and on the kink speed

$$C_k = \left(\frac{\rho_0 C_{A0}^2 + \rho_e C_{Ae}^2}{\rho_0 + \rho_e} \right)^{1/2},$$

where ρ_0 and ρ_e are the internal and external plasma mass densities, respectively. As, according to the Zaitsev-Stepanov-Edwin-Roberts dispersion relation (Zajtsev and Stepanov, 1975; Edwin and Roberts, 1983), phase speeds of kink waves are systematically lower than phase speeds of sausage waves with the same radial wave number, typical periods of kink oscillations are longer than sausage oscillation periods. Kink oscillations are identifiable by their non-exponential damping profile

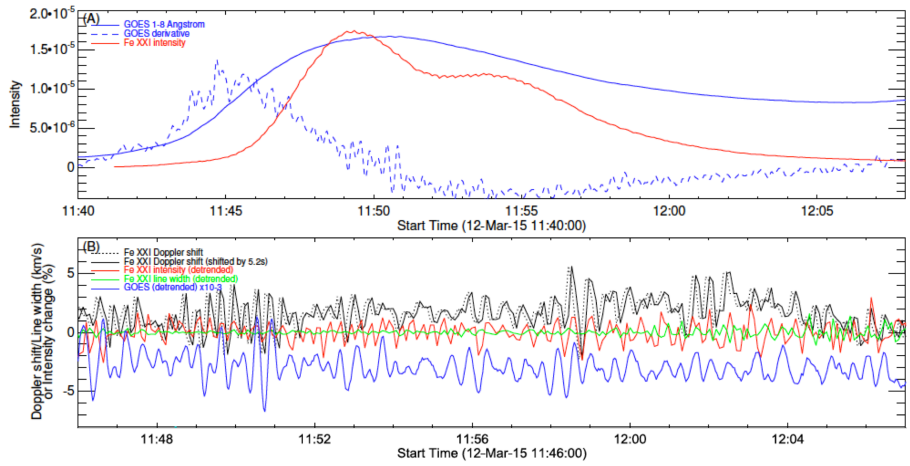

Fig. 4 Global sausage oscillations of flare loops detected by IRIS. (A) Temporal evolution of the Fe XXI 1354 Å line intensity, GOES 1–8 Å flux and its time derivative in an M1.6 flare peaked at 11:50 UT on 2015 March 12. (B) Detrended GOES flux and Fe XXI 1354 Å line parameters as a function of time. Adapted from Tian et al. (2016) with permission.

(De Moortel et al., 2002; Pascoe et al., 2012, 2016c) due to resonant absorption (Hood et al., 2013; Ruderman and Terradas, 2013) which can be used to infer the transverse structure of the oscillating loop (e.g. Pascoe et al., 2013a, 2016b, 2017a).

The trapped kink mode could exist in two regimes: low-amplitude decay-less oscillations (Anfinogentov et al., 2013b, 2015; Nakariakov et al., 2016a) and the high-amplitude rapidly decaying oscillations. The periods of the decay-less oscillations lie in the range between 1.5 and 10 min and their amplitudes are around 0.05–0.5 Mm (Anfinogentov et al., 2015). So, these oscillations are well resolved in time by the most modern instruments, however, special technique is needed to register the spatial displacements of a loop (Anfinogentov and Nakariakov, 2016).

The decaying kink oscillations were the first MHD mode detected in observations (Aschwanden et al., 1999; Nakariakov et al., 1999) in the imaging EUV data by TRACE, and since that time it is the most frequently observed MHD mode in the solar corona. The typical observed periods of decaying kink waves vary from one minute to few tens of minutes (Nechaeva et al., 2019). The absolute values of the exponential damping time are from 3 to 36 min, enveloping 1–6 cycles of oscillations, with the linear dependence on the period: $\tau_{kink} = (1.53 \pm 0.03)P_{kink}$ (Goddard et al., 2016a).

The initial amplitudes of the decaying kink oscillations are found from a few to a few tens of Mm (e.g., Liu and Ofman, 2014) with the most typical values of 3–5 Mm (Goddard et al., 2016a). Such the displacements are well resolved in the

imaging data of instruments with the highest spatial resolution, e.g., in optical and (E)UV bands. Simultaneously, this makes the kink oscillations invisible directly in data of those instruments, spatial resolutions of which greater than the amplitudes of the kink oscillations. In particular, the kink waves are not pronounced in the fluxes integrated over the whole solar disk. However, both the dependence of parameters of the kink oscillations on the plasma parameters in the oscillating volume and the line-of-sight (LOS) effect together with knowledge on mechanisms, where the kink oscillations could be involved, allow to identify them as QPPs in the light curves even in deficiency of the spatial resolution and use them as a tool for diagnostics of the flare plasma and magnetic field (e.g., Pascoe et al., 2016b).

Forward modelling, actively developing last several years, allows to calculate observable quantities as a result of the numerical simulations. Particularly, for the thermal emission, Antolin et al. (2017) found that the presence of a temperature gradient across a loop cause Kelvin–Helmholtz instability (KHI) at the loop boundaries leading to a modulation of intensity of the optically thin coronal line emission with double periods around several minutes, one of which corresponds to the global standing kink mode and another one, twice shorter, appears when the KHI is set up. Besides, the intensity and Doppler velocity are found to oscillate with a non-zero phase shift. Observable signatures of the fast MHD waves were defined also for the non-thermal emission observed in the radio wave band (Mossessian and Fleishman, 2012).

In the long-wavelength limit, kink oscillations do not modulate the plasma density. However, the LOS effect is based on dependence of the intensity of the emission on the column density. So, the waves can be detected as QPPs in the emission intensity light curves by imaging instruments. The effect consists in that the column depth of the oscillating loop (along the LOS) is changed by the wave (kink or sausage). This affects the actual amplitudes of the kink waves making the corresponding observed amplitudes of the QPPs larger by up to a factor of two than the actual ones. In contrast, the observed amplitudes of the QPPs for the sausage mode are always less than the actual amplitudes (Cooper et al., 2003).

Period of the QPPs associated with the kink mode can evolve because its dependence on the loop length changing during a flare. Stretching or contraction of a loop results in the QPP period drift towards longer or shorter values, respectively, being detected in the light curves of the both thermal (e.g., Zhang et al., 2020) and non-thermal emission (e.g., Jakimiec and Tomczak, 2010). Pascoe et al. (2017c) revealed a direct relationship between a decrease of the loop length and a decrease of the QPP period. Similarly, an increase of the QPP period can be associated with an increase of the loop length (Hayes et al., 2016).

Zhang et al. (2020) detected kink oscillations in the loop, one footpoint of which is the top of the circular ribbon structure and another footpoint is the remote sunspot. The circular ribbon produced two consequent flares causing the oscillations twice. The first flare triggered a lower-amplitude kink wave seen as QPPs in the time-distance plots in the 193 Å and 211 Å channels with the same period around 120 s. Kink wave excited by the second flare has higher amplitude. In each of the 171 Å, 193 Å and 211 Å EUV channels, QPPs had individual periods, period drift rate, and damping times. However, the ratios τ_{kink}/P_{kink} occurred to be similar for each channel. The authors connected the observed decreasing of periods with the loop contraction.

Indirect indication on the existence of the kink mode was found by Jakimiec and Tomczak (2010). The authors analysed light curves of the hard X-ray emission associated with the high cusp-shape coronal structures near the solar limb. They found that the QPP periods are around 10–60 s for different events. Moreover, the periods decreased in time implying the QPPs are originated from a dynamic volume. Above-the-limb location of the hard X-ray sources allowed estimation of the loop lengths (L), which occurred to be too long to produce so short-period oscillations even in the case of a fast MHD mode. However, such the periods could be explained in the framework of the model of collapsing magnetic trap developed by the authors. The model implies that not the entire loop could be evolved into the oscillatory process but only its short segment of size d ($d \ll L$), filled of the curved field lines, existing within a cusp structure above the loop top but under the current sheet. This triangle-shaped segment works as a magnetic trap for electrons accelerated during reconnection in the current sheet above. This volume is dynamic because the newly-formed by the reconnection magnetic field lines shrink down to the quasi-circular underlying coronal loops. During the contraction, a sequence of the magnetic traps appears. The contracted field lines bump the underlying loops and experience kink oscillations until the balance between the magnetic and gas pressures set up. The kink oscillations modulate the magnetic mirror ratio leading to the modulation of the loss-cone and number of precipitating energetic electrons and, thereby, to the QPPs in the intensity of hard X-ray emission.

In the microwave emission, where the spatial resolution does not allow to resolve oscillating loops directly, the kink oscillations can be identified applying theory of that emission, typically associated with the gyrosynchrotron emission of the electrons accelerated up to mildly relativistic energies. Intensity I of the gyrosynchrotron emission depends on both the magnetic field B and the angle θ between direction of the magnetic field and the LOS. According to (Dulk and Marsh, 1982), the intensity $I \propto \sin\theta^a B^b$, where indices a and b depend on the non-thermal electron energy spectral index δ, which is $2 < \delta < 7$. For such δ values, the indices a and b vary within, roughly, $1 < a < 4$ and $1.5 < b < 6$. This means that the small variations of the magnetic field, both its strength and direction, result in the significant variations of the intensity of microwave emission.

Depending on the trigger, kink oscillations could be polarized either in horizontal direction when the loop sways perpendicularly to its plane, or in vertical direction when the loop stretches and shrinks in the loop plane, or, in general case, could have an elliptical polarization. The recent statistical study revealed that the kink oscillations were associated with the low coronal eruptions in 57 of 58 studied cases. Among them, 44 events were accompanied by CME, 53 events were associated with flare (Zimovets and Nakariakov, 2015). All these phenomena could be considered as a trigger of the kink oscillations of a coronal loop. In the vast majority of the observed cases, the horizontally polarised kink oscillations are registered. However, Kohutova and Verwichte (2017) found that, in presence of coronal condensation at the loop top, the fundamental harmonic of a vertically polarised kink mode could be excited. Another model considers the vertical oscillations of a loop in a gravitationally stratified corona triggered by a periodic driver located at the top of the photosphere exactly under the loop top (Murawski et al., 2015). During the vertical kink oscillations, the top of oscillating loop moves between layers with slightly different balances of magnetic and gas pressures. This could result in small (around a few percent) variations of its cross-section radius (Aschwanden

and Schrijver, 2011) leading to variations of both the local plasma density and the local magnetic field in the loop which modulate both thermal (Aschwanden and Schrijver, 2011) and non-thermal (Kupriyanova et al., 2013) emissions. This property makes the vertically polarised kink mode similar to the sausage mode. However, in contrast to sausage mode, these kink oscillations are pronounced in the imaging data.

The fundamental (or global) harmonic ($j = 1$) is easiest to be excited, and it is the most frequently observed mode. However, depending on the trigger and its position relatively to the loop, the higher harmonics can be excited. For example, Pascoe et al. (2016a) connected the second harmonic ($j = 2$) with the coronal mass ejection which displaced one of the loop legs. Duckenfield et al. (2019) reported the specific case when the both fundamental and third harmonics were detected without any indications on presence of the second harmonic, while Pascoe et al. (2017a) found three first harmonics. Detection of two harmonics simultaneously is a useful tool for MHD diagnostics (Inglis and Nakariakov, 2009).

More about this mode is written in the review by Nakariakov et al. in this volume.

– **Torsional Alfven mode – mechanism [3].**

The period of the global torsional mode in a coronal loop is $P_{tors} = 2L/jC_{A0}$. In the linear regime, the torsional Alfvén wave does not perturb the density of a flux tube and so is an unlikely candidate to modulate emission as seen in QPPs. Their direct detection is instead based on asymmetric variations in Doppler shifts across the oscillating structure (Kohutova et al., 2020). On the other hand, the torsional Alfvén wave could modulate emission by periodic variations of the angle between the line of sight and the local magnetic field direction. However, the observed coherency of QPPs is not consistent with a non-collective nature of torsional Alfvén waves and the effect of phase mixing.

– **Slow magnetoacoustic mode – mechanism [4].**

The period of the global slow magnetoacoustic (or longitudinal) mode trapped into the magnetic loop is $P_{slow} = 2L/jC_{slow}$. In general case, depending on plasma parameters, its phase speed, C_{slow}, vary between the internal tube speed (or cusp speed) $C_{T0} = C_{s0}C_{A0}/\sqrt{C_{s0}^2 + C_{A0}^2}$ and the internal sound speed C_{s0}: $C_{T0} < C_{slow} < C_{s0}$. In the long-wavelength limit, $C_{slow} = C_{T0}$. In zero β approximation, $C_{slow} = C_{s0}$. Typical periods of the slow mode are from a few to a few tens of minutes. The slow mode is compressible, so, it modulates the plasma density inside a loop making the slow mode pronounced in the thermal emission. In the specific case, when the plasma density in a coronal loop is high while the magnetic field is relatively low, the modulation of intensity of the non-thermal gyrosynchrotron emission of mildly relativistic electrons by slow waves is possible at radio frequencies $f \leq f_R$, where $f_R \propto n_0/B$ is Razin frequency, n_0 is a number density of the thermal plasma inside the loop (Nakariakov and Melnikov, 2006). On the other hand, the accelerated electrons experience Coulomb collisions with thermal plasma usually producing weaker non-thermal bremsstrahlung hard X-ray emission in the coronal part of the flare loop (thin target) and stronger non-thermal hard X-ray emission in the loop's footpoints (thick-target). Slow waves, modulating the plasma density in the loop, could modulate the collision process resulting in QPPs in X-ray light curves. Intuitively, the amplitude of such QPPs is

expected to be low. However, as far as we know, there were no detailed simulations performed of this process yet.

A trigger of a slow wave could be a local perturbation of either density or temperature. For example, it could be evaporation of dense chromospheric plasma heated by a beam of energetic particles accelerated in the energy release site, including flares and microflares. Reale et al. (2019) found that large-amplitude QPPs within coronal loops could be efficiently driven by impulsive heating at the footpoint. A heating pulse generates a strong pressure imbalance, which could travel along a confined coronal loop and bounce back and forth as slow mode magnetoacoustic wave, the modulation depth could reach over 20% of the emission intensity of the coronal loop. An interplay between the coronal heating and cooling processes was shown to be a new natural mechanism for formation of quasi-periodicity in initially broadband slow magnetoacoustic waves, resulting into the development of quasi-periodic slow wave trains (Zavershinskii et al., 2019, see also discussion of the acoustic thermal overstability in Section 2.4.3). Kupriyanova et al. (2019) found correspondence between the Moreton wave and initiation of the QPPs in thermal and non-thermal emissions. Passing through the arcade, the Moreton wave increased the plasma density in the two footpoints simultaneously and, thereby, triggered the second harmonic of the slow wave, pronounced as QPPs with the characteristic period around 80 s in the X-ray (3-25 keV) and microwave (15.7 GHz) emissions. Moreover, QPPs with the same period are found in the time profiles of both the temperature and emission measure oscillating in the antiphase.

The periodic behavior of slow-mode magnetoacoustic waves is usually observed as a harmonic decaying QPP pattern during a solar flare (see e.g. Reznikova and Shibasaki (2011); Kim et al. (2012); Kolotkov et al. (2018c) for a few case studies, and Nakariakov et al. (2019a) for the most recent review). The damping of slow modes is defined mainly by the thermal conductivity along the magnetic field, or loop axis, with the conductive damping time depending on the loop temperature. The wave-induced perturbation of the thermal equilibrium of the coronal plasma was recently found to be of equal importance leading to the enhanced damping of slow waves, consistent with observations (Kolotkov et al., 2019). Cho et al. (2016) revealed a linear proportionality between the damping time and oscillation period of QPPs in solar flares, associated with the effect of slow-mode waves. Moreover, this relationship was demonstrated to hold true also for stellar flares (see Section 3.6). The slow mode could form a standing wave and modulate the plasma density and temperature, consistent with observations by SUMER (Wang, 2011; Nakariakov et al., 2019b) and synthetic results (Yuan et al., 2015). Alternatively it could form a reflective propagating wave, also known as "sloshing" oscillations (Reale, 2016); this scenario has been observed by (Kumar et al., 2015; Mandal et al., 2016) and reproduced by MHD simulations (Fang et al., 2015). In the case of QPPs modulated by slow-mode waves, it would be very unlikely to be observed in relatively cool ($\simeq 0.5-2$ MK) coronal loops, as the propagation speed is determined by the plasma temperature. Low-speed slow waves, e.g. $C_{slow} < 100$ km s^{-1}, are very unlikely to survive and transform into standing modes within a coronal loop of the 100 Mm scale. However, this phenomenon could happen in cooler ($\simeq 0.05-0.5$ MK) but much shorter chromospheric loops (Huang, 2018), in this case, we would observe short-period QPPs after small-scale explosive events.

In a low-β plasma, the propagation speed of slow magnetoacoustic mode is directed within a narrow angle to the guiding magnetic field. The slow wave excited

somehow in the corona and propagating down the magnetic arcade can be reflected at the footpoints due to strong plasma density inhomogeneity between the corona and the chromosphere. The reflected wave rises up the arcade at a slight angle to the field, and thus the wave front slowly drifts across the field. Due to this peculiarity, the slow mode could trigger successive episodes of magnetic reconnection in the current sheet above the arcade in two-ribbon flares (Nakariakov and Zimovets, 2011) (see mechanism [7]). Such the process could appear as quasi-periodic pulses of non-thermal radiation, the sources of which move along the flare ribbons and the PIL.

More about this mode is written in the review by Wang et al. in this volume.

– **Equivalent RLC circuit – mechanism [5].**

This model is based on a non-negligible electric conductivity across the field in the lower layers of the solar atmosphere due to which a current-carrying coronal loop could be modelled as a part of a closed electric contour with the effective resistance (R_l), inductance (L_l), and capacitance (C_l) (Zaitsev et al., 1998). In the linear regime, period of oscillations of the electric current in such a current-carrying coronal loop is $P_{\rm RLC} = (2\pi/c)\sqrt{L_l C_l (I_0)} \simeq 10 \times S_{[17]}/I_{0[11]}$ [s], which for practical purposes was re-written in terms of the loop cross-section $S_{[17]}$ measured in 10^{17} cm^2 and the equilibrium electric current $I_{0[11]}$ carried by the loop and measured in 10^{11} A (Zaitsev and Stepanov, 2008), and where c is the speed of light. For typical combinations of the coronal loop parameters, the oscillation period $P_{\rm RLC}$ ranges from a fraction of a second to several tens of minutes. However, the model assumes an instantaneous variation of the electric current in the entire oscillating system, neglecting the finite propagation time of the current perturbation along the loop. The latter is defined by the Alfvén transit time along the loop which is about a few minutes, hence the model adequately describes the oscillatory processes with time scales longer than that.

The damping of oscillations in this model is determined by the effective resistance coefficient R_l, connected with the ion-neutral collisions in the photosphere and also affected by the photospheric convection inducing the electromotive force. The latter suppresses the effective damping coefficient, so that for typical flaring conditions, the damping time caused by this effective photospheric resistance was found to be much longer than the oscillation period, suggesting the interpretation for short-period QPPs with distinctly high oscillation quality-factors, observed, for example, in sub-THz solar radio bursts (e.g. Kaufmann et al., 2009).

The discussed oscillations of the electric current in the loop may cause direct modulation of both thermal emission, e.g. via variations of the plasma temperature by Ohmic heating, and of non-thermal emission, e.g. via periodic acceleration/deceleration of charged particles. The most plausible conditions for the acceleration would be near the loop apex, where the Dreicer electric field is minimised. As a secondary effect, due to the interaction with the ambient magnetic field, oscillatory variations of the electric current in the loop may induce its horizontally- or vertically-polarised transverse oscillations (e.g. Kolotkov et al., 2016c, 2018b; Zaitsev and Stepanov, 2018). The latter would be seen as periodic variations in Doppler shift observations or in EUV imaging observations, similarly to kink oscillations of the loop. This effect may also be visible in the microwave emission associated with the gyrosynchrotron mechanism, which is known to be sensitive

to the angle between the line-of-sight and the local magnetic field. We also note, that the RLC mechanism can readily explain the variation of the QPP oscillation period with time. Indeed, a gradual decrease in the equilibrium electric current I_0 would cause increase in the oscillation period $P_{\rm RLC}$, observed, for example in the time derivative of the soft X-ray flare emissions (Dennis et al., 2017; Kolotkov et al., 2018c).

In multi-loop magnetic structures, e.g. coronal loop bundles or arcades, according to this mechanism each individual loop would experience oscillatory variations of the electric current with its own oscillation period, $P^i_{\rm RLC}$, prescribed by the loop parameters, unless there is a crosstalk between the oscillating loops, allowing for synchronization of oscillations. Such a crosstalk could be sustained through the effects of electromagnetic inductive interaction of coronal magnetic loops (Khodachenko et al., 2009). In this case, one would observe coherent oscillations of the entire loop arcade or at least its segment.

Below, we overview the most recent applications of the equivalent RLC circuit model of current-carrying coronal loops to observations of solar flare QPPs. A comprehensive review of the earlier applications of the model for the interpretation of the observed oscillatory phenomena in coronal loops and in the related radiation, including the case studies of low-frequency modulations of the microwave radiation during solar flares (Khodachenko et al., 2005), was performed by Khodachenko et al. (2009).

More recently, Hudson (2020) considered the inductive storage as a generic parameter with magnetic free energy in the corona in the flare toy model, in the context of correlation between the waiting times and magnitudes of solar flares observed by GOES/SXR. Another recent series of works by Sharykin et al. (2018, 2020) and Zimovets et al. (2020), presenting a direct observational evidence of the relationship between the time evolution of the photospheric vertical electric currents with soft and hard X-ray solar flare fluxes, demonstrated an important (but not yet clear) role of longitudinal currents in the processes of flare energy release and associated plasma heating and acceleration of charged particles. Li et al. (2020a,b) employed the RLC model for the interpretation of several-minute pre-flare QPPs seen in multi-instrumental observations by GOES/SXR, SDO/AIA, NoRH, and NVST.

More specifically, Li et al. (2020b) studied a QPP event simultaneously detected in both EUV images and microwave emission before a C1.1 flare on 2016 March 23. The authors first found a low-amplitude transverse oscillation with growing periods in the EUV coronal loop at AIA 171 Å, the oscillation period was estimated to be ≈ 397 s with a slowly growth rate of 0.045. Then they detected a small-scale QPPs with growing periods in the microwave flux at NORH 17 GHz, increasing from ≈ 300 s to ≈ 500 s. The growing periods could be explained by the modulation of RLC-circuit oscillating process in a current-carrying plasma loop. Likewise, a few-minute QPP in the simultaneous microwave observations of a solar flare by MUSER and NoRH, and in the UV and EUV wavebands by SDO/AIA before and during the flare was associated with the RLC model (Chen et al., 2019) (see also about these observations in the discussion of the mechanism [9] in Section 2.4.3). Tan et al. (2016) detected that at least one-third of all analysed isolated solar flares observed by GOES/SXR in the solar cycle 24 exhibit long-period QPPs with periods of 8-30 min before the flare onset, and connected them to the periodic modulation of the magnetic energy accumulation by oscillations of the electric

current in the loop system, caused by the RLC mechanism. High-quality and short-period (about a few seconds and shorter) QPPs in radio observations of solar flares were successfully interpreted by the model of a current-carrying loop as an equivalent electric RLC circuit (see e.g. Zaitsev et al., 2014). In Tan and Tan (2012), the model was used as a possible candidate for the interpretation of the very short period QPPs consisting of millisecond timescale superfine structures in the microwave flare emission observed by SBRS/Huairou. By applying the RLC model to the observed QPPs, the longitudinal electric current in the loop was seismologically estimated to be about 2×10^{12} A. However, this estimation would benefit from taking the finite propagation time of the electric current perturbation along the loop into account, as discussed above.

– **Dispersive wave trains – mechanism [13].**

The dispersive evolution of fast MHD waves was described by Roberts et al. (1984) as a mechanism for producing quasi-periodic wave trains from an impulsive perturbation (see also the review by Li et al. in this volume). Different frequencies propagate with different speeds along a wave-guiding structure such that the signal measured some distance away from the initial perturbation can exhibit significant period and amplitude modulation. Efficient generation of quasi-periodic wave trains by dispersive evolution depends on the spatial (e.g. Nakariakov et al., 2005) and temporal (Goddard et al., 2019) localisation of the driving perturbation. Aside from this, the dispersive behaviour is a robust feature of fast MHD waves in wave-guiding structures with a characteristic transverse scale. For example, it has also been demonstrated in numerical simulations of current sheets (Jelínek and Karlický, 2012; Jelínek et al., 2012), curved coronal loops (Nisticò et al., 2014), magnetic funnels (Pascoe et al., 2013b), coronal holes (Pascoe et al., 2014), and for a range of loop density profiles (e.g. Yu et al., 2017). Dispersion also has the effect of inhibiting steepening for large amplitude wave trains inside waveguides, but leaky components can also form quasi-periodic wave trains outside of structures which can experience steepening (Pascoe et al., 2017b), which may account for quasi-periodic radio bursts associated with a fast wave train (Goddard et al., 2016b; Kolotkov et al., 2018a). It can be convenient to use wavelet analysis to visualise the signal for a fast wave train, which reveals a characteristic 'tadpole' signature (Nakariakov et al., 2004). This tadpole signature has been detected by observations made with the *Solar Eclipse Coronal Imaging System* (SECIS; Katsiyannis et al., 2003) and in radio fiber bursts (Karlický et al., 2013). Quasi-periodic wave trains have also been observed using SDO/AIA (e.g. Shen and Liu, 2012; Yuan et al., 2013; Nisticò et al., 2014).

2.4.2 Group (ii): modulation of the efficiency of energy release processes by MHD oscillations

– **Reconnection triggered quasi-periodically by external MHD waves – mechanism [6].**

In Section 2.4.1, the flare is typically considered as an impulsive, forcing term. However, MHD waves can trigger, or back-react on, the flaring process itself. If this trigger/driver mechanism is itself periodic, then the periodicity of the reconnection is determined by the period of the driver. Chen and Priest (2006), Nakariakov

et al. (2006) and Jelínek and Karlický (2019) are examples of such a phenomenon, where reconnection is 'induced' or 'forced' periodically and the periodicity is dictated/transferred from the trigger mechanism. Both fast and slow magnetoacoustic waves can act as periodic triggers, or periodic inducers, of magnetic reconnection (e.g., Meszarosova and Gomory, 2020). A non-periodic external driver (e.g., external pulse) may also trigger the forced reconnection in the current sheets apart from the periodic wave activity (e.g., Srivastava et al., 2019).

Nakariakov et al. (2006) postulated this initial wave driver could come from an oscillating coronal loop outside, but close to, the flaring arcade, and that an external evanescent part of the oscillation could reach the null point in the arcade. Here, the period is determined by the period of the oscillating external loop, which is determined by the kink oscillation period (compare to mechanism [2]). The key to this mechanism is the interaction of a fast magnetoacoustic wave with a null point. As fast waves approach null points, they refract and concentrate into the vicinity of the null, ultimately accumulating at the null itself (see McLaughlin and Hood, 2004; McLaughlin et al., 2011; Thurgood and McLaughlin, 2012, for details). This leads to an (exponential) increase of the electric current density near the null point and these current variations can, in turn, induce current-driven plasma micro-instabilities which are known to cause anomalous resistivity.

It is worth noting here that we are not aware of direct observational studies in which it is unambiguously shown that an oscillating coronal loop causes QPPs with the same period in a nearby flare region. The opposite situation is usually observed – a solar flare and the associated low-coronal eruption excite kink oscillations of the surrounding coronal loops (e.g. Zimovets and Nakariakov, 2015, see also the review by Nakariakov et al. in this volume for more details). An indirect observation that could be explained by the mechanism in question was presented by Foullon et al. (2005). It was shown there that long-period QPPs with a period of 8-12 min, detected by RHESSI in the X-ray range from compact flare loops, can be initiated by the kink oscillations of a nearby long transequatorial loop. However, in contrast to (Nakariakov et al., 2006), the authors assumed that this transequatorial loop causes quasi-periodic variations of the magnetic field in the compact loops and, as a consequence, modulation of electron acceleration in them due to the effect of magnetic pumping (betatron effect). At the same time, the temporal and spatial resolution of the available instruments was not sufficient to resolve the possible kink oscillations of the transequatorial loop.

Another example of an indirect support of this mechanism is presented in the work by Zhang et al. (2016). Using multiwavelength observations from SDO/AIA, GOES, and IRIS, the authors studied the C3.1 circular-ribbon flare in the AR 12434 on 2015 October 16. During the impulsive phase of the flare, the circular ribbon in Si IV shows Doppler redshift, indicating a downflow or chromospheric condensation at the peak speeds of $45 - 52$ km s^{-1}. The downflow speeds are found to be positively correlated with the logarithm of the Si IV line intensity and time derivative of the soft X-ray flux in the GOES $1 - 8$ Å channel. The Si IV line intensity and the derivative of the soft X-ray flux show QPPs with periods of $32 - 42$ s, which are probably caused by episodic null-point magnetic reconnections modulated by the fast-mode wave propagating along the fan surface loops at phase speed of ~ 1000 km s^{-1}. Quasi-periodic accelerations and precipitations of the non-thermal electrons in the chromosphere generate quasi-periodic heating observed in the UV and soft X-ray wavelengths.

Chen and Priest (2006) conducted MHD simulations of transition-region explosive events (TREEs) driven by five-minute, solar p-mode oscillations that were driven at the photospheric base. This led to periodically-triggered reconnection, induced by slow magnetoacoustic waves (compare to mechanism [4]). Specifically, density variations in the vicinity of the reconnection site result in a periodic variation in the electron drift speed, which switches on/off anomalous resistivity.

A possible manifestation of the discussed mechanism is a connection between three-minute oscillations and QPPs observed in some solar flares. For example, Sych et al. (2009), based on the analysis of spatially resolved radio observations by NoRH at 17 GHz in two flares in the same AR 10756, found an increase in the power of three-minute oscillations in a sunspot before the flares. It was found that the light curves of the radio emission from the flare sites also contain QPPs with a period of 3 min. The authors argued that three-minute slow magnetoacoustic waves emanating from the sunspot can serve as a trigger of quasi-periodic energy releases in the flare site observed in the form of the microwave QPPs.

More recently, Kumar et al. (2016) detected QPPs with the period of about 3 min in an M1.9 flare with a quasi-circular ribbon on 2011 September 23-24. The pulsations occurred simultaneously (with no noticeable delay) in hard X-rays ($12 - 100$ keV) and microwaves ($2 - 17$ GHz). At the metric and decimetric radio wavelengths ($25 - 610$ MHz), repetitive type III bursts were detected too, which occurred simultaneously with the emission peaks in the hard X-ray and microwave emissions. This event seems to be an example of quasi-periodic magnetic reconnection with bidirectional (upward and downward) electron beams which produced emission in open (type III bursts) and closed (hard X-rays and microwaves) magnetic structures, respectively. The QPPs were also found to correlate with three-minute oscillations in a nearby sunspot, and hence the magnetic reconnection and particle acceleration was likely triggered quasi-periodically by slow-mode waves leaking from the sunspot.

It is worth noting here that not only five- and three-minute oscillations can affect the process of flare energy release, leading to QPPs, but disturbances of different layers of the solar atmosphere caused by flares can also affect the properties of these oscillations detected in various wavelength ranges (e.g. see Milligan et al., 2017; Chelpanov and Kobanov, 2018; Kobanov and Chelpanov, 2019). It is not excluded that the perturbations caused by the initial energy release of a flare can enhance these oscillations, which in turn could trigger further quasi-periodic energy releases in the flare region causing QPPs in different spectral ranges.

– **Autowave processes – mechanism [7].**

In the context of solar flares, autowave processes mean such processes when a disturbance (e.g., in the form of a magnetoacoustic wave) from one source of energy release is transmitted through the plasma of the solar atmosphere and is a trigger for energy release in another source, which in turn triggers a new disturbance, etc. In the Sun, an example of such an auto-wave process is a series of sympathetic flares. Illustrative examples from daily life are the effect of falling dominoes, the movement of a fire front in a dry forest or grass field, the spread of epidemics, etc.

We know of two models of solar flares that assume the presence of some autowave processes (Emslie, 1981; Nakariakov and Zimovets, 2011). Their development was motivated by the presence of sequential bursts of non-thermal radiation in the impulsive phase of many flares (often in the form of QPPs) and by signs

of sequential ignition of flare loops in magnetic arcades lined up along the magnetic polarity inversion line (PIL). These features include sequential brightening of arcade loops in the soft X-ray or EUV ranges (Vorpahl, 1976; Reva et al., 2015), expansion of flare ribbons along the PIL (Qiu et al., 2010), and the apparent movement of flare non-thermal hard X-ray (Bogachev et al., 2005; Grigis and Benz, 2005; Zimovets and Struminsky, 2009; Kuznetsov et al., 2016) and microwave (Kuznetsov et al., 2017) sources along the PIL.

The first such model – an interacting loop model – was proposed by Emslie (1981). This is a simple analytical model. According to this model, the initial energy release in one of the loops of the bipolar magnetic arcade leads to the acceleration of charged particles, chromospheric evaporation, and the filling of the loop with hot plasma, as a result of which the loop undergoes lateral expansion. Due to expansion, the poloidal component of the field of this loop (around the longitudinal axis) interacts with the oppositely directed poloidal component of the field of the neighboring loop in the magnetic arcade, which leads to magnetic reconnection, particle acceleration and heating of the plasma in the second loop, and the process continues until the edge of the arcade is reached. The period of QPPs is defined as the ratio of the characteristic distance between the neighboring flaring loops, D, and the speed of lateral expansion, v: $P \simeq D/v$. Emslie (1981) took this speed to be equal to the ion sound speed, which is approximately equal to the Alfvén speed in the coronal part of the loop at comparable values of gas and magnetic pressures ($\beta \sim 1$). At characteristic distances between loops $D \simeq 500 - 5000$ km and Alfvén velocities $v \simeq 500-2500$ km s^{-1}, the values of the QPP periods are in the range $P \simeq 0.2-10$ s. The model assumes: (a) the initial inhomogeneity of the magnetic arcade along the PIL in the form of dividing the arcade into separate loops, (b) a trigger for energy release in one of the arcade loops, (c) the presence of large-scale toroidal (longitudinal) currents in the arcade loops, providing the presence of a poloidal magnetic component. While these assumptions look quite realistic, this model does not fit some observations. First, there are observations showing that there are gaps with low EUV luminosity between flaring loops of a magnetic arcade (e.g. Reva et al., 2015). Second, within the framework of this model it is difficult to explain QPPs with longer periods ($P \gtrsim 10$ s). Third, it was found that the characteristic velocity of the trigger of energy release along the PIL is usually tens of km s^{-1} (e.g. Kuznetsov et al., 2016), which is less than the characteristic ion sound and Alfvén velocities in coronal loops.

To explain QPPs with greater periods $P \gtrsim 10$ s and the characteristic spread of the flare energy release process in a magnetic arcade along the PIL with velocities less than the sound speed ($v \simeq 10 - 100$ km s^{-1}), Nakariakov and Zimovets (2011) proposed a model based on the autowave process where the energy release is triggered by slow magnetoacoustic waves. It is suggested that there is a magnetic X-line or a current sheet above a magnetic arcade, like in the "standard" flare model. An initial energy release in one part of a current sheet (or in one loop) produces disturbances which spread as the slow magnetoacoustic waves propagate obliquely to the magnetic field. It is shown that the perpendicular group speed reaching maximum of $\approx 10 - 20\%$ of the sound speed for the propagation angles $\alpha \approx 25^\circ - 28^\circ$ to the magnetic field. The waves reflect from the loop footpoints (see the 2D ideal MHD simulation of this model performed by Gruszecki and Nakariakov, 2011) and reach the current sheet above the magnetic arcade in another place. There, they can trigger magnetic reconnection by variation of the plasma

density, which can result in some instabilities and hence anomalous resistivity (similar to mechanism [6]). This episode of energy release generates another slow magnetoacoustic disturbance, and the process continues until reaching the edge of the magnetic arcade and current sheet.

Each episode of reconnection and energy release can be accompanied by the acceleration of charged particles and a burst of non-thermal emissions. Due to the chromospheric evaporation, each episode can also produce a burst of thermal soft X-ray and EUV emissions. The sequence of bursts can be in the form of QPPs with a period $P \simeq 2H/v_s \cos\alpha$, where H is a distance from the loop footpoints to an X-point in the current sheet, v_s is the sound speed in the undisturbed pre-flare magnetic arcade, i.e. before the energy release and plasma heating ($T \approx 1-3\times10^6$ K, $v_s \approx 166-288$ km s^{-1}). In the case of a low-lying current sheet and X-point, we can put $H \approx L/2$, where L is the characteristic length of the loop of the magnetic arcade. By the time-of-flight analysis Aschwanden et al. (1996) showed that $H = (1.4 \pm 0.3)L/2$. However, the X-point could be located much higher in the case of a highly stretched current sheet (e.g. Reid et al., 2011). In this case $H > L/2$. For the estimates, we assume that $H \approx (0.5-5.0)L$ and that $L \approx (1-5)\times10^4$ km. Thus, the model predicts the QPP periods in the range $P \approx 40-3420$ s, which is consistent with many observations. An advantage of this model is its ability to explain the sometimes observed double-peak QPPs (e.g. Nakajima et al., 1983; Zimovets and Struminsky, 2009). For this, one needs to assume that the initial energy release and the region of generation of slow waves are located not in the middle of the magnetic loop, but on the side. In this case, the waves propagating in different legs of the loop take different times to reach X-points and they trigger energy release at different times, which result in double-peak pulsations.

This model was tested by Inglis and Dennis (2012) based on the analysis of RHESSI observations of the hard X-ray source dynamics in three powerful solar flares with QPP periods in the ranges 30-80, 50-200 and 100-250 s. It was found that the model does not agree with observations, namely, the model predicts a longer period of pulsations and a larger distance between hard X-ray sources of neighboring pulsations. However, the authors noted that they considered only the propagation of slow waves with maximum group velocity at an angle of $\approx 25^\circ-28^\circ$ to the magnetic field. It is not yet known whether the energy of the fastest (along the PIL) waves is really enough to trigger the energy release process. The possibility is not excluded that the trigger is wave packets propagating at smaller angles to the field, which will result in smaller distances between positions of emission sources of neighboring pulsations. To answer this question, it is necessary to carry out more advanced, 3D MHD simulations of a system with a current sheet above the magnetic arcade. Acceleration, propagation and emission of charged particles should be also modeled. Inglis and Dennis (2012) also pointed out that the model additionally needs to be checked on other flares, in particular, with larger QPP periods and with slower apparent displacements of the flare sources along the PIL, or vice versa.

– **Flapping oscillations – mechanism [8].**

Low-frequency oscillations of the magnetic field and plasma pressure with frequencies of $\sim 10^{-4}-10^{-1}$ Hz are often observed in the Earth's magnetotail before

and during magnetic substorms. One of the most discussed types is the flapping oscillations (see e.g. Nakariakov et al., 2016b). Erkaev et al. (2007, 2009) developed a double-gradient mechanism to explain these oscillations in the magnetotail. Artemyev and Zimovets (2012) suggested that a similar mechanism may also work in current sheets in flare regions on the Sun. They considered the problem of finding unstable symmetric (sausage) wave modes propagating along a two-dimensional vertical current sheet (along the PIL). Additionally, the influence of the presence of a magnetic shear and Coulomb collisions is considered. The linear MHD equations are solved analytically. It is shown that unstable modes with periods in a wide range $P \sim 10^{-1} - 10^{3}$ s and with wavelengths $\lambda \sim 10^{2} - 10^{7}$ km (along the PIL) can develop under the characteristic physical conditions in the solar corona. Based on the results obtained, the authors proposed a scenario that can naturally explain both the QPPs of non-thermal hard X-ray and microwave radiation and the apparent parallel motion of their sources along the PIL observed in some two-ribbon solar flares (see discussions of the mechanisms [7] and [15]). The idea is that symmetric modes lead to local thinnings of the current sheet, which cause local increases in the current density due to the conservation of the magnetic flux. Upon reaching the threshold values of the current density, this process can be responsible for the intensification of the tearing instability and magnetic reconnection. In turn, this can lead to more efficient energy release and particle acceleration in the regions of the current sheet compression. The beams of accelerated electrons injected in the corresponding loops will lead to local episodes of chromospheric evaporation and increased brightness of these loops in soft X-rays and EUV. Moreover, this mechanism can be used to explain the presence of two components of hard X-ray emission, which are distinguished in the light curves of some flares: 1) a slowly varying component, and 2) a fine structure of peaks against the background of a slowly varying component (e.g. Aschwanden, 2002). The first component can be interpreted as a result of modulation of the energy release and acceleration of electrons along the current sheet due to the considered oscillation modes; the second one, due to the bursty reconnection in the corresponding sections of the current sheet.

The proposed scenario is schematic. The authors did not simulate the development of unstable modes in realistic three-dimensional current sheets, or the acceleration of particles and the radiation generated by them in different spectral ranges. According to its observational features, this mechanism can be similar to the autowave process with successive episodes of energy release triggered by the slow magnetoacoustic waves (mechanism [7]) and to the mechanism [15] based on the thermal instability of the current sheet. To determine which of these mechanisms is responsible for QPPs in solar flare (or whether they present at all), first, more detailed modeling taking into account the acceleration of particles and their emissions, and, second, more detail comparison of the simulation results with the observations, are required.

– **Magnetic tuning fork model – mechanism [12].**

This model was proposed by Takasao and Shibata (2016), based on the 2D MHD simulation with high spatial resolution originally developed in (Takasao et al., 2015). The model includes essential physics for solar flares such as magnetic reconnection, heat conduction and chromospheric evaporation, however, it does

not implement directly the acceleration of non-thermal particles. The vertical current sheet is considered, where magnetic reconnection is triggered by the localized resistivity fixed in time and space to achieve a fast and quasi-steady reconnection with a single X-point. Due to the reconnection, magnetic energy is converted into the mechanical energy of the Alfvenic outflow. The plasma is heated by the slow mode MHD shocks. The heated plasma flows down along the reconnected magnetic field lines and form a magnetic loop structure, which later is filled with the hot and dense plasma evaporated from the chromosphere. This loop structure could be observed as the flare loops in the soft X-ray and EUV wavebands. A complex structure of fast mode MHD shocks is formed in the above-the-loop-top region due to the pile-up of reconnected magnetic fields and termination of plasma outflow there. The shock system has a V-shape composed of two oblique fast shocks, and from time-to-time another horizontal fast shock appears between them. Magnetic field lines in the above-the-loop-top region form an M-shape structure (with a characteristic vertical size w), which is called as a magnetic tuning fork. The gradient of the dynamic pressure by the backflow (with the characteristic speed v_{bf}) pushes the magnetic arms outward and compress their magnetic field. When magnetic pressure overcomes the backflow, the magnetic arms start to move back. This produces inward-propagating fast waves. These waves decelerate the backflow, however, it recovers quickly because of the constancy of the reconnection outflow speed. The same process repeats and oscillations are maintained. The distance between two arms of the magnetic fork changes quasi-periodically. The quasi-periodic termination of the outward motion of the arms causes quasi-periodic outward propagating fast waves. They could be observed as the quasi-periodic propagating fast-mode magnetoacoustic waves (QPFs) with characteristic periods from a few tens to a few hundred seconds (Liu et al., 2011; Yuan et al., 2013, see also the review by Liu et al. in this volume for more details).

The period of the magnetic tuning fork oscillations is estimated as $P_{MF} \propto w/v_{bf} \propto \beta^{15/14} L^{9/7} \propto B^{-2.1}$, where β is the plasma beta (ratio of the gas to magnetic pressure), L is the characteristic linear size of the system (i.e. the magnetic loop length), and B is the characteristic magnetic field induction in the magnetic fork. Thus, there is a strong dependency of the oscillation period on the magnetic field in the above-the-loop-top region. It is difficult to test this dependency at present due to difficulties with magnetic field measurement in the corona. However, there is hope that soon it will be possible (e.g. Fleishman et al., 2020).

It is important to note that the source of oscillations and waves is very compact, less than 10% of the size of the magnetic loop system, i.e. $w \ll L$, and is suited in the above-the-loop-top region. This circumstance can also be used to verify the model in the future. For example, in another model proposed by Ofman et al. (2011), the oscillation source of QPFs is located in the foots of the flare magnetic structure.

The magnetic fork model also predicts quasi-periodic changes of parameters of the termination shocks (e.g. the ratio of the pressure ahead and behind the oblique fast shocks). Since the termination shocks in the above-the-loop-top region are considered as one of possible accelerators of charged particles in flares (e.g. Tsuneta and Naito, 1998; Chen et al., 2015a; Kong et al., 2019), the found oscillations of these shocks can quasi-periodically modulate efficiency of particle acceleration and cause QPPs of non-thermal emissions. The thermal emission could be also modulated quasi-periodically due to quasi-periodic plasma heating by non-thermal

particles in flare loops. An important observational property of the model is the presence of simultaneous QPFs and QPPs with close periods P_{MF}.

In conclusion, we note that the discussed magnetic tuning fork model is still two-dimensional and does not take into account the processes of particle acceleration. Also, no forward modeling of emission from the flare region has been done. For a more accurate comparison of the model with observations, a significant development of the model is required.

At the moment, we are not aware of direct observations that unequivocally confirm the operation of this mechanism in solar flares. However, it is possible that some observations of QPPs in flares, which are interpreted by other mechanisms (for example, self-oscillatory processes [9], see Section 2.4.3), could be the result of this mechanism. For example, one can note the work of Liu et al. (2011), in which QPPs of the UV (SDO/AIA) and X-ray (RHESSI) emissions from a flare and QFPs (observed by SDO/AIA in the EUV channels) with a period of about 3 min were simultaneously observed. But these observations can also be interpreted by the mechanism [6] – reconnection triggered quasi-periodically by three-minute magnetoacoustic waves coming from the lower layers of the solar atmosphere. We can also note the observations of hard X-ray QPPs with periods in the ranges $P = 10-60$ s and $P > 120$ s from the tops of the flare loops (Jakimiec and Tomczak, 2010, 2012, 2013). However, the authors of these works interpreted the observations with the phenomenological model of oscillating magnetic traps, according to which the acceleration (Fermi and betatron) and injection of electrons are modulated by kink mode oscillations (see mechanism [2]) of collapsing magnetic traps formed by reconnected field lines in the cusp region.

– **KHI in loop-top – mechanism [14].**

The 2.5D numerical MHD simulation performed by Ruan et al. (2019) predicts the following main observational features of the mechanism under consideration: 1) QPPs can be observed in the integral flux of thermal soft X-ray radiation, although the source of the QPPs itself is localized in a tiny region at the top of the flare loop with size $l \ll L$, where L is the loop length; 2) QPPs are observed simultaneously and in-phase (i.e. without perceptible delays) in the soft X-ray flux, density and temperature of the plasma in the local source; 3) QPPs are not detected in non-thermal hard X-rays; 4) QPP period is estimated as $P = 2l/v_p$, where v_p is the local fast magnetoacoustic wave speed, which can be significantly higher than the local Alfven speed; with characteristic parameters at the top of the flare loop ($l \sim 10^3 - 10^4$ km and $v_p \sim 10^2 - 10^3$ km s^{-1}), the QPP period can take values from a second to hundred of seconds (note that Ruan et al. (2019) found $P \approx 26$ s in their simulation run); 5) QPPs in soft X-rays begin a few minutes after the peak of hard X-rays, which is associated with the time it takes for the evaporating chromospheric plasma to reach the top of the loop and develop the KHI instability.

It should be noted that the discussed model is 2.5-dimensional. In reality, deviations from the considered features may be observed. It is necessary to develop this model for the 3D case and realistic acceleration and ejection of charged particles (see the simulation by Ruan et al., 2020, where, however, the question of the origin of QPPs was not investigated). It would also be useful to investigate the observational manifestations of this model in different ranges of EUV and radio emissions to make more informative comparison with observations.

At the moment, we are not familiar with observational studies in which most of the observational features of this model (see Section 2.4.2) would be found. Hypothetically, the model can be applied to a number of observations of soft X-ray pulsations with a period of less than ~ 100 s for flares for which there is no information on the spatial structure of the QPP sources and without accompanying QPPs of non-thermal hard X-ray radiation in the range above ≈ 25 keV (e.g. Inglis et al., 2016; Hayes et al., 2020).

– **Thermal instability of a current layer – mechanism [15].**

This model proposed by Ledentsov and Somov (2016, 2017) is already briefly described in the end of Section 2.3. Therefore, here we only give some of its possible observational manifestations. It should be noted that this is still a two-dimensional analytical MHD model. Its application to observations is still very limited. In particular, the model in its present form considers only a neutral current sheet. However, most probably, current sheets in solar flare regions contain a strong magnetic guide field along the PIL (e.g. Qiu et al., 2017; Sharykin et al., 2020). The solution was obtained in the linear approximation; the nonlinear growth of instability has not yet been investigated. Realistic numerical three-dimensional calculations, including acceleration of particles and radiation in different spectral ranges, also have not yet been carried out.

Nevertheless, the model predicts that as a result of thermal instability in the current sheet, regions of hot and cold plasma will alternate in it with a spatial scale λ along the PIL. Since the heated plasma flows out of the current sheet along the field lines, the flare magnetic arcade under the current sheet will consist of alternating hotter (brighter) and colder (dimmer) coronal loops. According to the rough estimates made by Ledentsov and Somov (2016), $\lambda \simeq 10$ Mm. This is in agreement with some observations of flare arcades in soft X-ray and EUV ranges (e.g. Vorpahl, 1976; Zimovets et al., 2013; Reva et al., 2015). If the thermal instability propagates in the form of a wave along the current and the PIL, then it can be a trigger for flare energy release episodes in separate parts of the current sheet with a step λ, which can lead to a sequence of "elementary flare bursts" or QPPs in different wavelength ranges, including hard X-rays and microwaves, if electrons are accelerated. It could also explain the elongation of flare ribbons and apparent motion of the hard X-ray sources during flares (similar to mechanisms [7] and [8]). Successive injections of beams of accelerated electrons in different loops can lead to successive episodes of chromospheric evaporation. In the case without effective acceleration of electrons, the flows of heated plasma in the regions of the reconnecting current sheet, where thermal instability is developed, can reach the loop footpoints and cause gentle chromospheric evaporation, which can lead to pulsations of soft X-ray and EUV radiation.

Although this was not done in Ledentsov and Somov (2016), the characteristic period of QPPs can be roughly estimated as $P \simeq P_1 + P_2$, where $P_1 \simeq \lambda/v_{fma}$ is the transit time of the fast magnetoacoustic wave of the distance λ, and $P_2 \simeq 1/\Gamma$ is the reciprocal of the instability growth rate Γ. For the case of ion thermal conductivity, Ledentsov and Somov (2016) estimated $\Gamma \simeq 1/\tau_r$, where $\tau_r = \gamma 2 k_B T_s/(\gamma-1) n_s L_r\,(T_s)$ is the characteristic radiation cooling time of plasma with density n_s and temperature T_s in the current sheet, γ is the adiabatic exponent, k_B is the Boltzmann constant, $L_r\,(T_s)$ is the radiative loss rate. For $\lambda \simeq 1-10$ Mm and $v_{fma} \simeq 500-2500$ km s^{-1}, $P_1 \simeq 0.4-20$ s. For $\gamma = 5/3$, $n_s \sim 10^{10}-10^{12}$

cm^{-3}, $T_s \sim 10^6 - 10^7$ K, $L_r \sim 10^{-23} - 10^{-22}$ erg s^{-1} cm^{-3} (e.g. Aschwanden, 2005), one can estimate $P_2 \simeq \tau_r \sim 10^1 - 10^4$ s. Thus the possible QPP period is in the broad range $P \sim 10^1 - 10^4$ s.

2.4.3 Group (iii): spontaneous quasi-periodic energy release (DC-to-AC models)

According to the Standard Model, flares have their origin in magnetic reconnection, taking place in a coronal current sheet and with the reconnection accelerating particles in both the upwards and downward directions. Flares are also a finite-duration phenomenon, and so we should be cautious about applying steady-state reconnection models to such scenarios, and instead we should consider time-dependent reconnection theory.

– Self-oscillatory processes – mechanism [9].

A key advantage of time-dependent reconnection models is a natural explanation of the simultaneity of QPPs in different bands – in other words, the time-varying rate of electron acceleration is all produced by the same source. A subset of time-dependent reconnection, relevant here, is periodic reconnection or repetitive spontaneous reconnection or oscillatory reconnection. These are self-oscillatory processes (e.g. in electronics, self-oscillations are associated with the conversion of direct current, DC, to alternating current, AC, of a certain frequency) and so they naturally produce periodic outputs from aperiodic drivers. As with most of the QPP models described here, the Oscillatory Reconnection models are still being explored (for full details see McLaughlin et al. 2009; Thurgood et al. 2017, 2018, 2019 and references therein) but quantitative progress has been made: McLaughlin et al. (2012a) quantified the periodic nature of oscillatory reconnection for a 2D simple X-point. Driving amplitudes of 6.3 – 126.2 km s^{-1} resulted in periods in the range 56.3 – 78.9 s, e.g. a driving amplitude of 25.2 km/s corresponds to a period of 69.0 s. The authors reported that the system acts akin to a damped harmonic oscillator; hence, the greater the initial driving amplitude, the stronger and longer the current sheets formed at each stage, thus the greater the restoring force, which leads to shorter periods.

McLaughlin et al. (2012b) investigated the periodic signals associated with magnetic flux emergence, namely the emergence of an initially-submerged, buoyant flux tube into a pre-existing stratified atmosphere permeated by a unipolar magnetic field (representing a coronal hole). As the buoyant flux tube emerges into the pre-existing atmosphere, it was found that a null point is generated naturally and a series of reconnection reversals take place as the system searches for equilibrium. In other words, the system demonstrates oscillatory reconnection in a self-consistent manner. Parametric studies reported varying the strength of the initially-submerged, buoyant flux tube, $\mathbf{B}_{\rm buoyant}$, results in a range of associated periodicities of 105 – 212.5 s for 2.6×10^3 G $\leq \mathbf{B}_{\rm buoyant} \leq 3.9 \times 10^3$ G, where the stronger the magnetic strength of the initial flux tube, the longer the oscillation period (same conclusion as McLaughlin et al. 2012a). Of note is that there are natural limitations placed on the periods generated in the flux emergence system. If the magnetic strength of the initially-submerged, buoyant flux tube is too high (for McLaughlin et al. 2012b, this was found experimentally to be $\mathbf{B}_{\rm buoyant} > 3.9 \times 10^3$ G) then plasmoids are ejected from the current sheet,

and these plasmoids change the properties of the X-point (primarily expelling magnetic flux with them). Hence, there is still oscillatory behaviour but this represents a fundamentally different regime of oscillatory reconnection than that of reconnection-without-plasmoids. Conversely, when the magnetic strength of the initially-submerged flux tube is less than the buoyancy instability criterion, we have 'failed emergence' (for McLaughlin et al. 2012b the buoyancy instability criterion was $\mathbf{B}_{\mathrm{buoyant}} < 2.6\times10^{3}$ G) and thus, by definition, no emergence and so no associated periodicity. However, lower and higher periods could have been generated by modifying the equilibrium parameters of the model, such as modifying the strength of the pre-existing magnetic field. However, we utilise the values reported by McLaughlin et al. (2012b) in Table 1, as opposed to saying all values are possible. It is interesting to note that flux-emergence-driven, Oscillatory Reconnection systems have a natural upper and lower bound on generated periodicities, and thus observations could be used as constraints in such an model.

Additionally, for the Oscillatory Reconnection mechanism, the oscillations are generated with an exponentially-decaying signature. Note that the decay is not due to a specific dissipative mechanism and/or radiative losses, but arises from the generation mechanism itself. This is intuitive: there is a finite injection of energy and so, physically, the resultant periodic behaviour must also be finite in duration. Note that this is simply a result of injecting a finite amount of energy into the Oscillatory Reconnection mechanism, and a self-oscillation may itself be decayless if there is a continuous extraction of energy from the medium. Finally, properties of self-oscillations (e.g. period, amplitude, shape of the signal) are determined by the parameters of the system that support them. In other words, and in contrast with regular oscillations, the properties of self-oscillations are independent of the initial conditions.

Of course, Oscillatory Reconnection is just one example of a time-dependent reconnection process. Oscillatory Reconnection is a relaxation process - it may not occur if the reconnection is being driven/forced - and a different regime of time-dependent reconnection occurs during magnetic flux rope eruption. Here, converging motions in the photosphere bring magnetic field lines of opposite polarities together and drive reconnection, leading to the formation of a magnetic flux rope, which rises (i.e. erupts) into the corona. In such models, a current sheet is formed, during the eruption, where one end of the current sheet connects to the flare loop top (the 'lower end' of the current sheet, if we consider moving radially outwards from the Sun) and also connects to the bottom of the (rising) flux rope (the 'upper end' of the current sheet). QPPs have been reported in models of magnetic flux rope eruption. Takahashi et al. (2017) perform 2D MHD simulations of magnetic flux rope eruptions and propose a mechanism for quasi-periodic oscillations related to magnetic reconnection, where QPPs take place during the time when magnetic reconnection peaks as the flux rope is rising rapidly. The authors investigated various values of the global Lundquist number, finding that for their low Lundquist number run, no oscillatory behaviour was found, and for high and moderate Lundquist number runs, reconnection jets collide with material at the flare loop top and flux rope bottom of the simulation, and form termination shocks. These structure becomes unstable and quasi-periodic oscillations of supersonic backflows appear at both locally-confined high-beta regions. In this sense, the oscillations at the flare loop top (the 'lower end' of the current sheet) may be similar to those in the Magnetic tuning fork model [12]. Takahashi et al. (2017)

focus on the dynamics of the termination shocks at the end of the current sheet. However, once can also focus on the dynamics of the current sheet itself, namely a chain of plasmoids (magnetic islands) should form when the Lundquist number exceeds a critical value of 10^4 (due to the plasmoid instability - a super-Alfvénic tearing mode instability - see e.g. Tajima and Shibata 2002; Loureiro et al. 2007 and the reconnection rate is almost independent of the current sheet Lundquist number, once the critical value of 10^4 is reached - Bhattacharjee et al. 2009). Zhao et al. (2019) studied an MHD simulation of magnetic flux rope formation and eruption driven by photospheric converging motions, and then forward-modelled the results in SDO/AIA channels as well as for thermal X-ray. The authors found QPPs appeared in their forward-modelled results, corresponding to the chaotic (re)appearance and current-sheet-guided displacements of the magnetic islands. The QPPs appear at various stages of the evolution, and coincide with the evolution of the magnetic islands, during which the magnetic reconnection rate fluctuates significantly.

It should be noted that the models of Takahashi et al. (2017) and Zhao et al. (2019) are either 2D or 2.5D MHD models, assuming homogeneity along the PIL. However, the real eruptive flare is a three-dimensional object. As discussed above (see the discussion of mechanism [7] in Section 2.4.2), it is known from numerous observations that the energy release of a flare can progress along the PIL, accompanied by pulsations in different spectral ranges. The uneven (asymmetric) eruption of the magnetic flux rope along the PIL, most likely, can lead to reconnection in different loops of the magnetic arcade at different times, which can manifest itself in the form of pulsations, the sources of which appear in different places of the flare region (e.g. Grigis and Benz, 2005; Liu et al., 2009). Based on the comparison of observations with the extrapolation of magnetic field to the corona in the nonlinear force-free field (NLFFF) approximation, Zimovets et al. (2018) showed that hard X-ray pulsations are emitted from different parts of the magnetic flux rope or from different loops of magnetic arcades with which the flux rope can interact. This indicates the importance of taking into account the effects of inhomogeneity and non-uniformity of magnetic structures when constructing new 3D models of eruptive flares for studying the processes of generation of QPPs.

The QPP features that are usually interpreted as evidence of quasi-periodic particle acceleration are: a) high modulation depth when the emission itself is produced by an incoherent mechanism (e.g., gyrosynchrotron or bremsstrahlung); b) non-harmonic irregular intensity modulation; c) highly correlated (possibly, with a small delay) pulsations in multiple wavelength ranges, i.e., in a wide range of heights where a global phase-coherent MHD wave is unlikely to exist; d) evidence of propagating electron beams (e.g., type III bursts) that seem to be quasi-periodically injected. Below, we briefly summarize some recent observations where the QPPs demonstrated some (or all) of the mentioned signatures.

Huang et al. (2016) detected QPPs in an M7.7 flare on 2012 July 19: the microwave emission (17 GHz) from the loop footpoints, hard X-ray emission ($20-50$ keV) from a footpoint and the loop top, and reverse type III bursts (with positive drift, i.e., corresponding to downward-propagating electron beams) in the $0.7-3$ GHz range demonstrated prominent in-phase oscillations with the period of 270 s; an additional period of 100 s was detected in some channels, too. In this event, the source of energetic electrons (i.e., the probable site of quasi-periodic reconnection) was likely located above the loop top, at the level corresponding to ≈ 700

MHz emission frequency. Kupriyanova and Ratcliffe (2016) and Kupriyanova et al. (2016) analyzed a C9.3 flare on 2005 May 6; simultaneous QPPs with modulation depth of $30-80\%$ and typical periods of 50 and 30 s were detected in hard X-rays ($50-300$ keV) and microwaves ($9.4-35$ GHz). The hard X-ray spectral index variations correlated with the hard X-ray and microwave intensity: the spectrum was harder at the intensity maxima, which can be interpreted as a signature of quasi-periodic injection of new accelerated electrons. Several type III bursts (in $25-180$ MHz range) corresponding to the hard X-ray and microwave emission peaks were detected, which demonstrated the period of about $40-50$ s and were delayed after the microwave peaks by ≈ 10 s. Kumar et al. (2017) detected QPPs with a shorter period of about 13 s in a C4.2 flare on 2015 September 21; the pulsations occurred simultaneously in hard X-rays ($12-300$ keV) and microwaves ($4.9-34$ GHz). Three type III bursts (in the $25-180$ MHz range) were also detected, which likely corresponded to the hard X-ray and microwave emission peaks (had a similar repetition period), but were delayed with respect to the microwave peaks by ≈ 30 s. Li et al. (2015) observed an event with ever longer delay between the QPPs in hard X-rays and type III bursts: in an X1.6 flare on 2014 September 10, hard X-ray light curves ($27-296$ keV) contained three prominent peaks with a period of about 4 min; a similar period (but with up to 10 peaks) was detected in EUV emission. Some time (≈ 8 min) later, a sequence of quasi-periodic type III bursts with a similar ~ 4-minute period was detected at low radio frequencies ($\sim 0.1-10$ MHz); the delay is consistent with the propagation time of the energetic electrons from a supposed quasi-periodic acceleration site. For the same flare, Li and Zhang (2015) found quasi-periodic motions of bright knots in one of the flare ribbons with the apparent velocity of $20-110$ km s^{-1} and the associated period of $3-6$ min. These movements were accompanied by quasi-periodic changes in the intensity and red Doppler shifts of the Si IV 1403 Å line. The authors interpreted these observations as the quasi-periodic slipping reconnection involved in the flare process. However, other possibilities cannot be ruled out, such as mechanisms [7], [8], and [15].

Altyntsev et al. (2016) observed an M1.8 flare on 2012 August 18 and found a sequence of six broadband quasi-periodic pulses with the period of 11 ± 1 s (weaker periods of 8 and 15 s were also detected) in hard X-rays ($25-300$ keV) and microwaves ($\sim 3-35$ GHz). High correlation between the light curves at different energies/frequencies was found, but the microwave peaks were slightly delayed after the hard X-ray emission: by 1.3, 1.0 and 0.5 s at 9.4, 17 and 34 GHz, respectively (at higher frequencies, the peaks occurred earlier); these delays are consistent with propagation times of non-thermal electrons producing the gyrosynchrotron microwave emission. Li et al. (2017b) detected QPPs with the period of about 100 s in non-thermal emission of a M7.1 flare on 2014 October 27; hard X-ray ($12-25$ keV) and microwave ($17-34$ GHz) pulsations demonstrated high correlation. In the same event, QPPs with a period of 50 s were detected in thermal ($3-6$ keV) soft X-ray emission. Yu et al. (2020) observed a strong (X8.2) flare on 2017 September 10; broadband microwave ($2.5-18$ GHz) pulsations with a modulation depth of up to 30% and an average recurrence period of ≈ 300 s were detected, almost simultaneously at the loop top and a footpoint. QPPs in hard X-rays ($6-100$ keV) had the same period but a lower amplitude (a few percent); the microwave peaks correlated well with the hard X-ray ones, but were delayed by ≈ 10 s. The softer X-ray emission ($1-8$ Å) demonstrated QPPs with a period

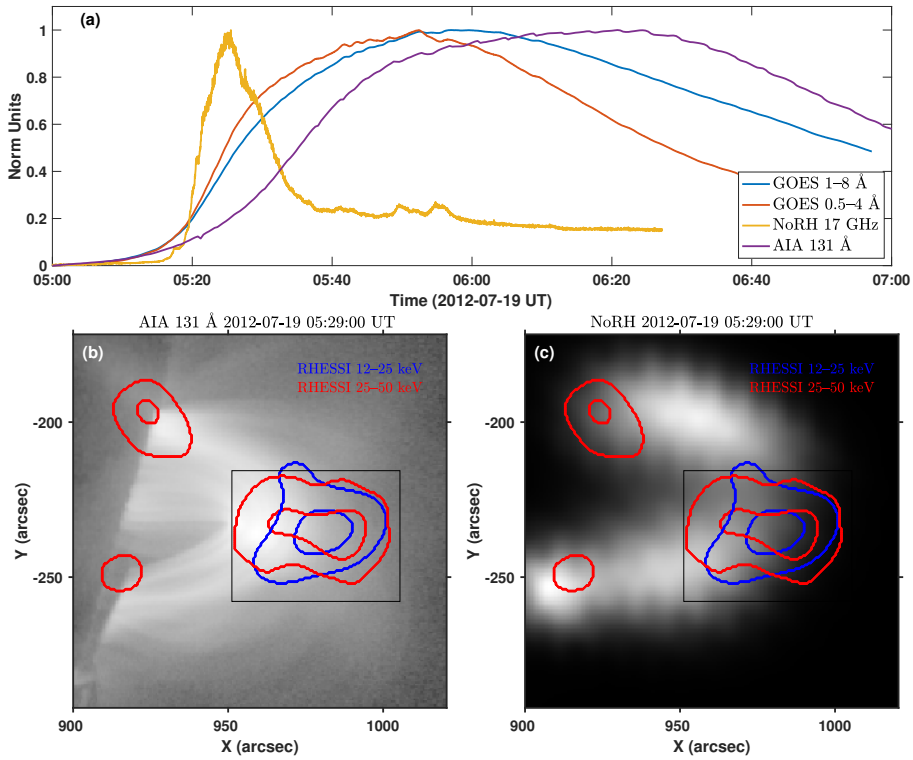

Fig. 5 (a) light curves showing the rise and decay of a solar flare recorded by GOES, NoRH and AIA 131Å (b) Coronal loop system observed by AIA 131 Å channle. (c) NoRH synthetic image of 17 GHz. The blue and red contours label the emission levels of RHESSI 12-25 keV nd 25-50 keV X-ray emissions. Adapted from Yuan et al. (2019) with permission.

of ≈ 150 s. We note that in the two latter examples the QPPs in thermal (soft X-ray) emission appeared to be a harmonic of the QPPs in non-thermal (hard X-ray and microwave) emission; this effect (if not a coincidence) may indicate the presence of some MHD oscillations which both modulate thermal emission and trigger quasi-periodic magnetic reconnection.

Yuan et al. (2019) studied the spatial extent of QPPs during an X7.7 flare that occurred at AR11520 on 19 July 2012. The authors removed every alternative SDO/AIA images that are subject to the CCD overflowing, so that the remaining image sequence had no saturation effect. The coronal loop system was located at the west limb of the Sun and well suited for spectral analysis (Figure 5). The NoRH 17 GHz radio flux reached peak earlier than the X-ray and EUV emission peaks and decayed rapidly. The radio flux oscillated with an 4-minute periodicity for about 30 minutes, the EUV emission flux in the AIA 131 Å channel started to oscillate 15 minutes after oscillation in the radio signal. The oscillatory signal detected in the EUV bandpass last for about 90 minutes. Yuan et al. (2019) analyzed the spatial distribution and correlation of this 4-minute oscillation. They found that this QPPs were only detected at the compact source above the loop top, this region has overlap with the hard X-ray source of the flaring core (Figure 6). The

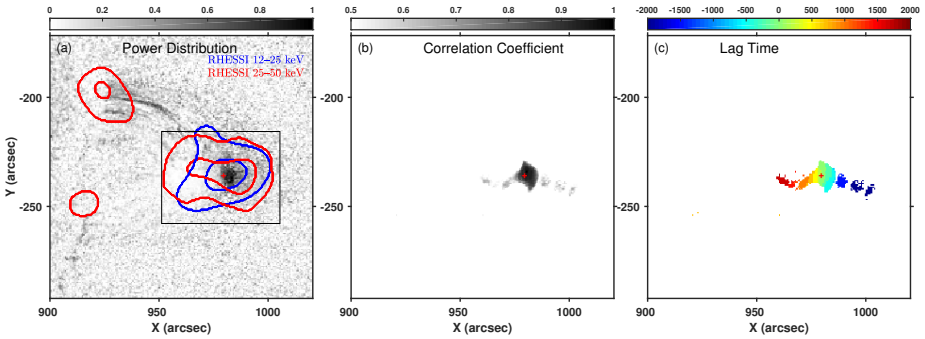

Fig. 6 Spatial distribution of the four-minute QPP Fourier power (a), correlation coefficient (b) and Lag time (c). Adapted from Yuan et al. (2019) with permission.

oscillations within this region were highly correlated with each other and exhibit gradual time shift. Thus, the authors suggest repetitive magnetic reconnection could be the cause of the QPPs detected.

Cai et al. (2019) investigated the supra-arcade fan region above the post-flare loop top in the famous 2017 September 10 eruption event, and found that the SJI 1330 Å intensity there (most likely dominated by the Fe XXI 1354 Å emission) reveals a quasi-periodic oscillating behavior with a $\approx$ 77 s period. This periodicity was suggested to be related to the quasi-periodic behavior of the magnetic reconnection process during the eruption. Their numerical simulation has also reproduced this periodicity.

With joint observations by the *Mingantu Spectral Radioheliograph* (MUSER) in Inner Mongolia, China and SDO/AIA, Chen et al. (2019) investigated an M8.7 circular-ribbon flare in the AR 12242 on 2014 December 17. Three different QPPs were detected: (1) UV QPPs with a period of $\approx$ 4 min near the center of the active region lasting from the pre-flare phase to the impulsive phase; (2) EUV QPPs with a period of $\approx$ 3 min along the circular ribbon during the pre-flare phase; (3) radio QPPs with a period of $\approx$ 2 min during the impulsive phase. Chen et al. (2019) has shown that the Type IV radio burst occurred simultaneously with the solar flare and also exhibited the QPP phenomenon. Furthermore, the QPP source region is co-spatial with the radio emission peak observed by MUSER, and the radio sources are situated above a magnetic null-point in the extrapolated magnetic field of this active region. It was suggested that the QPPs (1) were modulated by the nearby sunspot oscillations (mechanism [6]), and the QPPs (2) and (3) are connected and could be either a result of intermittent, quasi-periodic reconnection in the null-point region (mechanism [9]) or a result of oscillations in the LRC-circuit (mechanism [5]). This work clearly demonstrates that, first, QPPs with different periods can be observed in different phases of one flare, and probably are caused by different mechanisms; second, that modern observations with spatial resolution are not yet fully sufficient to reliably and unambiguously establish the mechanism of QPPs observed.

– **Thermal overstability – mechanism [10].**

In the corona, there is a continuous competition between the plasma heating/energy supply and the radiative losses. This misbalance can lead to the os-

cillatory regime of the thermal instability and, in the over-stable regime, an increase in the oscillation amplitude will become saturated due to nonlinear effects (Chin et al., 2010; Nakariakov et al., 2017). Modulation of plasma parameters by this overstability can produce QPPs. This acoustic over-stability phenomenon can occur in flaring regions and the oscillation frequency will be determined by the distance between the footpoints along the magnetic field line. The acoustic over-stability is most pronounced for long wavelength perturbations, which corresponds to the fundamental mode of long loops. Since they have an acoustic nature, typical periods are determined by the plasma temperature and the length of the oscillating loop. Thus, for typical flaring parameters, these oscillations range from a few to several minutes. Zavershinskii et al. (2019) investigated this phenomenon in a uniform plasma and demonstrated that a thermal misbalance can lead to the generation of a quasi-periodic slow magnetoacoustic wave pattern with the characteristic period determined as $P_{\rm TM} \propto \sqrt{C_V C_P / Q_\rho Q_T}$ where C_V and C_P are standard specific heat capacities, and Q_ρ and Q_T are the derivatives of the net plasma heating/cooling function with respect to the plasma density and temperature, evaluated at the equilibrium. The misbalance between plasma cooling and heating processes causes both dispersion as well as amplification or attenuation of the slow waves. The characteristic period is determined by the timescales of the thermal misbalance. Kolotkov et al. (2019) investigated the damping of linear standing slow magnetoacoustic waves through the misbalance of heating and radiative cooling processes. Depending on the magnitude of the misbalance timescales, three regimes for the evolution were identified, namely suppressed damping, enhanced damping and acoustic over-stability. The dynamics were found to be sensitive to the characteristic timescale of the thermal misbalance, but the observed properties of standing slow magnetoacoustic oscillations in the corona could be reproduced readily with a reasonable choice of the heating function.

For mechanism [10], it is expected that QPPs will be observed in the thermal radiation of the corona (soft X-rays, EUV), but detailed studies have not yet been carried out. It is unlikely that this mechanism can be accompanied by quasi-periodic acceleration of particles and generate QPPs of non-thermal emissions. We are unaware of any QPPs observations that have been interpreted as being generated via thermal overstability.

– **Periodic regimes of coalescence of two twisted loops – mechanism [11].**

Tajima et al. (1987) designed the first theoretical dynamic model for the phenomenon of the coalescence instability (CI) in solar flares, developing between magnetic ropes (plasmoids) twisted in the same direction (see also Finn and Kaw, 1977, for the first description of CI for laboratory plasmas). In the solar corona, this phenomenon occurs in such magnetic systems as current-carrying electrodynamically interacting coronal loops that may lead to lower-power energy releases (including microflares); and during strong solar flares associated with the standard flare model. In the latter case, CI can develop both between rising magnetic rope and the arcade, and between smaller-scale plasmoids in the fragmented macroscopic current sheet above the arcade (e.g., Shibata and Tanuma, 2001; Karlický, 2014). The onset of the CI is determined by the magnetic Ampere force pushing the plasmoids with co-directed electric currents towards each other and a counteracting gradient of the thermal pressure in the current sheet forming at the interface of the plasmoid interaction. Tajima et al. (1987) found that the imbalance between

these perturbing and restoring forces could lead to at least two natural scenarios for oscillatory variations of plasma parameters during CI. According to the first scenario, a quasi-steady magnetic inflow into the reconnection site causes repetitive events of CI resulting in quasi-periodic magnetic reconnections. The repetition rate of this pulsating reconnection was empirically found to be about a few hundreds of seconds, and is clearly defined by the inflow speed and the plasma parameters in the current sheet. However, the exact relationship between the oscillation period and the parameters of plasma and the magnetic inflow is not yet known. By its nature, this mechanism coincides with the concept of "magnetic dripping" (see Nakariakov et al., 2010b, and the discussion of self-oscillatory processes above). According to the second scenario, a current sheet between two coalescing flux ropes can experience transverse oscillations with periods of about one second and shorter at each elementary act of CI, driven by the interplay between the Ampere and thermal pressure gradient forces. In the pure MHD regime, the current sheet oscillation period P_{CI} is connected with the plasma parameter β and the transverse Alfvén transit time τ_A as $P_{CI} \propto \beta^{3/2}\tau_A$. The model of Tajima et al. (1987) for the current sheet oscillations of the latter kind was extensively exploited in a number of follow up numerical works (see e.g. Takeshige et al., 2015) for the study of finite-β effects on the current sheet dynamics. The first analytical generalisation of this model describing oscillatory regimes of finite amplitude in which the current sheet thickness may decrease beyond MHD scales was developed by Kolotkov et al. (2016b).

The expected observational manifestations of the CI are only poorly understood so far. For example, fragmentation of the macroscopic current sheets into smaller-scale plasmoids could be considered both as a result of the coalescence of the emerging magnetic rope with loops of the arcade and, on the other hand, as favourable physical conditions for CI onset between individual plasmoids. As a typical thickness of the coronal current sheet is less than a few hundred km, they could be observed with the existing instruments directly at the very limit of the available spatial resolution. Thus, Takasao et al. (2012) was able to reveal the appearance of several plasmoids ejected bidirectionally along a macroscopic current sheet structure above the flaring arcade, analysing the SDO/AIA images of a GOES C4.5-class solar flare. The upward and downward propagation speeds were 220–460 km s^{-1} and 250–280 km s^{-1}, respectively. In the follow up study, the authors found that each plasmoid ejection produced an impulsive microwave burst at 34 GHz with the period of a few tens of seconds (Takasao et al., 2016). The authors discussed the observed dynamics of these plasma blobs in terms of rapid ejection of plasmoids along the macroscopic current sheet, their coalescence, and collision with the post-flare loops.

2.5 Review of recent statistical studies on QPPs in solar flares

Over several decades, there have been many single-event studies of QPP signatures in a solar flare. Such studies have been and remain important to improve the body of knowledge of this phenomenon and to highlight novel observations. However, studying a scientific phenomenon purely in this way limits our ability to answer some key questions. In the context of QPPs, these questions include:

- what is the prevalence of QPP signatures in solar and stellar flares, i.e. how often does a flare play host to a QPP signature?
- Are there different, distinct populations (types) of the QPP phenomenon, and what might the distribution of these various populations be?
- Are there relationships between observable QPP properties and their surrounding system, and can these identify the emission mechanism?

The most effective way to address questions like those listed above is to study QPPs in a statistical fashion. Historically this has proven difficult, but recently several authors have successfully carried out such studies (e.g. Balona et al., 2015; Simões et al., 2015; Cho et al., 2016; Inglis et al., 2016; Pugh et al., 2016, 2017b; Dominique et al., 2018; Pugh et al., 2019; Hayes et al., 2020), obtaining new insights into solar and stellar flares respectively.

In the solar domain, Simões et al. (2015) carried out a survey of all the X-class flares of solar cycle 24 that had occurred to date, searching for pulsations in the soft X-ray regime using GOES/XRS, an energy range that corresponds to thermal emission during flares. This wavelet-based study analysed a total of 35 flares. The key result from this work was the estimate that $\approx 80\%$ of flares exhibited significant pulsations in soft X-rays. The typical periods observed were found to be in the $16 - 53$ s range.

Subsequently, Inglis et al. (2016) carried out a survey of all GOES M and X class solar flares that occurred between 2011 and 2015 inclusive, in search of strong QPP-like signatures. This involved a total of around 700 solar flares, which were studied using soft X-rays observed by GOES and hard X-rays observed by Fermi/GBM. The study was carried out using a methodology called AFINO (Automated Flare Inference of Oscillations; see the review by Anfinogentov et al. in this volume), which fits different models to the Fourier power spectra of solar flares and performed a model comparison test to identify those with possible QPP signatures. Using this approach, the authors found approximately 30% of the solar flares examined showed evidence for a QPP signature in the GOES soft X-ray data, a very different result from that of Simões et al. (2015). Furthermore, only $\approx 8\%$ of those same flares showed evidence for QPP signatures in hard X-rays, which may have been partially explained by signal-to-noise differences. The authors also determined that the characteristic periods were primarily in the $10 - 30$ s range, broadly consistent with the Simões et al. (2015) study. These periods appeared to be independent of the flare magnitude. Both of these studies suggest that QPP signatures are a relatively common occurrence during solar flare thermal-dominated emission, an interesting finding since historically many QPP studies have focused on non-thermal emission accessible via hard X-rays and radio data. The difference in detection rates could be partially explained by the different choice of methodology; the wavelet analysis technique used by Simões et al. (2015) is able to detect shorter-lived, and more non-stationary signals, compared with the global methodology used by Inglis et al. (2016).

A further study focused primarily on thermal emission was carried out by Dominique et al. (2018), who analysed all the flares from solar Cycle 24 with a GOES magnitude greater than M5 in search of QPP signatures, a total of 90 events. In this work, the authors applied a wavelet analysis technique to the PROBA2/LYRA and SDO/EVE/ESP data from these flares, which observe in the EUV and soft X-ray wavelengths respectively. The authors developed a set of detection criteria

for the wavelet analysis designed to prevent false detections due to windowing or detrending. Despite these extra conditions, a quasi-periodic signal was identified in around 90% of the studied flares, an even larger prevalence of QPP signals than was found in Simões et al. (2015). As with other studies, the typical periods observed were primarily in the < 30 s range.

Related works by Pugh et al. (2017b) and Pugh et al. (2019), have explored the link between QPPs observed in solar flares and the properties of their source active regions. Such links can provide important insights into the QPP generation mechanism. In the Pugh et al. (2017b) work, all of the flares from a single, unusually long-lived active region were studied. This region completed multiple Carrington rotations and thus had three designations: NOAA 12172, 12192 and 12209. In total, this study included 181 solar flares observed by GOES. Of these, 37 were found to show significant evidence of pulsations. The mean period for these flares was ≈ 20 s, similar to both the Simões et al. (2015) and Inglis et al. (2016) results. This work also identified a correlation between the QPP period and the flare duration. However, the main focus of the work was to explore the connection with the host active region properties. Several properties were explored on this basis, including active region area, bipole separation distance, and average magnetic field strength. No correlations between these parameters and the QPP period was found, indicating that the generation mechanism is largely insensitive to the host active region. However, a follow-on study of 20 flares by Pugh et al. (2019) found a correlation between observed flare pulsations and the flare ribbon parameters as observed by SDO/AIA. The strongest correlations found were between period and ribbon area, as well as period and total unsigned magnetic flux below the ribbons.

A recent study by Hayes et al. (2020) has addressed further these questions about the relationship between QPP signatures and their host flares and active regions. This work employed the AFINO methodology, studied GOES X-ray data in the time interval 2011 — 2018 inclusive, and also included data on C-class flares, bringing the total number of events studied to 5519. In this work, the authors found that $\approx 46\%$ of X-class flares and $\approx 29\%$ of M-class flares exhibited QPP signatures. While only $\approx 9\%$ of C-class events contained evidence of such a signature, reduced signal-to-noise may be a factor in this finding. For all studied flares, the observed QPP properties showed no correlation with the flare magnitude (see Figure 7a) and the underlying active region properties, a result that is consistent with the Pugh et al. (2017b) study. However, correlations were found between QPP properties and estimates of underlying flare ribbon properties, including separation, ribbon area and magnetic flux. Another key result of this study was a strong dependence of the QPP period and the flare duration, i.e. longer-lasting flares exhibited longer QPP periods (see Figure 7b). When further examined by breaking flares into impulsive and decay phases, the measured decay phase periods were indeed longer on average than those observed in the impulsive phase. This raises the question of whether flare evolution causes a QPP-generating process to produce longer periods over time during a flare, or whether distinct, separate generating processes are at play in these different flare phases.

These recent works have shown that the potential of statistical studies of QPPs in solar flares has begun to be realized and taken advantage of. It has been established that pulsations are not rare phenomena in flares, although their exact prevalence remains unclear. It also appears that, statistically speaking, the pulsation periods are independent of flare magnitude and the properties of the underlying

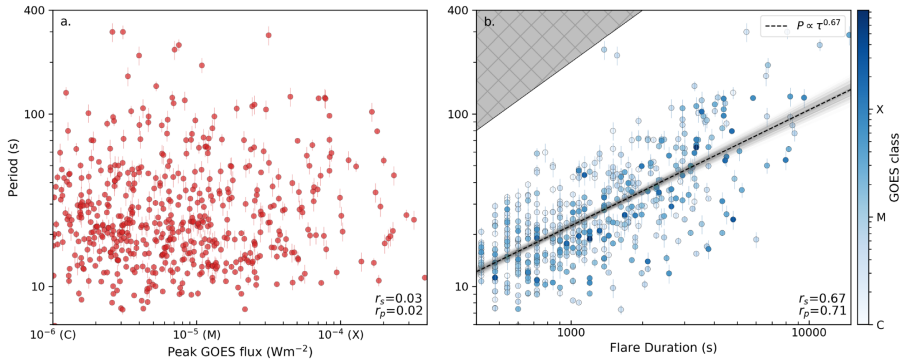

Fig. 7 Scatter plots of QPP periods with flare peak magnitude (a) and flare duration in the GOES 1−8 Å X-ray channel. Reproduced from Figure 4 in Hayes et al. (2020) with permission.

active region, but correlated with certain flare properties such as chromospheric ribbons. Untangling these findings to better understand the QPP generation mechanism(s) is an ongoing task.

3 Review of observations of stellar flare QPPs

The application of the theoretical models developed for QPP events in solar flares and described in detail in Section 2.3 needs to be adjusted for stellar QPPs on the basis of their characteristic properties, such as observational wavebands and apparent emission formation heights, flare emission mechanisms, QPP periods and damping times, and typical spatial and temporal scales of stellar active regions. For example, flares in the soft X-ray and radio bands are usually associated with the radiation from coronal loops and the regions above them, while for optical and UV flares the emission mechanism is deemed to be connected with the lower atmospheric layers heated by non-thermal electrons. On the other hand, MHD waves (one of the potential mechanisms for QPPs, see Section 2.4.1) are known to possess different properties at different layers of the solar and stellar atmospheres. In particular, the fundamental standing fast magnetoacoustic oscillations have nodes and antinodes near the loop footpoints and at the apex, respectively (see also the reviews by Nakariakov et al. and Li et al. in this volume for more details). Thus, assuming the flaring loop is large enough so that its apex is situated in the corona and the footpoints are anchored in the chromosphere, the impact of the standing fast modes on the flare emission source is maximised in the corona and is almost absent in the chromosphere. Hence, standing kink and sausage oscillations (mechanisms [1] and [2]) are not likely to directly modulate a chromospheric flare source and be responsible for stellar QPPs in the chromospheric lines, e.g. those observed in the UV or optical bands. On the other hand, these modes can affect the chromospheric flare emission indirectly via periodic triggering of reconnection higher up in the corona by a kink-oscillating remote loop (mechanism [6]) or through changing the magnetic mirror ratio in the flaring loop (Zaitsev and Stepanov, 1982), both leading to periodic precipitations of energetic particles down to the chromosphere and local chromospheric plasma heating. In contrast, the fundamental standing

slow magnetoacoustic waves (mechanism [4]) can affect the flare emissions in the lower atmosphere and cause longer-period QPPs directly via perturbation of the plasma density near the loop footpoints (see also the review by Wang et al. in this volume for more details).

To enable an effective transfer of the models for QPPs from the realm of solar flares to stellar flares, in this section we overview typical properties of stellar QPPs in different wavebands and point out their differences and similarities with solar QPPs. Historically, observations of stellar flares were performed by ground-based optical instruments (e.g. Haisch et al., 1991). However, the most recent progress in the analysis of QPPs in stellar flares has been achieved via space-borne observatories such as *Chandra* Orion Ultradeep Project (COUP, e.g. Getman et al. 2005), XMM-Newton (e.g. Jansen et al. 2001), GALEX (e.g. Martin et al. 2005), *Kepler* (e.g. Borucki et al. 2010) and also the ground-based facilities (e.g. NGTS, JVLA and Arecibo) providing observations of stellar flares in X-rays, UV, optics, and radio.

3.1 Observations of stellar flare QPPs in optical bands

Stellar flare QPPs detected in optical bands may be significant as they provide us with information about the evolution of MHD modes in multi-temperature loop plasma (if near simultaneous X-ray and UV QPPs are also present) or solely the dynamical plasma processes related to the chromospheric or photospheric response to stellar flares, including the detection of superflares. To the best of our knowledge, the first observation of QPPs in a stellar flare (duration: 13 min) was reported by Rodono (1974) in the Hyades flare star H II 2411 (M4e). The average period $\langle P \rangle = 13.08 \pm 0.06$ s was detected which changes during the flare from $P_1 = 13.70$ s (between periods $n = 0$ and $n = 31$) to $P_2 = 12.35$ s (between $n = 31$ and $n = 61$). The basic physical cause of the QPPs were unknown. Zhilyaev et al. (2007) have also reported a quantitative colorimetric UBVRI analysis of two stellar flare events on the red dwarf EV Lac. The photometric data were recorded and analyzed in September 2004 during the multi-site synchronous monitoring and continuous observations from the four observatories based respectively in Ukraine, Russia, Greece and Bulgaria. These QPP observations during the stellar flares confirm the presence of small-scale high-frequency oscillations as earlier observed by Rodono (1974). After such an early detection of the optical stellar QPPs by Rodono (1974), there were several investigations in 1980-1990 about the observations of micro-flaring processes and quasi-periodic pulsations in dMe flare stars. An interesting example is Andrews (1990) who performed a photometric micro-variability study of AT Mic (G799B) following a small stellar flare ($\geq 1.9 \times 10^{32}$ erg) in the U-band with a time resolution of 1 s. Quasi-periodic fluctuations with the periods $P_1 \approx 13.2$ and $P_2 \approx 7.9$ s were detected 10–15 min after the peak of the flare lightcurve using a modified auto-correlation (MAC) analysis (Andrews, 1989a,b). QPPs with $P_1 \approx 13.2$ s were detected only from the earlier stage of the flare decay, while the QPPs with $P_2 \approx 7.9$ s were found both in the earlier and later stages of the flare decay. However, it is noted that these QPPs, abbreviated as "time signatures" following the flare, cannot be distinguished from those for quiescent dMe stars. Thus, it was not fully convincing that the detected pulsations were directly related to the observed stellar flare.

In the beginning of 1990's, Houdebine et al. (1993a,b) observed oscillations with a period of 2.68 min in the centroids of Ca II H & K lines in the decay phase of a flare on AD Leo (M4Ve). These oscillations were interpreted as periodic motions in a prominence triggered by a flare disturbance. Later, it was found that this star was likely to be associated to a planetary companion separated by 0.024 AU (Tuomi et al., 2018). Such observations of QPPs in the modern era may shed new light on the dynamics of stellar prominences, their diagnostics, in analogy with our established understanding of the solar prominence seismology (e.g. Arregui et al., 2012, and references cited therein). Optical stellar QPPs continued to be detected, and some of them could not be understood in terms of their physical mechanisms: Qian et al. (2012) have reported an optical flare in the R band from CU Cancri and observed oscillatory bumps during the peak phase of the flare. CU Cancri is known to be a detached eclipsing binary consisting of a M3.5Ve primary and unresolved secondary. Three quasi-periodic emission peaks with $P \approx 3$ min were observed in the R-band during a flare. Four quasi-periodic peaks were also detected after the main flare peak on the growing bump with an average period of ≈ 13 min. Visual analysis of light curves yielded the observed QPPs, however, the underlying physical causes remain unclear in the present study. Jackman et al. (2019) have also detected QPPs in a giant flare on a PMS M star, NGTSJ121939.5-35555 in the optical band ($520 - 890$ nm). This star is found to be free from a circumstellar disk and known to be an X-ray saturated star. The multiple periods of 320 s and 660 s at around the flare peak were detected with an amplitude of 10%. A detection of the spike lasting around 30 seconds before the starting time of the shorter oscillation was also detected during the flare epoch. Vander Haagen (2019) have performed a high cadence flare search of X-ray star 47 Cas (F0V). They have detected 46 B-band flares at 0.26 to 0.78 mag peak above the mean. Their detailed flare analysis led to the detection of numerous QPPs accompanying the spikes with predominant frequencies of 2 to 12 Hz. There were no conclusive arguments given for the most possible physical mechanisms behind the observed QPPs.

From above examples, it is clear that the detected optical QPPs could not establish clear information on their triggering mechanisms, however, they are present during the flare epochs in a variety of stellar atmospheres. Some efforts have also been initiated to understand the most likely physical causes in the evolution of the optical stellar QPPs. Therefore, during the past three to four decades, there are plenty of scientific studies that show the detection of optical stellar QPPs, and suggest their possible underlying physical mechanisms. Below we will describe some of the most significant of these investigations, which fall into two broad categories of the physical phenomena.

3.1.1 Optical stellar QPPs and their association with possible MHD modes

Likewise solar flare QPPs and their association with flare-generated MHD modes, there are several observations that have been interpreted in terms of MHD oscillations in the stellar flaring loops. A significant attempt is noted in the later part of 1990's when three flare events were studied in detail by Zhilyaev et al. (2000) using many-site multicolor synchronous monitoring of the flare star EV Lacertae. The EV Lac is a faint red dwarf M3.5e, which is 16.5 light years away from the Earth and acts as an X-ray emitter. Its mass, radius and surface temperature

are respectively $0.35M_\odot$, $0.36R_\odot$ and 3400 K. The typical integration time of the observed flare light curves was 0.1 s. Two of these flares were observed at more than one site using distant telescopes operating synchronously to an accuracy of 0.1 s. One flare possessed QPPs during the flare maximum in the U-band with a period of around 13 s. The flare, detected by two instruments simultaneously, was associated with the QPPs with a period $P = 12.8 \pm 0.7$ s during the flare maximum of around 180 s duration. The other flare, observed by two different instruments in the B- and U-bands, showed QPPs which first appeared with a period $P = 25.7 \pm 1.8$ s and, after ≈ 200 s, changed its period to ≈ 13 s near the flare maximum. Fourier analysis with filtering was applied to detect these significant QPPs present during various flaring epochs. The observed QPPs were interpreted in terms of coherent oscillations of one or two magnetic loops, but the exact physical scenario of the oscillations was not clarified. This physical scenario resembles the observations by Zimovets and Struminsky (2010) of double-periodic QPPs in a solar flare, which occurred in a system of interacting coronal loops. Later, Stepanov et al. (2005) investigated ≈ 10 s QPPs found by Zhilyaev et al. (2000) on the EV Lac star. They conjectured that the observed pulsations were associated with fast magnetoacoustic oscillations in the stellar flaring loops. They diagnosed the magnetic field $B \approx 320$ G, temperature $T \approx 3.7 \times 10^7$ K and plasma number density $n \approx 1.6 \times 10^{11}$ cm^{-3}, in the region of flare energy release. It was argued that the optical emission source was localized at the footpoints of the flaring loop.

Mathioudakis et al. (2003) analysed the intensity oscillations as observed in the gradual phase of a white-light stellar flare on the RS CVn binary II Peg using a Fast Fourier Transform (FFT) power spectra and wavelet analysis, and found a period of 220 s. II Peg is a RS CVn type eclipsing binary that consists of K2IV-V primary and unresolved secondary stars. It seems that the flare occurred at the secondary star in this particular case. By analogy with the Sun, the oscillating coronal loop models are used to derive the parameters such as temperature, electron density and magnetic field associated with the flaring loop. The magnetic field strength and number density inside the flaring loop were determined to be 1200 G and 6.4×10^{11} cm^{-3}, respectively, using the seismological technique developed by Nakariakov and Ofman (2001). The derived parameters are consistent with the near-simultaneous X-ray observations of the flare. There is no evidence for oscillations in the quiescent state of the binary, which infer that the oscillations are uniquely set into the stellar loops during the flare energy release. This work could test the seismological aspects of more than one wave modes, however, it could not support any particular oscillation mode in its given observational baseline.

Using the wavelet technique, Zhilyaev et al. (2011) detected QPPs with a period $P \approx 11$ s in the U-band around the maximum of one of the most powerful and long-duration (around 1 h) flares on the active red dwarf YZ CMi (dM 4.5e). An initial modulation depth of the emission intensity was found to be 5.5% with an exponential damping time of 29 s. This red dwarf is situated at 5.93 pc distance from the Earth. It possesses respectively the radius, mass and surface temperature as $R_* \approx 0.36R_\odot$, $M_* \approx 0.34M_\odot$ and $T_* \approx 2900$ K. It is one of the brightest ($V = 11.1^m$) and most active flare stars. It was interpreted that the observed QPPs are caused by fast MHD oscillations of a flare loop. Using coronal seismology methods, the number density, temperature and magnetic field have been estimated as 2×10^{10} cm^{-3}, 3×10^7 K and 150 G, respectively. Similarly, Tsap et al. (2011)

have used coronal seismology and investigated 10 s QPPs in the optical flare emission from the active red dwarf EQ Peg B detected using the William Herschel Telescope commissioned on the La Palma. The underlying mechanism was found to be associated with the sausage oscillations of a coronal flare loop (mechanism [1]). The temperature, density and magnetic field were diagnosed respectively as $\approx 6 \times 10^7$ K, $\approx 2.7 \times 10^{11}$ cm^{-3} and ≈ 540 G in the flaring corona. The estimated flare loop length of $\approx 0.4 R_\star$ indicates the existence of extended coronae on red dwarf stars.

Anfinogentov et al. (2013a) have reported QPPs in the U-band light curve of a stellar mega-flare on YZ CMi (dM4.5e) as observed on 2009 January 16 in the decaying phase of the flare with a period and damping time of 32 and 46 min, respectively, and the relative amplitude of 15%. These damped oscillations in the decaying phase are typical of slow magnetoacoustic waves (mechanism [4]) observed in solar flares in the EUV and radio wavelengths. The flare-generated oscillations are fitted well using an exponentially-decaying harmonic function. It was noted that the macroscopic variations of the plasma parameters in the observed oscillations can modulate the ejection/precipitation of non-thermal electrons to the lower layers of the stellar atmosphere. The phase speed of the longitudinal slow magnetoacoustic waves in the flaring loop or arcade, the tube speed, of about 230 km s^{-1} will require a loop length of about 200 Mm. This length is consistent with the loop length estimated for a flare on a similar M-type dwarf AT Mic by Mitra-Kraev et al. (2005) (see Section 3.3.1). Nevertheless, other mechanisms, e.g. quasi-periodic triggering of magnetic reconnection by standing kink oscillations (mechanism [6]) or quasi-periodic occultations by an oscillating prominence (e.g. Doyle et al., 1990; Kolotkov et al., 2016c), may also have taken place in the flaring region. Pugh et al. (2015) also reported multiple damped QPPs in the decaying phase of a white-light flare on KIC 9655129 with a period of 78 and 32 min. These multi-periodic oscillations could be evidence of MHD oscillations typical for solar flares. The star is known to be an Algol type eclipsing (semi-detached) binary whose spectral type and luminosity class are not known.

Mancuso et al. (2020) found an anharmonic shape of QPPs in the decaying phase of a super-flare observed by *Kepler* on KIC8414845, which is a young, fast-rotating (1.88 ± 0.22 days) solar-like active star. It was revealed that the anharmonicity results from a superposition of two intrinsic modes with periods of 49 min and 86 min in coronal loops with the length of $(1.2 - 2.1) \times 10^{11}$ cm. The authors analyzed the QPP signal using a data-driven, non-parametric method known as singular spectrum analysis (SSA). This method has certain advantages because it is not based on a prescribed choice of basis functions, and is suitable for analyzing non-stationary, non-linear signals such as those observed in QPPs during major flares. The amplitude modulation of the two QPPs may be interpreted as the excitation of the second harmonic of standing slow-mode magnetoacoustic oscillations (mechanism [4]) and global kink oscillations of a coronal loop, which quasi-periodically trigger magnetic reconnection in a nearby flaring loop (mechanism [6]). It is, however, emphasized that the available observations do not allow to reject possible concurrent mechanisms.

These examples clearly indicate that some of the evolved optical stellar flare QPPs may be associated with the various MHD modes, and may be utilized to diagnose the crucial physical parameters of the flaring regions using coronal magnetoseismology. However, this can be done only under the condition that the mech-

anism for generating QPPs is reliably established, which is not yet possible due to limited observations.

3.1.2 Optical stellar QPPs and their association with transient energetic processes

In contrast to Section 3.1.1, many QPPs are not found to be associated with the MHD modes in the flaring regions, but they are probably associated with a transient energetic phenomena (e.g. self-oscillatory processes including quasi-periodic regimes of magnetic reconnection, mechanism [9]). Such QPPs are important candidates for probing the energy release processes in the stellar flaring regions. Some such examples are described in this subsection.

Mathioudakis et al. (2006) performed high time-resolution observations of a white-light flare on the magnetically-active star EQ PegB and reported evidence of intensity oscillations with a period of ≈ 10 s. Period drifts are seen towards its larger values during the decay phase of the stellar flare (a similar situation was also found in solar flares, e.g. Hayes et al. 2016; Dennis et al. 2017; Hayes et al. 2019, 2020). Considering that the oscillation is interpreted as an impulsively-excited standing acoustic wave in a flaring stellar loop (similar to mechanism [4]), the observed period shows its existence in a loop length of ≈ 3.4 Mm and ≈ 6.8 Mm for the case of the fundamental mode and the second harmonics, respectively. However, the small stellar loop lengths demonstrate the presence of a very high modulation depth, making the acoustic wave mode interpretation less likely. A more realistic physical interpretation may be associated with the evolution of the fast-MHD modes (e.g. the sausage mode, mechanism [1]) causing the modulation of the emissions most likely due to the magnetic field variations. On the contrary, the quasi-periodic intensity variations could be due to some other mechanisms. The authors also considered different possibilities, e.g. mechanisms [6], [7] (by Emslie, 1981), [9], and [11]. However, the limited observational capabilities did not allow them to choose a definitive mechanism operating in the flare studied.

Lovkaya (2013) observed the fine temporal structure of two stellar flares on the red-dwarf flare star AD Leo on February 4, 2003 using the 1.25-m telescope of the Crimean Astrophysical Observatory in a rapid-photometry mode. The time duration of the first flare was approximately 5 min and another was more than 8 min. The amplitudes in the U-band were found to be 1.65^m and 1.76^m respectively. Quasi-periodic brightness pulsations were detected during the flares with a period of ≈ 10 s. The various estimations invoke for the first time the signature of rapid cooling of the plasma near the maxima of the first flare. At the end of the first flare, the plasma becomes optically thin in the Balmer continuum while the final stage of the second flare was not observed. The underlying physical cause of the QPPs was not associated to any MHD modes, however, it might be linked with the quasi-periodic energy release processes of the observed giant flares covering $\approx 0.07\% - 0.11\%$ of the visible stellar disk.

Using the 30-inch Cassegrain telescope of the Stephanion Observatory, Greece, Contadakis et al. (2012) reported the analysis of the B-light curve for the flares of the red dwarf YZ CMin (dM4.5e) observed in February 2002. A Discrete Fourier Transform (DFT) and Brownian Walk noise estimated the proper random noise and detected the plausible weak transient optical oscillations present during the stellar flare. Transient high-frequency oscillations were observed during the flare event and the quiet-star phase with frequencies (periods) ranging between 0.0083

Hz (∼2 min) to 0.3 Hz (∼3 s). The QPPs were most pronounced during the flare state. The oscillations with periods 2 min to 1.5 min, 60 s, 11 s, 7.5 s, and 4 s appeared around the maximum and continued to appear during the whole flare state. From the flare maximum phase, a progressive increase of the oscillations with periods 30 s, 20 s down to 4.0 s was obtained. At the end of the flare, only the oscillation of the pre-flare state remained and the rest had disappeared. These observations were consistent with the physical scenario of the impulsively-excited oscillations of a coronal magnetic loop and a subsequent chromospheric heating by electron flux at the foot of the loop resulting in soft X-ray coronal emissions. It also indicates that more than one impulsive event may occur in the course of an observed flare. In a different study, Contadakis et al. (2013) found the presence of high-frequency oscillations in two weak flares of the G8 dwarf V390 Auri. It was found that transient high-frequency oscillations occurred during the flare event, and the observed frequencies (periods) ranged between 0.011 Hz (∼1.5 min) and 0.083 Hz (∼12 s). They found it in accordance with the results of the observation of transient optical oscillations on strong and medium flares (e.g. Contadakis et al., 2004, 2012; Contadakis, 2013, and references cited there).

Vida et al. (2019) have analyzed ≈ 50-day long light curve (roughly white light) of the M5.5 dwarf Proxima Centauri as obtained with the *Transiting Exoplanet Survey Satellite* (TESS, e.g. Ricker et al. 2014). The mass, radius and surface temperature of this star are respectively $M_\star = 0.120 \pm 0.003 M_\odot$, $R_\star = 0.146 \pm 0.007 R_\odot$ and $T_{\star eff} = 2980 \pm 80$ K. Overall in this observational epoch 72 flares were identified, therefore, the flare rate is 1.49 events per day. Most of flares appeared in groups, while two flare events exhibited QPPs during their decay phase. In the first flare, QPPs had a period of about 6.5 hr, lasting for around 1 day with the decreasing amplitude. As far as we know, these QPPs have the longest period detected in stellar (and solar) flares to date (see Figure 12 in Section 3.6). The second flare was found to be more energetic, and its decay phase shows QPPs with two periods about 2.7 and 5.4 hr with the possibility of harmonics. Due to the lack of observational data, the authors did not make an unambiguous conclusion about the mechanism of the detected QPPs. They suggested that a mechanism based on oscillatory reconnection caused by magnetic flux emergence could take place (mechanism [9]). However, they did not rule out the possibility that the QPPs could be a consequence of some MHD oscillations of stellar coronal loops.

3.2 Observations of stellar flare QPPs in radio

Due to large distances and hence very low (in comparison to the solar radio bursts) apparent radio fluxes, even the most sensitive radio telescopes (such as JVLA and Arecibo) currently provide rather limited and fragmentary information about the stellar radio emission; this is especially true for the related quasi-periodic processes. To date, QPPs in radio emission of stellar flares have been identified only in a few events, mostly on the so-called "flare stars" – highly active red dwarfs (of dMe spectral class), and in a certain (the brightest one) spectral component of the flaring radio emission[3]. In contrast to the solar case, the bulk of the flaring radio emission from the red dwarfs (at the frequencies $\lesssim$ 5 GHz) seems to be

[3] We do not consider here the periodically occurring radio bursts detected on some red and brown dwarfs and magnetic Ap/Bp stars (e.g., Trigilio et al., 2000; Hallinan et al., 2007;

produced due to a coherent (most likely, maser) mechanism, as indicated by its high brightness temperature and high polarization degree (e.g., Bastian, 1994; Güdel, 2002). The stellar coherent radio bursts resemble in many aspects the solar decimetric-metric spike bursts, but (a) are much more powerful and (b) extend to higher frequencies. Like the solar decimetric and metric radio emissions, the stellar coherent radio flares often demonstrate a variety of fine temporal and spectral structures, including short broadband and/or narrowband pulses, bursts with frequency drifts, etc, sometimes with quasi-periodic patterns.

The periods of QPPs detected in stellar radio flares vary from tens of milliseconds to about one minute. E.g., Lang and Willson (1986) detected on the M4 dwarf AD Leo, at the frequency of 1415 MHz, a sequence of QPPs with a mean periodicity of 3.2 ± 0.3 s; the brightest pulse itself was found to consist of shorter quasi-periodic spikes with a period of 32 ± 5 ms (likely, these fast pulsations persisted in other time intervals as well, but were not resolved due to insufficient sensitivity). Bastian et al. (1990) detected on AD Leo broadband pulsations (covering the 40 MHz band around 1415 MHz) with nearly 100% circular polarization and modulation depth of $\gtrsim 50\%$; in a 8-second interval, the pulsations were almost monochromatic with the period of 0.7 s, while in a longer time interval, the Fourier transform revealed a broader range of periods (from ~ 0.3 to ~ 1 s). Abada-Simon et al. (1995) observed on AD Leo, in the $1365 - 1415$ MHz band, a cluster of short (down to $\lesssim 20$ ms) 100%-polarized spikes with a complicated dynamic spectrum, including broadband, narrowband and frequency-drifting pulses; oscillations with a quasi-period of $\sim 5 - 10$ s were also detected in the cluster envelope. Gary et al. (1982) detected on the M5.5 dwarf BL Cet, at the frequency of 4.9 GHz, QPPs with nearly 100% polarization and a period of about 56 ± 5 s.

Like on the Sun, stellar radio QPPs often demonstrate multiple and/or variable periods. In addition to the above examples, we can mention the event observed by Lang et al. (1983) on AD Leo, at the frequency of 1400 MHz: during the rise phase of a weakly-polarized flare, a bright 100% polarized burst occurred, which consisted of shorter spikes and demonstrated quasi-periodic fluctuations at the time scales of about 2, 10, and 25 s. Stepanov et al. (2001) and Zaitsev et al. (2004) analyzed the broadband pulsations detected on AD Leo in the 480 MHz band around 4.85 GHz, at the decay phase of a flare; the Wigner-Ville transformation revealed two components of QPPs: a periodic sequence of pulses with a repetition period of about 0.5 s, and a quasi-periodic component with the period steadily increasing from ~ 0.5 s to $\sim 2 - 3$ s. On the other hand, many stellar radio bursts with fine temporal structure have revealed no evidence for periodicities (e.g. Osten and Bastian, 2006, 2008): the Fourier transform of the light curves demonstrated no distinctive periods. The most common (although largely qualitative) interpretation of the QPPs in stellar radio flares is modulation of the coherent maser emission mechanism by some MHD oscillations in the emission source.

Brown and Crane (1978) reported QPPs with a period of about 4 min in the flaring radio emission from the binary HR 1099 (of the RS CVn type), at the frequency of 2695 MHz. High polarization degree of the pulsating component, again, favors the maser emission mechanism. The authors argue that the radio

Zic et al., 2019), where the periods (from a few hours to a few days) coincide with the stellar rotation periods, and thus the repetitive patterns are evidently caused by the rotational modulation.

emission originated from a magnetic structure "shared" by both components of the interacting binary; therefore, a relatively long period of pulsations is consistent with MHD oscillations in a long magnetic tube connecting two stars. In this regard, the MHD model by Gao et al. (2008), developed to interpret the quasi-periodicity in the flaring rate, observed with a period of 48 ± 3 min in the YY Gem binary star system (containing two dM1e late-type stars with $M_{\star 1} = M_{\star 2} \approx 0.57 M_{\odot}$, $R_{\star 1} = R_{\star 2} \approx 0.6 R_{\odot}$, the orbital period of $P_{orb} \approx 0.81$ days, and the separation distance $a \approx 3.83 R_{\odot}$), can be noted. This model is based on interacting magnetic loops rooted in both components. In the interaction region of the loops, the energy is released due to magnetic reconnection, the efficiency of which can be modulated by fast-mode magnetoacoustic waves trapped between the surfaces of two stars (mechanism [6]). The authors also derived an empirical relationship between the pulsation period, P, and the mean coronal temperature, T, and plasma density, ρ, as well as the magnetic field, B: $P \sim \rho^{0.42} T^{-0.49} B^{0.84}$.

In some stellar flares, microwave emission of probably gyrosynchrotron origin (i.e., similar to the solar flaring microwave continuum) has been detected (e.g. Osten et al., 2005). However, no definite QPPs in this emission component have been detected so far – mostly due to instrumental limitations.

3.3 Observations of stellar flare QPPs in X-rays

Before the advent of XMM-Newton observatory (Jansen et al., 2001), there was plenty of evidence about the QPPs in optical (see Section 3.1) and UV bands (Section 3.4) as observed during the occurrence of stellar flares. Later, the observed X-ray QPPs revealed a variety of plasma and wave processes in the atmosphere of solar-like stars. A sequential significant development of the observations of X-ray QPPs and their derived physical implications over the last two decades are described in this subsection.

3.3.1 X-ray QPPs and their association with MHD modes

The first QPPs in the X-ray emissions (0.2-12 keV) during a stellar flare were detected on the M star AT Mic by Mitra-Kraev et al. (2005). The detection of a QPP period of 750 s with an exponential damping time of ≈ 2000 s and relative peak-to-peak amplitude of around 15%, further helps making the diagnostics of standing slow mode oscillations in the flaring stellar loop of length $(2.5 \pm 0.2) \times 10^{10}$ cm. The interpretation of the presence of highly-damped slow magnetoacoustic oscillations in the flaring corona of AT Mic (mechanism [4]) is very similar to the observed damped SUMER oscillations in hot solar coronal loops (Ofman and Wang, 2002). The diagnosed magnetic field (≈ 105 G) using the concept of centrifugal model of the oscillating loop (Zaitsev and Stepanov, 1989), and the considered loop length ($\approx 2.5 \times 10^{10}$ cm) where slow waves are detected, was found to be consistent with the one derived from the pressure-balance model of the solar flare (Shibata and Yokoyama, 2002). An important conclusion is drawn from this analyses that the comparable loop length and magnetic field suggests a similar physical nature of the coronae of AT Mic and the Sun. Following Jansen et al. (2001), Stepanov et al. (2006) found that these QPPs with $P_{QPP} \approx 750$ s in the flare on AT Mic are associated with the excitation of standing slow magnetoacoustic waves evolved

most likely due to the piston mechanism in stellar flaring loops, and further decay due to the electron thermal conduction. Later, López-Santiago (2018) refined the wavelet analysis using synthetic light curves and investigated the effect of background noise while determining the confidence levels in the wavelet scalogram. The developed technique was applied to the light-curve of the AT Mic flaring star studied by Mitra-Kraev et al. (2005), and two overlapped oscillations were found. The first QPPs ($P_1 \approx 750$ s) had already been detected by Mitra-Kraev et al. (2005), while the second QPPs were detected with a period $P_2 \approx 2000$ s. The high period QPPs were not mentioned in the previous works as reported by Mitra-Kraev et al. (2005). Their physical mechanism is not yet clear.

In the quest of deriving a better understanding of stellar QPPs and their inherent physical mechanism(s), Pandey and Srivastava (2009) reported the observations of X-ray ($0.3 - 10$ keV) oscillations during the decay phase of a flare on 19 January 2001 in a cool active star ξ Boo using EPIC/MOS of XMM-Newton. The star is a well-known binary with magnitude 4.55, at a distance 6 pc, encompassing of a primary G8 dwarf and a secondary K4 dwarf along with an orbital period of 151 yr. The X-ray light curve was investigated with wavelet and periodogram analyses, and significant QPPs with $P_{QPP} \approx 1019$ s were detected. By using four different approaches (the hydrodynamic, rise and decay, pressure balance, and Haisch's models), the derived loop length ($\approx [3.6 - 3.9] \times 10^{10}$ cm) along with the estimated magnetic field of 36 G by a pressure-balanced method (Shibata and Yokoyama, 2002), yielded convincingly for the first time the observed QPP period matching with the theoretically-estimated period of the fast kink mode waves (mechanism [2]) (cf., Table 2 in Pandey and Srivastava 2009). This was the first (possible) detection of the fast magnetoacoustic kink modes in a binary Sun-like star.

The works described above (Mitra-Kraev et al., 2005; Stepanov et al., 2006; Pandey and Srivastava, 2009) reported only a single MHD mode (e.g. the fundamental mode of slow or kink oscillations) for X-ray QPPs associated with the coronae of various magnetic stars. In contrast, Srivastava et al. (2013) presented the first observational evidence of multiple slow acoustic oscillations in the post-flaring loops of the corona of Proxima Centauri (M5.5Ve) making use of XMM-Newton X-ray observations (0.3-10.0 keV). They found multiple oscillation periodicities of $P_1 \approx 1261$ s and $P_2 \approx 687$ s, which could be accompanying with the first two harmonics of slow magnetoacoustic waves in a loop of length $\approx 7.5 \times 10^9$ cm. The fundamental mode oscillations showed dissipation with a damping time of 47 min. The period ratio P_1/P_2 is found to be 1.83, less than its canonical value 2.0. This infers that such oscillations are most likely excited in the longitudinal density-stratified stellar loops of Proxima Centauri, possessing an average scale height of 23 Mm. This work elaborated that Proxima Centauri loops are very similar to the longitudinally-structured Sun's coronal loops as diagnosed via the observations of multiple harmonics of slow waves (McEwan et al., 2006; Srivastava and Dwivedi, 2010, see also Reale et al. 1988).

Another example of the detection of multiple X-ray QPPs has been reported by López-Santiago et al. (2016) who analyzed the oscillatory patterns in the young Classical T Tauri stars (CTTS) of the Orion Nebula Cluster that were observed by the *Chandra*/COUP to determine the properties of their flaring loops (see also Section 3.3.3). Oscillations were interpreted to be caused by the fundamental mode and/or the first harmonic of slow magnetoacoustic waves inside the loop (mech-

anism [4]). Higher order harmonics require higher energies to be released (Selwa et al., 2005). The results showed that flares may take place in magnetic tubes connecting the star with its accretion disk (see Section 3.3.3 for more details). In particular, it was found that at least three stars, COUP 332 (2MASS J05350934-0521415), COUP 597 (V2252 Ori), and COUP 1608 (OW Ori) have magnetic fluxtubes that potentially connect the star with its accretion disk, and are subjected to oscillatory processes.

These findings of multiple wave harmonics in different types of stellar atmosphere (e.g. Proxima Centauri and CTTS) indicate that their loop-like structures do exist and possess flare-like energy release, which can result in oscillatory processes. Further systematic analysis should be performed in the future to diagnose such stellar atmospheres in terms of their magnetic structuring and the energetic plasma processes, taking into account the analogy with the Sun.

3.3.2 X-ray QPPs and their association with other energetic plasma processes

Apart from the association of the observed X-ray QPPs in the stellar flares with a variety of MHD modes, there are several reports that such QPPs may also be associated with other energetic plasma processes. Therefore, these QPPs can play an important role in diagnosing the stellar atmospheres of the distant Sun-like stars to understand the flare-generated heating and particle acceleration processes there.

For example, using the observations by the *ASCA* satellite, Tsuboi et al. (2000) detected quasi-periodic X-ray flares from the class I protostar YLW 15 in the ρ Oph cloud. It was found that three flares occurred every ≈ 20 hr. They exhibited an exponential decay with time constant 30–60 ks typical of the stellar flares. The total energy released in each flare was $[3-6]\times10^{36}$ erg, which is at least 10^3 times more powerful than the known solar flares. The first flare was well explained by a quasi-static cooling model, which is similar to solar flares where the heated plasma eventually cools down mainly due to radiation. The two consecutive flares were consistent with the reheating of the same magnetic structure where the first flare occurred. The large-scale magnetic structure and the periodicity of the multiple gigantic stellar flares suggested that the reheating events of the same magnetic stellar loop develops during an interaction between the star and the disk of the star owing to their differential rotation.

Broomhall et al. (2019b) detected QPPs in a flare on the solar analogue, EK Draconics (G1.5V) in the X-ray bands of low-energy (0.2 – 1.0 keV) with a period of 76 ± 2 min and high-energy (1.0 – 12.0 keV) with a period of 82 ± 2 min. EK Draconics is a young solar analogy G1.5V that possesses a stronger magnetic field. It was found that the QPPs in the low-energy band lag the QPPs in the high-energy band, which is consistent with the Neupert effect typically observed in solar flares. It was not possible to reliably establish the mechanism of generation of the QPPs detected, but they may have been caused by modulations of the propagation speed or acceleration of particles. Also, we cannot exclude the alternative possibility that the observed processes took place in two different systems of flare loops (something similar was observed in solar flares, e.g. Zimovets and Struminsky 2010). The authors concluded that the similarity of the observed properties of QPPs in solar and stellar flares may indicate the presence of similar processes in flare regions on different stars.

In conclusion, X-ray QPPs should also be examined in future studies to diagnose a variety of physical processes that may be related to the energetic response of intense stellar flares making changes in the plasma equilibrium as well as related X-ray emissions. Such classical plasma processes are well known in the solar atmosphere, and demonstrate a pathway to understanding the physics of flaring stellar atmospheres in the framework of the solar-stellar analogy.

3.3.3 Observations and modelling of QPPs in X-ray flares of star forming regions

Quasi-periodic pulsations have been detected on several CTTS in the Orion star-forming region during day-long X-ray flares within the *Chandra* Orion Ultradeep Project (COUP) by López-Santiago et al. (2016), during a 13 day observation of the Orion Nebula Cluster. These flares were very intense and easily demonstrated temperatures above 100 MK. CTTS are young stars which still accrete mass from a surrounding disk made of gas and dust. These stars are strong X-ray emitters (e.g. Favata et al., 2005) and are sites of intense photospheric magnetic fields (Johns-Krull et al., 1999; Johnstone et al., 2014), and therefore of very active magnetic coronae. It is believed that the inner regions of the disk are significantly ionized by the stellar radiation and that accreting material flows along magnetic channels that connect the disk to the star (Koenigl, 1991; Hartmann et al., 2016). In this framework, a suggestive scenario is that such long-lasting flares might involve such huge magnetic channels. Despite limited photon statistics, QPPs were detected in the flare light curves of COUP at high significance with wavelet analysis tools (Torrence and Compo, 1998; López-Santiago, 2018). Related periodograms clearly showed oscillation patterns in five light curves of day-long flares at high significance. All of them were long-period and large amplitude in a similar way, with periods approximately in the range 1-10 ks, and amplitudes on the order of 10%. As a first interpretation, the pulsations were associated with the fundamental mode and/or the first harmonic of MHD sausage modes inside single flaring loops, with damping often driven by thermal conduction processes (Ofman and Wang, 2002). A coherent oscillation in the flare light curve of a star is likely to come from a single magnetic channel or loop since the ignition of different loops in an arcade would be produced at distinct times, and possible oscillations would be out-of-phase and overall wash out each other. One obvious implication of a long-lasting intense flare in single magnetic tubes is that such tubes must then be extremely long - several solar/stellar radii - so long as to possibly connect the star to the circumstellar disk. This possibility had already been pointed out in the systematic analysis of the COUP flares (Favata et al., 2005), but the presence of QPPs further confirms this hypothesis.

The systematic analysis of QPPs was supported with simple analytic estimates (López-Santiago et al., 2016). A couple of very well-observed modulated flares on V772 Ori and OW Ori were instead studied with detailed loop modelling. Hydrodynamic loop modelling had already shown that it could reproduce very well both the light curves and the spectral evolution of flares which do not show QPPs. In particular, it was confirmed that there are long-lasting flares with negligible heating during the decay. Pure cooling in a simple flare evolution, i.e. a regular light curve and spectral evolution, is another way to have coherent evolution and therefore it is also strong evidence for single flaring loops (Reale, 2007). In this case, a slow decay must then correspond to a long loop, which was the case of

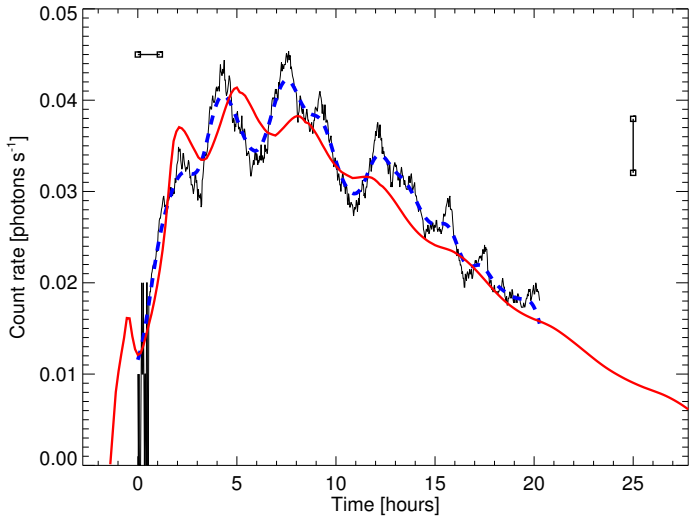

Fig. 8 Flare light curves observed with Chandra/ACIS from V772 Ori (COUP 43), after smoothing with a boxcar of 4000 s (black solid) and with a Gaussian with $\sigma = 2000$ s (blue dashed). The observed light curves are compared to those obtained by a hydrodynamic simulations of a flaring flux tube $20R_{\odot}$ long and heat pulses of ~ 1 hour (red solid). The vertical bar on the right marks a typical data error bar, the horizontal bar on the left is the boxcar width (see also Reale et al., 2018).

a specific flare in COUP (Favata et al., 2005). V772 Ori and OW Ori are two young M stars, with about half of the solar mass and a radius about twice the Sun. There is evidence for an accretion disk for both of them. QPPs were detected in their flare light curves with a very fine time-binning at very high significance as well-defined peaks in the wavelet power spectrum after convolution with a Morlet function (López-Santiago et al., 2016) and assuming a red noise.

The pulsations show up very clearly in the flare light curves smoothed with a wider boxcar. Figure 8 shows the smoothed COUP flare light curve of V772 Ori. We clearly see that the period is ~ 10 ks and the amplitude is $\sim 20\%$. The coherence over such a long period and the large amplitude suggest that low-order compressible modes might explain the observation, similar to those described in (Reale, 2016). This hypothesis was tested against detailed hydrodynamic modelling of the plasma confined in a long magnetic channel (Reale et al., 2018). A wave with a period of 10 ks, propagating in a plasma at ~ 100 MK, i.e. with a speed ~ 1000 km/s means a waveguide of the order of 10^7 km long. A good reproduction of the observation, as shown in Figure 8, is obtained assuming a channel $\sim 20R_{\odot}$ long, where a 1-hr heat pulse of $\sim 10^{11}$ erg cm^{-2} s^{-1} is released. The pulse duration is well below the sound crossing time along the tube, which is the upper limit to trigger the pulsations (Reale, 2016). Despite the simplified single loop model and simple assumptions on the heating, the model is able to reproduce both the period and the amplitude of the observed pulsations, together with the flare envelope light curve. The implication of this model is that it is evidence for a very long flaring magnetic tube, so long as to connect the star to the surrounding disk, as shown

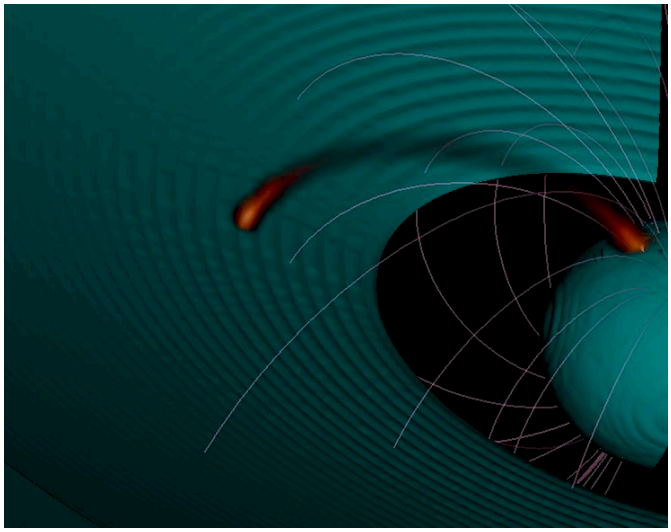

Fig. 9 Possible scenario of the flaring magnetic tube in the V772 Ori flare. The framework is a young stellar object surrounded by an accretion disk (cyan, Romanova et al., 2002) with a bundle of magnetic field lines (white lines). The flare X-ray emission from the simulation is mapped along a tube around a magnetic field line with a constant cross section (volumetric rendering, linear red scale) that links the star to the disk and $\approx 20 R_{\odot}$ long (from Reale et al., 2018).

in Figure 9. In turn, such a strong mass and energy exchange between the star and the disk may drive strong perturbations to the disk and to trigger more mass accretion (Orlando et al., 2011). Therefore, the observation of coherent quasi-periodic pulsations in stellar flares becomes a very important probe for physical conditions in young stellar systems.

3.4 Observations of stellar flare QPPs in UV/EUV: a possible clue to MHD wave activities

The coronae of the Sun and Sun-like stars emit optically-thin radiation in UV/EUV, which delivers important information about the ongoing dynamics of the emitting regions. There are plenty of examples obtained in the EUV emission of different kinds of MHD wave activities in the solar corona, either in direct imaging or in the form of time-resolved QPPs. However, there are just a few examples of UV/EUV QPPs coming from the stellar coronae, which also possibly provides possible clues to MHD wave activity occurring there.

As far as we know, the first detection of stellar flare QPPs in the UV range was presented by Welsh et al. (2006). Light curves for flares on four nearby dMe-type stars (GJ 3685A, CR Dra, AF Psc, and SDSS J084425.9+513830.5) were obtained with the GALEX satellite in the near-ultraviolet (NUV: $1750 - 2800$ Å) and far-ultraviolet (FUV: $1350 - 1750$ Å) with high temporal resolution (< 0.01 s). Significant oscillations were detected during the flare events observed on all four stars, with the periods found in the range of 30 to 40 s. These observed stellar UV QPPs could be interpreted as acoustic waves in the stellar flaring loops (mechanism [4]) of length $\simeq 10^9$ cm (less than 1/10th of the stellar radii of these M-dwarfs) for an assumed plasma temperature of $[5-20]\times 10^6$ K. Of course, other mechanisms for these QPPs cannot be ruled out yet.

Doyle et al. (2018) detected QPPs on several dMe stars (AF Psc, CR Dra, GJ 3685A, Gl 65, SDSS J084425.9+513830, and SDSS J144738.47+035312.1) in GALEX NUV light curves, in the rising and peak flare phases, suggesting that the QPPs are generated by periodic reconnection driven by large-scale magnetoacoustic waves interacting with the flare current sheets, as often assumed for solar flares (mechanism [6]). Some of these flares also showed QPPs in the decay phases that were interpreted as the presence of fast sausage mode oscillations either driven externally by some quasi-periodic drivers (such as the oscillatory reconnection, mechanism [9]) or intrinsically in the post-flare loop system (mechanism [1]).

As articulated above, the UV/EUV spectral window may provide us with the transparent light from stellar coronae modulated by certain wave activity or the activity related to the transient energy release processes in the stellar flaring loops. This aspect is less explored in the context of the stellar flares, and large-scale campaigns should be conducted to observe UV/EUV QPPs in stellar flares and perform diagnostics of the flaring regions based on the solar-stellar analogy.

3.5 On multiwavelength observations of stellar flare QPPs

As in the solar case, multiwavelength observations of QPPs in stellar flares could provide crucial hints about the origin of the pulsations. To date, stellar flare QPPs at several wavelengths within the same spectral range have been observed in optical (e.g. Zhilyaev et al., 2000, see Section 3.1.1), radio (see Section 3.2) and soft X-rays (Broomhall et al., 2019b, see Section 3.3.2). However, no QPPs occurring simultaneously in different spectral ranges (e.g. X-rays and optical) have been detected so far – which it is assumed is due mostly to the technical limitations. For example, Guarcello et al. (2019) analyzed stellar flares observed simultaneously in optical (with *Kepler*) and soft X-ray (with XMM-Newton) ranges, and detected

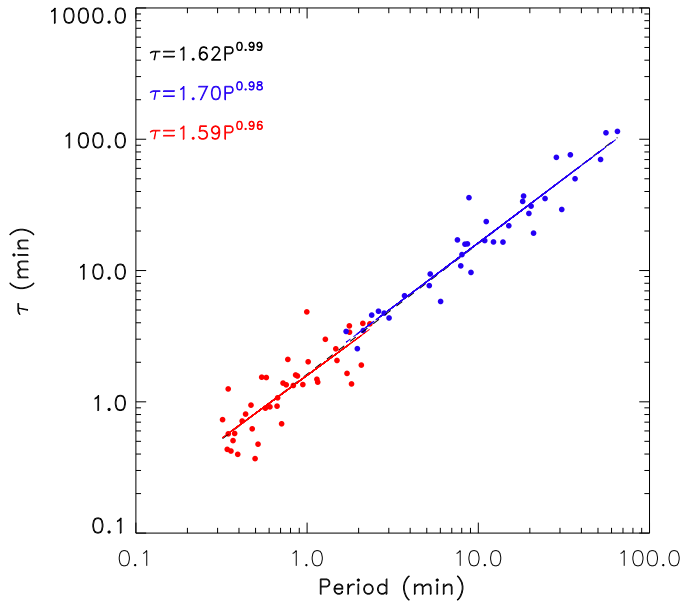

Fig. 10 Damping time, τ, as a function of period of X-ray QPPs in solar (red) and stellar (blue) flares. The blue and red straight lines represent the best-fitting power-law dependencies. The black dashed line is the least-squares approximation of the combined dataset, composed of both solar and stellar flare QPPs. Figure taken from Cho et al. (2016) with the permission of the authors.

QPPs with a period of 500 ± 100 s in the X-ray light curve at the decay phase of a flare at the M2 class star HCG 273. However, the time resolution of the simultaneous *Kepler* observations (30 min) was insufficient to detect any associated pulsations in the optical range.

3.6 Statistical Studies of QPPs in stellar flares

Statistical studies of flare pulsations have become topical in the stellar domain. Balona et al. (2015) analyzed 257 stellar flare light curves in white light and found that only seven flares show clearly damped oscillations in the decay phase, typical in solar flares - an occurrence rate of less than 3%. It was found that the periods of QPPs are not correlated with any stellar parameters. The authors also found that 18% of flares showed a distinct bump in the decay phase, which could hardly be interpreted as a result of simultaneous multiple flares. It was found that the period of the bump did not correlate with any stellar parameter. Pugh et al. (2016) performed a statistical study of 1439 flares from 216 different stars observed in white light by *Kepler*, finding 56 instances of a QPP signature. Similar to the Balona et al. (2015) result, this corresponds to only a ∼4% occurrence rate. This study found that the QPP periods were not correlated with stellar temperature, radius, rotation period, or surface gravity, suggesting that the QPPs

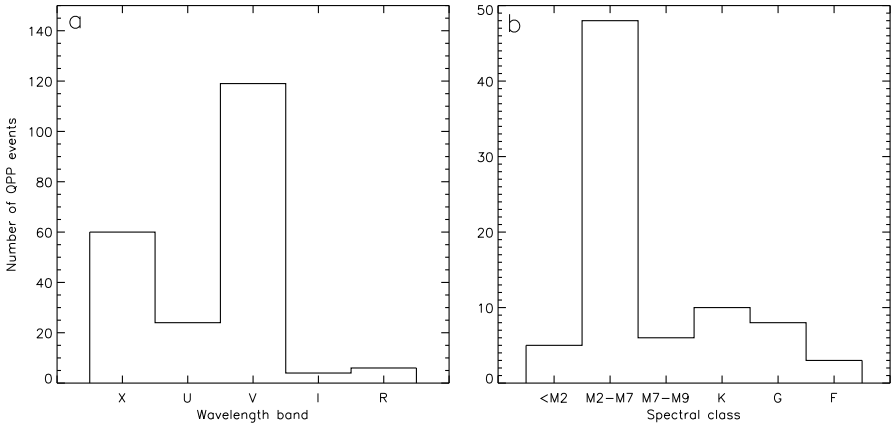

Fig. 11 The number of detected QPP events in stellar flares as a function of (a) observational wavelength band and (b) stellar spectral class. The sample parameters are mostly provided by the statistical studies given in Section 3.6 and also by the case studies given in Sections 3.1 - 3.4. The number of samples in panels (a) and (b) are 213 and 80, respectively.

are independent of global stellar parameters and likely to be result of processes occurring in local environments. It was also found that the QPP period is not correlated with flare energy. Crucially however, it was found that the observed period scales with the QPP decay time.

Cho et al. (2016) observed 42 solar flares with pronounced X-ray QPPs as observed with RHESSI, and 36 stellar flares with X-ray QPPs as observed with XMM-Newton. The empirical mode decomposition (EMD) method and least-squares fit by a damped sinusoidal function were applied to obtain the periods (P) and damping times (τ) of both the solar and stellar flare QPPs. The authors reported that the periods and damping times of the stellar flare QPPs are $P = 16.21 \pm 15.86$ min and $\tau = 27.21 \pm 28.73$ min, while those of the solar flare QPPs are $P = 0.90 \pm 0.56$ and $\tau = 1.53 \pm 1.10$ min, respectively. It was noticed that the ratios of the damping times to the periods observed in the stellar QPPs ($\tau/P = 1.69 \pm 0.56$) are statistically identical to those of solar QPPs ($\tau/P = 1.74 \pm 0.77$). It was estimated that the scalings of the QPP damping time with the period are well described by a power law in both solar and stellar cases (Figure 10). The power indices of the solar and stellar flare QPPs are found to be 0.96 ± 0.10 and 0.98 ± 0.05, respectively. These estimated scaling are found to be consistent with the scalings for the standing slow magnetoacoustic (mechanism [4]) and kink modes (mechanism [2]) in solar coronal loops. This analysis provides a comprehensive physical picture that the underlying mechanism responsible for the stellar QPPs (at least of some type) can be the natural magnetohydrodynamic oscillation in the flaring loops simply identical to the case of the solar flare-driven MHD oscillations.

To conclude this section, we now consider all the available global parameters of the flare-active stars where QPPs have been detected in various wavelength bands, based on the case studies reviewed in Sections 3.1–3.4 and the statistical studies described above. In total, this sample contains 213 QPP events and, for

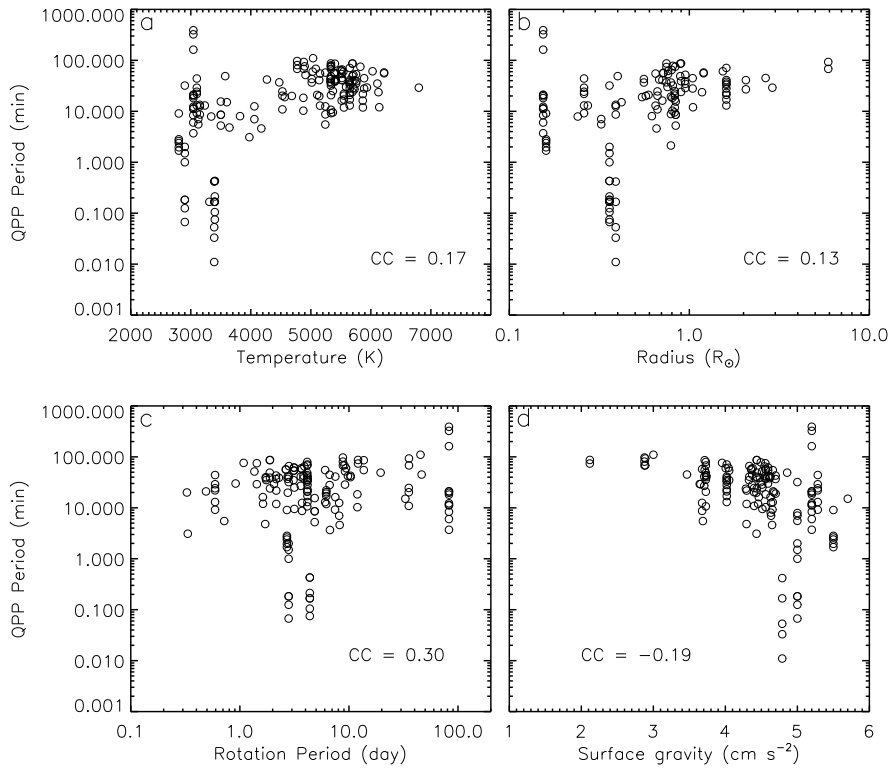

Fig. 12 Scatter-plots of QPP periods in stellar flares as a function of (a) stellar surface temperature, (b) radius, (c) rotation period, and (d) surface gravity. The sample parameters are mostly provided by the statistical studies given in Section 3.6 and also by the case studies given in Sections 3.1 – 3.4. The number of the samples in four panels is 169, 129, 151, and 149, respectively. The values of the linear correlation coefficient (CC) are shown in the panels.

each event, information on the wavelength range of the QPP observation is available. More than half of the QPPs were detected in the visible range (V), mainly due to the observations by the *Kepler* observatory (see Figure 11a). Furthermore, in descending order, there are QPP events detected in the ranges of X-ray, UV, radio and infrared radiation. The total number of QPP events with information on the spectral type of host stars is 80 (Figure 11b). It is striking that most of the QPPs were observed on red dwarfs of spectral classes M2–M7. This is not surprising, since such stars are very numerous, demonstrate very high flare activity and have received a lot of attention (e.g. Gershberg, 2005). The dependencies of the QPP periods on stellar temperature, stellar radius, rotation period, and surface gravity are shown in Figure 12 for the samples of 169, 129, 151, and 149 events, respectively. It seems that there is only a very weak dependency between the QPP periods and global stellar parameters, but no strong and obvious correlation. Besides, the QPP periods for a given global parameter value have very large scatter.

4 Summary and prospects

The phenomenon of QPPs in solar and stellar flares has been known and studied about 50 years (Parks and Winckler, 1969; Rodono, 1974). Over the past five decades, great progress has been made in studies of solar and stellar flares in general, and QPPs in particular. In this work, we have given an overview of the most important and interesting results on QPPs in solar flares, with an emphasis on the results of recent years, as well as on the analogy between QPPs in solar and stellar flares. Here, we will try to briefly summarize our view on the current state-of-the-art in QPP research:

QPPs in solar flares:

- QPPs are a common phenomenon accompanying many solar flares. They are observed in all ranges of the electromagnetic spectrum, from radio waves to γ-rays, at various stages of flares. QPPs are observed both in very weak flare events (such as microflares and bright X-ray points) and in the most powerful flares. Recent statistical studies have shown different probabilities of occurrence of QPPs in powerful solar flares (above M5), from 30% to 90%. The difference can be interpreted by the fact that the significance of the quasi-periodicity was determined using different methods and criteria, for data from different instruments in different ranges of the spectrum, on different samples of events. Nevertheless, it can be concluded that QPPs are not rare and not 'black sheep' — they occur in a large percentage of powerful solar flares. The probability of detecting QPPs decreases with decreasing flare magnitude. This may be due to the lower signal-to-noise ratio for these events. The question of the actual prevalence of QPPs in solar flares is still open. It is necessary to conduct further statistical studies based on new methods for determining the significance of quasi-periodicity and more precise observational data in various ranges of the spectrum. Since they are established as a regularly occurring phenomenon, QPPs remain a critical attribute of solar flares in that flare models must necessarily include mechanisms that naturally explain their appearance.

- To date, at least fifteen physical mechanisms / models have been proposed to explain QPPs in solar flares. According to Kupriyanova et al. (2020), they can be divided into three groups: (i) *direct modulation by MHD and electrodynamic oscillations of all types*, (ii) *modulation of the efficiency of energy release processes by MHD oscillations*, (iii) *spontaneous quasi-periodic energy release including quasi-periodic regimes of magnetic reconnection (DC-to-AC models)*. The division into these groups is not unambiguous. There is also another classification of the models by McLaughlin et al. (2018): (A) *oscillatory processes*, (B) *self-oscillatory processes*, (C) *autowave processes*. Some mechanisms, by their physical nature, can be attributed to several groups.

- There have been several hundred observational studies of QPPs in solar flares. Despite improvements in observation capabilities, it can be stated that for most events it has not yet been possible to draw an unambiguous conclusion about the underlying QPP mechanism. Usually, the observed QPPs can be interpreted simultaneously within the framework of several different mechanisms.

The problem is twofold: On the one hand, at present, most of the models are of a qualitative nature – it is not yet possible to quantitatively obtain all the necessary observational properties of the models for realistic conditions in flare regions. A serious drawback of most models is that they are developed within the MHD approximation and do not take into account the particle acceleration processes, which play a very important role in flares. It is necessary to follow the path of developing realistic 3D models, taking into account inhomogeneities along the PIL, the processes of acceleration and propagation of particles, as well as direct modelling of the emission of flare regions in different spectral ranges for a detailed comparison with observations of various instruments. On the other hand, modern observations usually do not yet provide all the necessary information about the physical properties of flare regions and sources of QPPs. It is extremely important to have detailed information about the spatial structure of QPP sources and their dynamics in different spectral ranges. It is also important to have reliable information on the geometry and dynamics of magnetic fields, electric currents and plasmas in the flare region for an adequate choice of the model. A promising avenue for the QPP-based solar coronal seismology is the detection of spatially-resolved multi-periodic, multi-modal QPPs.

QPPs in stellar flares:

– First of all, it is important to note that progress in the study of QPPs in stellar flares is largely based on the solar-stellar analogy. Based on numerous observations, it is assumed that physical processes in flare regions on the Sun and on other magnetoactive stars are of a similar nature; namely, flare processes occur in magnetic loop systems, where, as a result of reconnection, free magnetic energy can be transformed into other energy channels (kinetic energy of plasma and accelerated particles, electromagnetic radiation, various waves and oscillations). It is important to note that the presence of the QPPs themselves in stellar flares and the similarity of a number of their characteristics with the properties of QPPs in solar flares is in itself an important additional argument in favor of the existence of physical analogies between solar and stellar flares.

– Among the properties of QPPs in stellar flares, the following properties stand out as similar to those of QPPs in solar flares: (1) A similar range of characteristic periods from seconds to several minutes, although it should be noted that QPPs with periods of up to several hundred minutes are also found in stellar flares, which is possible, due to the fact that stellar flares can be much more powerful (superflares) and longer duration than solar flares; (2) Observation of QPPs in stellar flares in different spectral ranges, as well as in solar flares. However, it should be noted that QPPs in several principally different ranges (e.g. radio and optical) simultaneously have not yet been detected in stellar flares, which is probably due to the difficulties of multiwavelength observations of stellar flares; (3) The presence of multiperiodic QPPs in stellar flares; (4) Similar scaling for the ratios of the QPP decay time and period in solar and stellar flares. The last two properties are well-known characteristics of MHD oscillations of solar coronal loops; (5) Adequate explanation of X-ray QPPs in

flares in the star-formation regions using the hydrodynamic model of sloshing oscillations, which is also applicable to flare loops on the Sun; (6) Statistical studies indicate that the properties of flare QPPs do not explicitly depend on the global characteristics of parent stars, as well as on the physical parameters of parent active regions on the Sun. Also, no connection was found between the characteristics of QPPs and the flare magnitude. This indicates that the properties of QPPs in both solar and stellar flares are determined by local processes occurring in flare regions.

– Based on solar-stellar analogies, the same mechanisms (but with different parameters), developed for solar flares, are usually used to interpret QPPs in stellar flares. As in the interpretation of QPPs in solar flares, it is most often assumed that QPPs in stellar flares are associated either with MHD oscillations of coronal loops or with quasi-periodic regimes of magnetic reconnection. The assumption of MHD oscillations makes it possible to apply the methods of coronal MHD seismology to estimate the physical parameters of flare loops, such as the average temperature and plasma density, magnetic field, and electric current. For a number of stellar flares, it has been shown that the parameters of flare loops obtained using MHD seismology are close to those obtained by other independent methods. This gives rise to hope that the proposed mechanisms may indeed take place in the studied stellar flares. Nevertheless, estimates are still rather rough and do not exclude the possibility that QPPs may be the result of other mechanisms. It is necessary to be cautious about the estimates obtained and to develop additional diagnostic methods to verify the results. In general, the information available on stellar flares is still much scarcer than for solar flares. In all likelihood, the development of theories of stellar flare QPPs will proceed, as before, following the development of theories of solar flare QPPs.

– Further progress in studies of QPPs in stellar flares can also be associated with the implementation of sessions of multiwavelength observations of stellar flares using instruments with high temporal resolution (seconds) and high signal-to-noise ratio. Of particular interest are simultaneous observations of QPPs of thermal and non-thermal emissions (e.g. gyrosynchrotron emission of accelerated electrons in the radio range and bremsstrahlung X-ray radiation of heated plasma in flare loops). In particular, new results can be obtained in the radio range with the introduction of new instruments such as the *Square Kilometre Area* (SKA, e.g. Weltman et al. 2020). We also expect new data from the *Transiting Exoplanet Survey Satellite* (TESS) observations in the optical range with a cadence of 20 s (improving on the 120 s cadence provided in the initial prime mission). These data could provide many new possibilities for identifying stellar QPPs if the signal-to-noise ratio is sufficient. One important task is to understand whether the mechanisms of superflares on solar-type stars are similar to those of solar flares, and also to understand why QPPs in the optical continuum (in white light) have not yet been seen in solar flares, while there are now many white-light observations of QPPs in stellar flares.

Acknowledgements This work is an output of the international workshop "Oscillatory processes in solar and stellar coronae" held in ISSI-Bj, China, on October 14-18, 2019. We thank

ISSI-Bj for hosting this encouraging meeting. I.V.Z. is supported by the budgetary funding of Basic Research program “PLASMA”. J.A.M. acknowledges UK Science and Technology Facilities Council (STFC) support from grant ST/T000384/1. A.A.K. is supported by budgetary funding of Basic Research program II.16. D.Y.K. acknowledges support from the STFC consolidated grant ST/T000252/1 and the budgetary funding of Basic Research program No. II.16. H.T. is supported by the National Natural Science Foundation of China (NSFC) Grants No. 11825301 and No. 11790304(11790300). D.Y. is supported by NSFC (grants No. 11803005, 11911530690) and Shenzhen Technology Project (JCYJ20180306172239618). I.H.C. acknowledges support from the National Research Foundation of Korea (grang No. NRF-2019R1C1C1006033) and Korea Astronomy and Space Science Institute (Project No. 2020-1-850-07). D.J.P. was supported by the European Research Council (ERC) under the European Union’s Horizon 2020 research and innovation programme (grant agreement No 724326) and the C1 grant TRACEspace of Internal Funds KU Leuven.

Conflict of interest

The authors declare that they have no conflict of interest.

A Appendix: Model-Property Table

Here, in Table 1, we summarize the main expected properties of models (mechanisms) [1]-[15] discussed in Sections 2.4.1-2.4.3. Since most of the models are not yet fully developed, it is necessary to consider the given properties as preliminary and possible, but not as final and irrevocable. This table is a rough guide only and should be used with care when choosing the model to interpret the observations of QPPs in a particular flare. This table also partly reflects the current state of development of the models. In particular, it can be seen that analytical formulas for the periods of QPPs are not yet available for all models. Thus, the table also indicates the possible gaps and directions of development of the models.

Table 1: Possible observational properties of solar flare QPP mechanisms. (Designations: P - period, j - harmonic number, L - loop length, a - loop cross-section radius, Q - quality factor, C_{s0} and C_{A0} - sound and Alfvén speeds inside the loop, respectively, η_j - zeros of the Bessel function $J_0(\eta)$, C_k - kink speed, C_{T0} - internal tube speed, $S_{[17]}$ - loop cross-section measured in 10^{17} cm^2, $I_{0[11]}$ - equilibrium electric current in the loop measured in 10^{11} A, c - speed of light in vacuum, C_V and C_P - standard specific heat capacities, Q_ρ and Q_T - derivatives of the net plasma heating/cooling function with respect to the plasma density and temperature evaluated at the equilibrium.)

Signal shape in the time & frequency domains	**Intensity amplitude modulation**	**Periodicity**	**Source Structure & Emission**	**Peculiarities**
Group (i): Direct modulation by MHD and electrodynamic oscillations of all types				
[1] Standing sausage mode				
Narrow-band harmonic, possible presence of higher harmonics	Monotonic decreasing, from a few to a few tens of percent; $Q \simeq 10-100$	Seconds - tens of seconds; variations are possible due to changes of loop's parameters; $P_{GSM} = 2L/C_p$ (global trapped at $j=1$) or $P_{saus} = \frac{2\pi a}{\eta_j\sqrt{C_{s0}^2+C_{A0}^2}}$ (leaky at $j \geq 1$ & trapped at $j>1$)	Flare loops Thermal, non-thermal (compressive and LOS effects, modulation of non-thermal particle loss-cone and precipitation)	$\pi/2$ difference between intensity and Doppler shift; small-amplitude variations of flare loop cross-section (not yet resolved)
[2] Standing kink mode				
Narrow-band harmonic, possible presence of higher harmonics	Mainly monotonic decreasing with $Q \simeq 1-6$	Tens of seconds - a few tens of minutes; variations are possible due to changes of loop's parameters, $P_{kink} = 2L/jC_k$	Flare loops Thermal, non-thermal (LOS effects, no particle acceleration)	Quasi-periodic intensity variations are due to changes of angle between LOS and loop's axis (magnetic field direction)
[4] Standing slow mode				
Narrow-band harmonic, possible presence of higher harmonics	Mainly monotonic decreasing with $Q \simeq 1-2$	Tens of minutes; variations are possible due to changes of loop's parameters (i.e. density, temperature, and magnetic field perturbations), $P_{slow} = 2L/jC_{T0}$	Flare loops Mainly thermal, could be non-thermal (e.g. Razin suppression effect, modulation of non-thermal bremsstrahlung)	Amplitude could increase due to thermal overstability (see mechanism [10])

Signal shape in the time & frequency domains	**Intensity amplitude modulation**	**Periodicity**	**Source Structure & Emission**	**Peculiarities**
[5] RLC contour				
Narrow-band harmonic	Monotonic decreasing with high Q-factor	Minutes and more; modulation by oscillations of electric current in the loop, $P_{RLC} \simeq 10 \times S_{[17]}/I_{0[11]}$	Flare loops Thermal, non-thermal (periodic plasma heating & particle acceleration is possible; modulation of microwave emission due to oscillations of magnetic field)	Presence of strong ($\gtrsim 10^{10}$ A) vertical electric currents in the loop's footpoints
[13] Dispersive wave trains				
Broadband (tadpole)	Non-monotonic wave train	Tens of seconds with, e.g., $\approx P_{saus}$ in leaky regime	Various open structures, e.g. coronal fan, current sheet, also coronal loops Thermal, non-thermal (particle acceleration could be possible, e.g., if there is a steepening of the fronts to shocks	
Group (ii): Modulation of the efficiency of energy release processes by MHD oscillations				
[6] Reconnection triggered by MHD waves				
Quasi-periodic asymmetric bursts (fast rise, slower decay) or symmetric triangular bursts; pronounced higher harmonics in the spectrum	Irregular, up to 100%, no pronounce decay	Seconds - a few tens of minutes; irregular if trigger is aperiodic (i.e. propagating fast wave pulse) or regular if trigger is periodic (e.g. external kink or leaky sausage modes)	Different geometries are possible, the presence of X-point or X-line is needed Thermal, non-thermal (particle acceleration)	Requires an external source of waves (e.g. oscillating loop, propagating fast wave, three-, five-minute oscillations, etc.)
[7] Reconnection triggered by MHD autowave processes				

Signal shape in the time & frequency domains	**Intensity amplitude modulation**	**Periodicity**	**Source Structure & Emission**	**Peculiarities**
Quasi-periodic asymmetric bursts (fast rise, slower decay)	Irregular, up to 100%	Fraction of seconds - tens of minutes	Flare arcade of loops with longitude electric currents or flare arcade with a current sheet above Thermal, non-thermal (particle acceleration)	Systematic progression of energy release source and emission sources along PIL
[8] Reconnection triggered by flapping oscillations				
Quasi-periodic asymmetric bursts (fast rise, slower decay)	Irregular, up to 100%	Fraction of seconds - tens of minutes	Current sheet above a flare arcade Thermal, non-thermal (particle acceleration)	Systematic progression of energy release source and emission sources along PIL
[12] Magnetic tuning fork				
Quasi-periodic asymmetric bursts (fast rise, slower decay)	Irregular, up to 100%	Seconds - minutes	Current sheet and flare loop/arcade, above-the-loop-top source Thermal, non-thermal (particle acceleration) is possible	Simultaneous presence of both QPPs and QPFs with equal periods
[14] KHI in loop-top				
Narrow-band harmonic, possible presence of higher harmonics	Decreasing	Seconds – tens of seconds	Flare loop-top Thermal	QPPs appear after chromospheric evaporation
[15] Thermal instability of current layer				
Quasi-periodic asymmetric bursts (fast rise, slower decay)	Irregular, up to 100%	Seconds – tens of minutes	Current sheet above a flare arcade Thermal, non-thermal (possible particle acceleration)	Alternating hotter and colder loops in a flare arcade
Group (iii): Spontaneous quasi-periodic energy release (DC-to-AC models)				
[9] Self-oscillatory processes				

Signal shape in the time & frequency domains	**Intensity amplitude modulation**	**Periodicity**	**Source Structure & Emission**	**Peculiarities**
Quasi-periodic asymmetric bursts (fast rise, slower decay); power-law spectral shape is possible	Irregular, up to 100%	Seconds - minutes	Various structures with X-points or X-lines, current sheets Thermal, non-thermal (particle acceleration)	Reconfiguration of magnetic structure due to reconnection
[10] Thermal overstability of standing slow waves or propagating dispersive slow wave trains				
Increasing or stable amplitude	High	A few minutes to tens of minutes. For standing waves, period coincides with the acoustic period; for propagating slow wave trains period is prescribed by properties of the coronal heating and cooling functions, $P_{TM} \simeq \sqrt{\frac{C_V C_P}{Q_\rho Q_T}}$	Flare loops Thermal	
[11] Periodic regimes of coalescence of twisted loops				
Quasi-periodic asymmetric bursts (fast rise, slower decay); double-peak bursts are possible	Decreasing; up to 100%	Seconds - minutes	E.g. two interacting loops, erupting flux rope and overlying arcade, merging plasmoids Thermal, non-thermal (particle acceleration)	Interacting current-carrying magnetic structures

References

Abada-Simon M, Lecacheux A, Aubier M, Bookbinder JA (1995) High-Resolution Dynamic Spectrum of a Spectacular Radio Burst from AD Leonis, vol 454, p 32. DOI 10.1007/3-540-60057-4_224

Altyntsev A, Meshalkina N, Mészárosová H, Karlický M, Palshin V, Lesovoi S (2016) Sources of Quasi-periodic Pulses in the Flare of 18 August 2012. Solar Phys. 291(2):445–463, DOI 10.1007/s11207-016-0846-9, 1601.02332

Altyntsev A, Lesovoi S, Globa M, Gubin A, Kochanov A, Grechnev V, Ivanov E, Kobets V, Meshalkina N, Muratov A, Prosovetsky D, Myshyakov I, Uralov A, Fedotova A (2020) Multiwave Siberian Radioheliograph. Solar-Terrestrial Physics 6(2):30–40, DOI 10.12737/stp-62202003

Andrews AD (1989a) Investigation of micro-flaring and secular and quasi-periodic variations in dMe flare stars. I. Suspected ultra-short "waves" in the dM2-3estar V1285 Aquilae. Astron. Astrophys. 210:303–310

Andrews AD (1989b) Investigation of micro-flaring and secular and quasi-periodic variations in the dMe flare stars. II. "Time signatures" of micro-variabilityin V1285 Aquilae, V645 Centauri, V1054 Ophiuchi and AU Microscopii. Astron. Astrophys. 214:220–226

Andrews AD (1990) Investigation of micro-flaring and secular and quasi-periodic variations in dMe flare stars. III. Micro-variability of AT MIC following a stellar flare. Astron. Astrophys. 227:456–464

Anfinogentov S, Nakariakov VM (2016) Motion Magnification in Coronal Seismology. Solar Phys. 291(11):3251–3267, DOI 10.1007/s11207-016-1013-z, 1611.01790

Anfinogentov S, Nakariakov VM, Mathioudakis M, Van Doorsselaere T, Kowalski AF (2013a) The Decaying Long-period Oscillation of a Stellar Megaflare. Astrophys. J. 773(2):156, DOI 10.1088/0004-637X/773/2/156

Anfinogentov S, Nisticò G, Nakariakov VM (2013b) Decay-less kink oscillations in coronal loops. Astron. Astrophys. 560:A107, DOI 10.1051/0004-6361/201322094

Anfinogentov SA, Nakariakov VM, Nisticò G (2015) Decayless low-amplitude kink oscillations: a common phenomenon in the solar corona? Astron. Astrophys. 583:A136, DOI 10.1051/0004-6361/201526195, 1509.05519

Anfinogentov SA, Stupishin AG, Mysh'yakov II, Fleishman GD (2019) Record-breaking Coronal Magnetic Field in Solar Active Region 12673. Astrophys. J. Lett. 880(2):L29, DOI 10.3847/2041-8213/ab3042, 1907.06398

Antolin P, Van Doorsselaere T (2013) Line-of-sight geometrical and instrumental resolution effects on intensity perturbations by sausage modes. Astron. Astrophys. 555:A74, DOI 10.1051/0004-6361/201220784, 1303.6147

Antolin P, De Moortel I, Van Doorsselaere T, Yokoyama T (2017) Observational Signatures of Transverse Magnetohydrodynamic Waves and Associated Dynamic Instabilities in Coronal Flux Tubes. Astrophys. J. 836(2):219, DOI 10.3847/1538-4357/aa5eb2

Argiroffi C, Peres G, Orlando S, Reale F (2008) The flaring and quiescent components of the solar corona. Astron. Astrophys. 488(3):1069–1077, DOI 10.1051/0004-6361:200809355, 0805.2685

Argiroffi C, Caramazza M, Micela G, Sciortino S, Moraux E, Bouvier J, Flaccomio E (2016) Supersaturation and activity-rotation relation in PMS stars: the young cluster h Persei. Astron. Astrophys. 589:A113, DOI 10.1051/0004-6361/201526539, 1602.03696

Arregui I, Oliver R, Ballester JL (2012) Prominence Oscillations. Living Reviews in Solar Physics 9(1):2, DOI 10.12942/lrsp-2012-2

Artemyev A, Zimovets I (2012) Stability of Current Sheets in the Solar Corona. Solar Phys. 277(2):283–298, DOI 10.1007/s11207-011-9908-1

Aschwanden MJ (1987) Theory of Radio Pulsations in Coronal Loops. Solar Phys. 111(1):113–136, DOI 10.1007/BF00145445

Aschwanden MJ (2002) Particle acceleration and kinematics in solar flares - A Synthesis of Recent Observations and Theoretical Concepts (Invited Review). Space Sci. Rev. 101(1):1–227, DOI 10.1023/A:1019712124366

Aschwanden MJ (2003) Review of Coronal Oscillations - An Observer's View. arXiv e-prints astro-ph/0309505, astro-ph/0309505

Aschwanden MJ (2005) Physics of the Solar Corona. An Introduction with Problems and Solutions (2nd edition)

Aschwanden MJ, Peter H (2017) The Width Distribution of Loops and Strands in the Solar

Corona—Are We Hitting Rock Bottom? Astrophys. J. 840(1):4, DOI 10.3847/1538-4357/aa6b01, 1701.01177

Aschwanden MJ, Schrijver CJ (2011) Coronal Loop Oscillations Observed with Atmospheric Imaging Assembly—Kink Mode with Cross-sectional and Density Oscillations. Astrophys. J. 736(2):102, DOI 10.1088/0004-637X/736/2/102, 1105.2191

Aschwanden MJ, Kosugi T, Hudson HS, Wills MJ, Schwartz RA (1996) The Scaling Law between Electron Time-of-Flight Distances and Loop Lengths in Solar Flares. Astrophys. J. 470:1198, DOI 10.1086/177943

Aschwanden MJ, Fletcher L, Schrijver CJ, Alexander D (1999) Coronal Loop Oscillations Observed with the Transition Region and Coronal Explorer. Astrophys. J. 520(2):880–894, DOI 10.1086/307502

Aschwanden MJ, Caspi A, Cohen CMS, Holman G, Jing J, Kretzschmar M, Kontar EP, McTiernan JM, Mewaldt RA, O'Flannagain A, Richardson IG, Ryan D, Warren HP, Xu Y (2017) Global Energetics of Solar Flares. V. Energy Closure in Flares and Coronal Mass Ejections. Astrophys. J. 836(1):17, DOI 10.3847/1538-4357/836/1/17, 1701.01176

Baker D, van Driel-Gesztelyi L, Brooks DH, Valori G, James AW, Laming JM, Long DM, Démoulin P, Green LM, Matthews SA, Oláh K, Kővári Z (2019) Transient Inverse-FIP Plasma Composition Evolution within a Solar Flare. Astrophys. J. 875(1):35, DOI 10.3847/1538-4357/ab07c1, 1902.06948

Balona LA (2012) Kepler observations of flaring in A-F type stars. Mon. Not. Roy. Astron. Soc. 423(4):3420–3429, DOI 10.1111/j.1365-2966.2012.21135.x

Balona LA (2013) Activity in A-type stars. Mon. Not. Roy. Astron. Soc. 431(3):2240–2252, DOI 10.1093/mnras/stt322

Balona LA, Broomhall AM, Kosovichev A, Nakariakov VM, Pugh CE, Van Doorsselaere T (2015) Oscillations in stellar superflares. Mon. Not. Roy. Astron. Soc. 450(1):956–966, DOI 10.1093/mnras/stv661, 1504.01491

Bárta M, Büchner J, Karlický M, Kotrč P (2011) Spontaneous Current-layer Fragmentation and Cascading Reconnection in Solar Flares. II. Relation to Observations. Astrophys. J. 730(1):47, DOI 10.1088/0004-637X/730/1/47, 1011.6069

Bastian TS (1994) Stellar flares. Space Sci. Rev. 68(1-4):261–274, DOI 10.1007/BF00749152

Bastian TS, Bookbinder J, Dulk GA, Davis M (1990) Dynamic Spectra of Radio Bursts from Flare Stars. Astrophys. J. 353:265, DOI 10.1086/168613

Benz AO (2017) Flare Observations. Living Reviews in Solar Physics 14(1):2, DOI 10.1007/s41116-016-0004-3

Benz AO, Güdel M (2010) Physical Processes in Magnetically Driven Flares on the Sun, Stars, and Young Stellar Objects. Annu. Rev. Astron. Astrophys. 48:241–287, DOI 10.1146/annurev-astro-082708-101757

Benz AO, Guedel M (1994) X-ray/microwave ratio of flares and coronae. Astron. Astrophys. 285:621–630

Bhattacharjee A, Huang YM, Yang H, Rogers B (2009) Fast reconnection in high-Lundquist-number plasmas due to the plasmoid Instability. Physics of Plasmas 16(11):112102, DOI 10.1063/1.3264103, 0906.5599

Bogachev SA, Somov BV, Kosugi T, Sakao T (2005) The Motions of the Hard X-Ray Sources in Solar Flares: Images and Statistics. Astrophys. J. 630(1):561–572, DOI 10.1086/431918

Borucki WJ, Koch D, Basri G, Batalha N, Brown T, Caldwell D, Caldwell J, Christensen-Dalsgaard J, Cochran WD, DeVore E, Dunham EW, Dupree AK, Gautier TN, Geary JC, Gilliland R, Gould A, Howell SB, Jenkins JM, Kondo Y, Latham DW, Marcy GW, Meibom S, Kjeldsen H, Lissauer JJ, Monet DG, Morrison D, Sasselov D, Tarter J, Boss A, Brownlee D, Owen T, Buzasi D, Charbonneau D, Doyle L, Fortney J, Ford EB, Holman MJ, Seager S, Steffen JH, Welsh WF, Rowe J, Anderson H, Buchhave L, Ciardi D, Walkowicz L, Sherry W, Horch E, Isaacson H, Everett ME, Fischer D, Torres G, Johnson JA, Endl M, MacQueen P, Bryson ST, Dotson J, Haas M, Kolodziejczak J, Van Cleve J, Chandrasekaran H, Twicken JD, Quintana EV, Clarke BD, Allen C, Li J, Wu H, Tenenbaum P, Verner E, Bruhweiler F, Barnes J, Prsa A (2010) Kepler Planet-Detection Mission: Introduction and First Results. Science 327(5968):977, DOI 10.1126/science.1185402

Brasseur CE, Osten RA, Fleming SW (2019) Short-duration Stellar Flares in GALEX Data. Astrophys. J. 883(1):88, DOI 10.3847/1538-4357/ab3df8, 1908.08377

Briggs KR, Güdel M, Telleschi A, Preibisch T, Stelzer B, Bouvier J, Rebull L, Audard M, Scelsi L, Micela G, Grosso N, Palla F (2007) The X-ray activity-rotation relation of T Tauri stars in Taurus-Auriga. Astron. Astrophys. 468(2):413–424, DOI 10.1051/0004-6361:20066823,

astro-ph/0701422
Broomhall AM, Davenport JRA, Hayes LA, Inglis AR, Kolotkov DY, McLaughlin JA, Mehta T, Nakariakov VM, Notsu Y, Pascoe DJ, Pugh CE, Van Doorsselaere T (2019a) A Blueprint of State-of-the-art Techniques for Detecting Quasi-periodic Pulsations in Solar and Stellar Flares. Astrophys. J. Suppl. 244(2):44, DOI 10.3847/1538-4365/ab40b3, 1910.08458
Broomhall AM, Thomas AEL, Pugh CE, Pye JP, Rosen SR (2019b) Multi-waveband detection of quasi-periodic pulsations in a stellar flare on EK Draconis observed by XMM-Newton. Astron. Astrophys. 629:A147, DOI 10.1051/0004-6361/201935653, 1908.06033
Brosius JW, Daw AN (2015) Quasi-periodic Fluctuations and Chromospheric Evaporation in a Solar Flare Ribbon Observed by IRIS. Astrophys. J. 810(1):45, DOI 10.1088/0004-637X/810/1/45
Brosius JW, Daw AN, Inglis AR (2016) Quasi-periodic Fluctuations and Chromospheric Evaporation in a Solar Flare Ribbon Observed by Hinode/EIS, IRIS, and RHESSI. Astrophys. J. 830(2):101, DOI 10.3847/0004-637X/830/2/101
Brown RL, Crane PC (1978) On the rapidly variable circular polarization of HR 1099 at radio frequencies. Astron. J. 83:1504–1509, DOI 10.1086/112352
Cai Q, Shen C, Raymond JC, Mei Z, Warmuth A, Roussev II, Lin J (2019) Investigations of a supra-arcade fan and termination shock above the top of the flare-loop system of the 2017 September 10 event. Mon. Not. Roy. Astron. Soc. 489(3):3183–3199, DOI 10.1093/mnras/stz2167
Cantiello M, Braithwaite J (2019) Envelope Convection, Surface Magnetism, and Spots in A and Late B-type Stars. Astrophys. J. 883(1):106, DOI 10.3847/1538-4357/ab3924, 1904.02161
Chelpanov AA, Kobanov NI (2018) Oscillations Accompanying a He i 10830 Å Negative Flare in a Solar Facula. Solar Phys. 293(11):157, DOI 10.1007/s11207-018-1378-2, 1810.10153
Chen B, Bastian TS, Shen C, Gary DE, Krucker S, Glesener L (2015a) Particle acceleration by a solar flare termination shock. Science 350(6265):1238–1242, DOI 10.1126/science.aac8467, 1512.02237
Chen PF, Priest ER (2006) Transition-Region Explosive Events: Reconnection Modulated by p-Mode Waves. Solar Phys. 238(2):313–327, DOI 10.1007/s11207-006-0215-1
Chen SX, Li B, Xiong M, Yu H, Guo MZ (2015b) Standing Sausage Modes in Nonuniform Magnetic Tubes: An Inversion Scheme for Inferring Flare Loop Parameters. Astrophys. J. 812(1):22, DOI 10.1088/0004-637X/812/1/22, 1509.01442
Chen X, Yan Y, Tan B, Huang J, Wang W, Chen L, Zhang Y, Tan C, Liu D, Masuda S (2019) Quasi-periodic Pulsations before and during a Solar Flare in AR 12242. Astrophys. J. 878(2):78, DOI 10.3847/1538-4357/ab1d64
Cheng X, Li Y, Wan LF, Ding MD, Chen PF, Zhang J, Liu JJ (2018) Observations of Turbulent Magnetic Reconnection within a Solar Current Sheet. Astrophys. J. 866(1):64, DOI 10.3847/1538-4357/aadd16, 1808.06071
Chin R, Verwichte E, Rowlands G, Nakariakov VM (2010) Self-organization of magnetoacoustic waves in a thermally unstable environment. Physics of Plasmas 17(3):032107, DOI 10.1063/1.3314721
Cho IH, Cho KS, Nakariakov VM, Kim S, Kumar P (2016) Comparison of Damped Oscillations in Solar and Stellar X-Ray flares. Astrophys. J. 830(2):110, DOI 10.3847/0004-637X/830/2/110
Contadakis M (2013) Transient high frequency optical oscillations on red dwarfs. In: 11th Hellenic Astronomical Conference, pp 43–43
Contadakis ME, Avgoloupis S, Seiradakis J, Zhilyaev BE, Romanyuk YO, Verlyuk IA, Svyatogorov OA, Khalack VR, Sergeev AV, Konstantinova-Antova RK, Antov AP, Bachev RS, Alekseev IY, Chalenko VE, Shakhovskoy DN (2004) Detection of high-frequency optical oscillation during the flare phase of EV Lac in 1999. Astronomische Nachrichten 325(5):427–432, DOI 10.1002/asna.200310250
Contadakis ME, Avgoloupis SJ, Seiradakis JH (2012) Detection of transient high frequency optical oscillations of the flare star YZ CMin. Astronomische Nachrichten 333(7):583, DOI 10.1002/asna.201111690
Contadakis ME, Avgoloupis SJ, Seiradakis JH (2013) Transient high frequency optical oscillations on two weak flares of the red dwarf V390 Auri. Astronomical and Astrophysical Transactions 28(1):9
Cooper FC, Nakariakov VM, Tsiklauri D (2003) Line-of-sight effects on observability of kink and sausage modes in coronal structures with imaging telescopes. Astron. Astrophys.

397:765–770, DOI 10.1051/0004-6361:20021556, astro-ph/0207167
Dal HA, Evren S (2010) A New Method for Classifying Flares of UV Ceti Type Stars: Differences Between Slow and Fast Flares. Astron. J. 140(2):483–489, DOI 10.1088/0004-6256/140/2/483, 1206.5791
Davenport JRA, Hawley SL, Hebb L, Wisniewski JP, Kowalski AF, Johnson EC, Malatesta M, Peraza J, Keil M, Silverberg SM, Jansen TC, Scheffler MS, Berdis JR, Larsen DM, Hilton EJ (2014) Kepler Flares. II. The Temporal Morphology of White-light Flares on GJ 1243. Astrophys. J. 797(2):122, DOI 10.1088/0004-637X/797/2/122, 1411.3723
De Moortel I, Hood AW, Ireland J (2002) Coronal seismology through wavelet analysis. Astron. Astrophys. 381:311–323, DOI 10.1051/0004-6361:20011659
De Pontieu B, Title AM, Lemen JR, Kushner GD, Akin DJ, Allard B, Berger T, Boerner P, Cheung M, Chou C, Drake JF, Duncan DW, Freeland S, Heyman GF, Hoffman C, Hurlburt NE, Lindgren RW, Mathur D, Rehse R, Sabolish D, Seguin R, Schrijver CJ, Tarbell TD, Wülser JP, Wolfson CJ, Yanari C, Mudge J, Nguyen-Phuc N, Timmons R, van Bezooijen R, Weingrod I, Brookner R, Butcher G, Dougherty B, Eder J, Knagenhjelm V, Larsen S, Mansir D, Phan L, Boyle P, Cheimets PN, DeLuca EE, Golub L, Gates R, Hertz E, McKillop S, Park S, Perry T, Podgorski WA, Reeves K, Saar S, Testa P, Tian H, Weber M, Dunn C, Eccles S, Jaeggli SA, Kankelborg CC, Mashburn K, Pust N, Springer L, Carvalho R, Kleint L, Marmie J, Mazmanian E, Pereira TMD, Sawyer S, Strong J, Worden SP, Carlsson M, Hansteen VH, Leenaarts J, Wiesmann M, Aloise J, Chu KC, Bush RI, Scherrer PH, Brekke P, Martinez-Sykora J, Lites BW, McIntosh SW, Uitenbroek H, Okamoto TJ, Gummin MA, Auker G, Jerram P, Pool P, Waltham N (2014) The Interface Region Imaging Spectrograph (IRIS). Solar Phys. 289(7):2733–2779, DOI 10.1007/s11207-014-0485-y, 1401.2491
Dennis BR, Tolbert AK, Inglis A, Ireland J, Wang T, Holman GD, Hayes LA, Gallagher PT (2017) Detection and Interpretation of Long-lived X-Ray Quasi-periodic Pulsations in the X-class Solar Flare on 2013 May 14. Astrophys. J. 836(1):84, DOI 10.3847/1538-4357/836/1/84, 1706.03689
Dolla L, Marqué C, Seaton DB, Van Doorsselaere T, Dominique M, Berghmans D, Cabanas C, De Groof A, Schmutz W, Verdini A, West MJ, Zender J, Zhukov AN (2012) Time Delays in Quasi-periodic Pulsations Observed during the X2.2 Solar Flare on 2011 February 15. Astrophys. J. Lett. 749(1):L16, DOI 10.1088/2041-8205/749/1/L16, 1203.6223
Dominique M, Zhukov AN, Dolla L, Inglis A, Lapenta G (2018) Detection of Quasi-Periodic Pulsations in Solar EUV Time Series. Solar Phys. 293(4):61, DOI 10.1007/s11207-018-1281-x
Doyle JG, Butler CJ, van den Oord GHJ, Kiang T (1990) A periodicity in the flaring rate on the eclipsing binary YY Geminorum. Astron. Astrophys. 232:83
Doyle JG, Kellett BJ, Byrne PB, Avgoloupis S, Mavridis LN, Seiradakis JH, Bromage GE, Tsuru T, Makishima K, Makishima K, McHardy IM (1991) Simultaneous detection of a large flare in the X-ray and optical regions on the RS CVn-type star II Peg. Mon. Not. Roy. Astron. Soc. 248:503, DOI 10.1093/mnras/248.3.503
Doyle JG, Shetye J, Antonova AE, Kolotkov DY, Srivastava AK, Stangalini M, Gupta GR, Avramova A, Mathioudakis M (2018) Stellar flare oscillations: evidence for oscillatory reconnection and evolution of MHD modes. Mon. Not. Roy. Astron. Soc. 475(2):2842–2851, DOI 10.1093/mnras/sty032
Dröoge F (1967) Beobachtungen solarer Radiobursts mit hoher Zeitauflösung. Zeitschr. Astrophys. 66:200
Duckenfield TJ, Goddard CR, Pascoe DJ, Nakariakov VM (2019) Observational signatures of the third harmonic in a decaying kink oscillation of a coronal loop. Astron. Astrophys. 632:A64, DOI 10.1051/0004-6361/201936822
Dulk GA, Marsh KA (1982) Simplified expressions for the gyrosynchrotron radiation from mildly relativistic, nonthermal and thermal electrons. Astrophys. J. 259:350–358, DOI 10.1086/160171
Edwin PM, Roberts B (1983) Wave Propagation in a Magnetic Cylinder. Solar Phys. 88(1-2):179–191, DOI 10.1007/BF00196186
Emslie AG (1981) An interacting loop model for solar flare bursts. Astrophys. Lett. 22:171–177
Emslie AG, Dennis BR, Shih AY, Chamberlin PC, Mewaldt RA, Moore CS, Share GH, Vourlidas A, Welsch BT (2012) Global Energetics of Thirty-eight Large Solar Eruptive Events. Astrophys. J. 759(1):71, DOI 10.1088/0004-637X/759/1/71, 1209.2654
Erkaev NV, Semenov VS, Biernat HK (2007) Magnetic Double-Gradient Instability and Flapping Waves in a Current Sheet. Phys. Rev. Lett. 99(23):235003, DOI 10.1103/PhysRevLett.

99.235003, 0707.0935
Erkaev NV, Semenov VS, Kubyshkin IV, Kubyshkina MV, Biernat HK (2009) MHD model of the flapping motions in the magnetotail current sheet. Journal of Geophysical Research (Space Physics) 114(A3):A03206, DOI 10.1029/2008JA013728
Fang X, Yuan D, Van Doorsselaere T, Keppens R, Xia C (2015) Modeling of Reflective Propagating Slow-mode Wave in a Flaring Loop. Astrophys. J. 813(1):33, DOI 10.1088/0004-637X/813/1/33, 1509.04536
Fang X, Yuan D, Xia C, Van Doorsselaere T, Keppens R (2016) The Role of Kelvin-Helmholtz Instability for Producing Loop-top Hard X-Ray Sources in Solar Flares. Astrophys. J. 833(1):36, DOI 10.3847/1538-4357/833/1/36
Favata F, Flaccomio E, Reale F, Micela G, Sciortino S, Shang H, Stassun KG, Feigelson ED (2005) Bright X-Ray Flares in Orion Young Stars from COUP: Evidence for Star-Disk Magnetic Fields? Astrophys. J. Suppl. 160(2):469–502, DOI 10.1086/432542, astro-ph/0506134
Feigelson ED, Broos P, Gaffney I James A, Garmire G, Hillenbrand LA, Pravdo SH, Townsley L, Tsuboi Y (2002) X-Ray-emitting Young Stars in the Orion Nebula. Astrophys. J. 574(1):258–292, DOI 10.1086/340936, astro-ph/0203316
Feigelson ED, Gaffney I James A, Garmire G, Hillenbrand LA, Townsley L (2003) X-Rays in the Orion Nebula Cluster: Constraints on the Origins of Magnetic Activity in Pre-Main-Sequence Stars. Astrophys. J. 584(2):911–930, DOI 10.1086/345811, astro-ph/0211049
Finn JM, Kaw PK (1977) Coalescence instability of magnetic islands. Physics of Fluids 20(1):72–78, DOI 10.1063/1.861709
Fitzpatrick R, Bhattacharjee A, Ma ZW, Linde T (2003) Wave driven magnetic reconnection in the Taylor problem. Physics of Plasmas 10(11):4284–4290, DOI 10.1063/1.1617983
Fleishman GD, Gary DE, Chen B, Kuroda N, Yu S, Nita GM (2020) Decay of the coronal magnetic field can release sufficient energy to power a solar flare. Science 367(6475):278–280, DOI 10.1126/science.aax6874
Fletcher L, Dennis BR, Hudson HS, Krucker S, Phillips K, Veronig A, Battaglia M, Bone L, Caspi A, Chen Q, Gallagher P, Grigis PT, Ji H, Liu W, Milligan RO, Temmer M (2011) An Observational Overview of Solar Flares. Space Sci. Rev. 159(1-4):19–106, DOI 10.1007/s11214-010-9701-8, 1109.5932
Foullon C, Verwichte E, Nakariakov VM, Fletcher L (2005) X-ray quasi-periodic pulsations in solar flares as magnetohydrodynamic oscillations. Astron. Astrophys. 440(2):L59–L62, DOI 10.1051/0004-6361:200500169
Fuhrmeister B, Liefke C, Schmitt JHMM, Reiners A (2008) Multiwavelength observations of a giant flare on CN Leonis. I. The chromosphere as seen in the optical spectra. Astron. Astrophys. 487(1):293–306, DOI 10.1051/0004-6361:200809379, 0807.2025
Gao DH, Chen PF, Ding MD, Li XD (2008) Simulations of the periodic flaring rate on YY Gem. Mon. Not. Roy. Astron. Soc. 384(4):1355–1362, DOI 10.1111/j.1365-2966.2007.12830.x, 0712.2300
Gao Q, Xin Y, Liu JF, Zhang XB, Gao S (2016) White-light Flares on Close Binaries Observed with Kepler. Astrophys. J. Suppl. 224(2):37, DOI 10.3847/0067-0049/224/2/37, 1602.07972
Gary DE, Hurford GJ (1994) Coronal Temperature, Density, and Magnetic Field Maps of a Solar Active Region Using the Owens Valley Solar Array. Astrophys. J. 420:903, DOI 10.1086/173614
Gary DE, Linsky JL, Dulk GA (1982) An unusual microwave flare with 56 second oscillations on the M dwarf L726-8 A. Astrophys. J. Lett. 263:L79–L83, DOI 10.1086/183928
Gary DE, Chen B, Dennis BR, Fleishman GD, Hurford GJ, Krucker S, McTiernan JM, Nita GM, Shih AY, White SM, Yu S (2018) Microwave and Hard X-Ray Observations of the 2017 September 10 Solar Limb Flare. Astrophys. J. 863(1):83, DOI 10.3847/1538-4357/aad0ef, 1807.02498
Gershberg RE (2005) Solar-Type Activity in Main-Sequence Stars. DOI 10.1007/3-540-28243-2
Getman KV, Flaccomio E, Broos PS, Grosso N, Tsujimoto M, Townsley L, Garmire GP, Kastner J, Li J, Harnden J F R, Wolk S, Murray SS, Lada CJ, Muench AA, McCaughrean MJ, Meeus G, Damiani F, Micela G, Sciortino S, Bally J, Hillenbrand LA, Herbst W, Preibisch T, Feigelson ED (2005) Chandra Orion Ultradeep Project: Observations and Source Lists. Astrophys. J. Suppl. 160(2):319–352, DOI 10.1086/432092, astro-ph/0410136
Getman KV, Feigelson ED, Micela G, Jardine MM, Gregory SG, Garmire GP (2008) X-Ray Flares in Orion Young Stars. II. Flares, Magnetospheres, and Protoplanetary Disks. Astrophys. J. 688(1):437–455, DOI 10.1086/592034, 0807.3007

Gizis JE, Paudel RR, Mullan D, Schmidt SJ, Burgasser AJ, Williams PKG (2017) K2 Ultracool Dwarfs Survey. II. The White Light Flare Rate of Young Brown Dwarfs. Astrophys. J. 845(1):33, DOI 10.3847/1538-4357/aa7da0, 1703.08745

Goddard CR, Nisticò G, Nakariakov VM, Zimovets IV (2016a) A statistical study of decaying kink oscillations detected using SDO/AIA. Astron. Astrophys. 585:A137, DOI 10.1051/0004-6361/201527341, 1511.03558

Goddard CR, Nisticò G, Nakariakov VM, Zimovets IV, White SM (2016b) Observation of quasi-periodic solar radio bursts associated with propagating fast-mode waves. Astron. Astrophys. 594:A96, DOI 10.1051/0004-6361/201628478, 1608.04232

Goddard CR, Nakariakov VM, Pascoe DJ (2019) Fast magnetoacoustic wave trains with time-dependent drivers. Astron. Astrophys. 624:L4, DOI 10.1051/0004-6361/201935401

Grechnev VV, Lesovoi SV, Smolkov GY, Krissinel BB, Zandanov VG, Altyntsev AT, Kardapolova NN, Sergeev RY, Uralov AM, Maksimov VP, Lubyshev BI (2003) The Siberian Solar Radio Telescope: the current state of the instrument, observations, and data. Solar Phys. 216(1):239–272, DOI 10.1023/A:1026153410061

Grigis PC, Benz AO (2005) The Evolution of Reconnection along an Arcade of Magnetic Loops. Astrophys. J. Lett. 625(2):L143–L146, DOI 10.1086/431147, astro-ph/0504436

Grigis PC, Benz AO (2008) Spectral Hardening in Large Solar Flares. Astrophys. J. 683(2):1180–1191, DOI 10.1086/589826, 0708.2472

Gruber D, Lachowicz P, Bissaldi E, Briggs MS, Connaughton V, Greiner J, van der Horst AJ, Kanbach G, Rau A, Bhat PN, Diehl R, von Kienlin A, Kippen RM, Meegan CA, Paciesas WS, Preece RD, Wilson-Hodge C (2011) Quasi-periodic pulsations in solar flares: new clues from the Fermi Gamma-Ray Burst Monitor. Astron. Astrophys. 533:A61, DOI 10.1051/0004-6361/201117077, 1107.2399

Gruszecki M, Nakariakov VM (2011) Slow magnetacoustic waves in magnetic arcades. Astron. Astrophys. 536:A68, DOI 10.1051/0004-6361/201117549

Guarcello MG, Micela G, Sciortino S, López-Santiago J, Argiroffi C, Reale F, Flaccomio E, Alvarado-Gómez JD, Antoniou V, Drake JJ, Pillitteri I, Rebull LM, Stauffer J (2019) Simultaneous Kepler/K2 and XMM-Newton observations of superflares in the Pleiades. Astron. Astrophys. 622:A210, DOI 10.1051/0004-6361/201834370, 1901.07263

Güdel M (2002) Stellar Radio Astronomy: Probing Stellar Atmospheres from Protostars to Giants. Annu. Rev. Astron. Astrophys. 40:217–261, DOI 10.1146/annurev.astro.40.060401.093806, astro-ph/0206436

Güdel M (2004) X-ray astronomy of stellar coronae. Astron. Astrophys. Rev. 12(2-3):71–237, DOI 10.1007/s00159-004-0023-2, astro-ph/0406661

Güdel M, Nazé Y (2009) X-ray spectroscopy of stars. Astron. Astrophys. Rev. 17(3):309–408, DOI 10.1007/s00159-009-0022-4, 0904.3078

Güdel M, Guinan EF, Skinner SL (1997) The X-Ray Sun in Time: A Study of the Long-Term Evolution of Coronae of Solar-Type Stars. Astrophys. J. 483(2):947–960, DOI 10.1086/304264

Guedel M, Benz AO (1993) X-Ray/Microwave Relation of Different Types of Active Stars. Astrophys. J. Lett. 405:L63, DOI 10.1086/186766

Guenther EW, Stelzer B, Neuhäuser R, Hillwig TC, Durisen RH, Menten KM, Greimel R, Barwig H, Englhauser J, Robb RM (2000) A multi-wavelength study of pre-main sequence stars in the Taurus-Auriga star-forming region. Astron. Astrophys. 357:206–218

Haisch B, Strong KT, Rodono M (1991) Flares on the Sun and other stars. Annu. Rev. Astron. Astrophys. 29:275–324, DOI 10.1146/annurev.aa.29.090191.001423

Hallinan G, Bourke S, Lane C, Antonova A, Zavala RT, Brisken WF, Boyle RP, Vrba FJ, Doyle JG, Golden A (2007) Periodic Bursts of Coherent Radio Emission from an Ultracool Dwarf. Astrophys. J. Lett. 663(1):L25–L28, DOI 10.1086/519790, 0705.2054

Hartmann L, Herczeg G, Calvet N (2016) Accretion onto Pre-Main-Sequence Stars. Annu. Rev. Astron. Astrophys. 54:135–180, DOI 10.1146/annurev-astro-081915-023347

Hayes LA, Gallagher PT, Dennis BR, Ireland J, Inglis AR, Ryan DF (2016) Quasi-periodic Pulsations during the Impulsive and Decay phases of an X-class Flare. Astrophys. J. Lett. 827(2):L30, DOI 10.3847/2041-8205/827/2/L30, 1607.06957

Hayes LA, Gallagher PT, Dennis BR, Ireland J, Inglis A, Morosan DE (2019) Persistent Quasi-periodic Pulsations during a Large X-class Solar Flare. Astrophys. J. 875(1):33, DOI 10.3847/1538-4357/ab0ca3, 1903.01328

Hayes LA, Inglis AR, Christe S, Dennis B, Gallagher PT (2020) Statistical Study of GOES X-Ray Quasi-periodic Pulsations in Solar Flares. Astrophys. J. 895(1):50, DOI 10.3847/

1538-4357/ab8d40, 2004.11775
Hood AW, Ruderman M, Pascoe DJ, De Moortel I, Terradas J, Wright AN (2013) Damping of kink waves by mode coupling. I. Analytical treatment. Astron. Astrophys. 551:A39, DOI 10.1051/0004-6361/201220617
Houdebine ER, Foing BH, Doyle JG, Rodono M (1993a) Dynamics of flares on late type dMe stars. II. Mass motions and prominence oscillations during a flare on AD Leonis. Astron. Astrophys. 274:245–264
Houdebine ER, Foing BH, Doyle JG, Rodono M (1993b) Dynamics of flares on late-type dMe stars. III. Kinetic energy and mass momentum budget of a flare on AD Leonis. Astron. Astrophys. 278:109–128
Huang J, Kontar EP, Nakariakov VM, Gao G (2016) Quasi-periodic Acceleration of Electrons in the Flare on 2012 July 19. Astrophys. J. 831(2):119, DOI 10.3847/0004-637X/831/2/119
Huang Z (2018) Magnetic Loops above a Small Flux-emerging Region Observed by IRIS, Hinode, and SDO. Astrophys. J. 869(2):175, DOI 10.3847/1538-4357/aaef86, 1811.03219
Hudson HS (2020) A correlation in the waiting-time distributions of solar flares. Mon. Not. Roy. Astron. Soc. 491(3):4435–4441, DOI 10.1093/mnras/stz3121, 1908.08749
Hurford GJ, Read RB, Zirin H (1984) A Frequency Angle Interferometer for Solar Microwave Spectroscopy. Solar Phys. 94(2):413–426, DOI 10.1007/BF00151327
Imanishi K, Tsujimoto M, Koyama K (2001) X-Ray Detection from Bona Fide and Candidate Brown Dwarfs in the ρ Ophiuchi Cloud with Chandra. Astrophys. J. 563(1):361–366, DOI 10.1086/323697
Inglis AR, Dennis BR (2012) The Relationship between Hard X-Ray Pulse Timings and the Locations of Footpoint Sources during Solar Flares. Astrophys. J. 748(2):139, DOI 10.1088/0004-637X/748/2/139, 1303.6309
Inglis AR, Nakariakov VM (2009) A multi-periodic oscillatory event in a solar flare. Astron. Astrophys. 493(1):259–266, DOI 10.1051/0004-6361:200810473
Inglis AR, Zimovets IV, Dennis BR, Kontar EP, Nakariakov VM, Struminsky AB, Tolbert AK (2011) Instrumental oscillations in RHESSI count rates during solar flares. Astron. Astrophys. 530:A47, DOI 10.1051/0004-6361/201016322, 1102.5349
Inglis AR, Ireland J, Dominique M (2015) Quasi-periodic Pulsations in Solar and Stellar Flares: Re-evaluating their Nature in the Context of Power-law Flare Fourier Spectra. Astrophys. J. 798(2):108, DOI 10.1088/0004-637X/798/2/108, 1410.8162
Inglis AR, Ireland J, Dennis BR, Hayes L, Gallagher P (2016) A Large-scale Search for Evidence of Quasi-periodic Pulsations in Solar Flares. Astrophys. J. 833(2):284, DOI 10.3847/1538-4357/833/2/284, 1610.07454
Jackman JAG, Wheatley PJ, Pugh CE, Kolotkov DY, Broomhall AM, Kennedy GM, Murphy SJ, Raddi R, Burleigh MR, Casewell SL, Eigmüller P, Gillen E, Günther MN, Jenkins JS, Louden T, McCormac J, Raynard L, Poppenhaeger K, Udry S, Watson CA, West RG (2019) Detection of a giant flare displaying quasi-periodic pulsations from a pre-main-sequence M star by the Next Generation Transit Survey. Mon. Not. Roy. Astron. Soc. 482(4):5553–5566, DOI 10.1093/mnras/sty3036, 1811.02008
Jakimiec J, Tomczak M (2010) Investigation of Quasi-periodic Variations in Hard X-rays of Solar Flares. Solar Phys. 261(2):233–251, DOI 10.1007/s11207-009-9489-4, 0908.0656
Jakimiec J, Tomczak M (2012) Investigation of Quasi-periodic Variations in Hard X-Rays of Solar Flares. II. Further Investigation of Oscillating Magnetic Traps. Solar Phys. 278(2):393–410, DOI 10.1007/s11207-012-9934-7, 1103.3165
Jakimiec J, Tomczak M (2013) Quasi-periodic Variations in the Hard X-ray Emission of a Large Arcade Flare. Solar Phys. 286(2):427–440, DOI 10.1007/s11207-013-0275-y, 1303.0977
Jansen F, Lumb D, Altieri B, Clavel J, Ehle M, Erd C, Gabriel C, Guainazzi M, Gondoin P, Much R, Munoz R, Santos M, Schartel N, Texier D, Vacanti G (2001) XMM-Newton observatory. I. The spacecraft and operations. Astron. Astrophys. 365:L1–L6, DOI 10.1051/0004-6361:20000036
Jeffries RD, Jackson RJ, Briggs KR, Evans PA, Pye JP (2011) Investigating coronal saturation and supersaturation in fast-rotating M-dwarf stars. Mon. Not. Roy. Astron. Soc. 411(3):2099–2112, DOI 10.1111/j.1365-2966.2010.17848.x, 1010.2152
Jelínek P, Karlický M (2012) Magnetoacoustic waves in diagnostics of the flare current sheets. Astron. Astrophys. 537:A46, DOI 10.1051/0004-6361/201117883
Jelínek P, Karlický M (2019) Pulse-beam heating of deep atmospheric layers, their oscillations and shocks modulating the flare reconnection. Astron. Astrophys. 625:A3, DOI 10.1051/0004-6361/201935188

Jelínek P, Karlický M, Murawski K (2012) Magnetoacoustic waves in a vertical flare current-sheet in a gravitationally stratified solar atmosphere. Astron. Astrophys. 546:A49, DOI 10.1051/0004-6361/201219891
Johns-Krull CM, Valenti JA, Koresko C (1999) Measuring the Magnetic Field on the Classical T Tauri Star BP Tauri. Astrophys. J. 516(2):900–915, DOI 10.1086/307128
Johnstone CP, Jardine M, Gregory SG, Donati JF, Hussain G (2014) Classical T Tauri stars: magnetic fields, coronae and star-disc interactions. Mon. Not. Roy. Astron. Soc. 437(4):3202–3220, DOI 10.1093/mnras/stt2107, 1310.8194
Kaneda K, Misawa H, Iwai K, Masuda S, Tsuchiya F, Katoh Y, Obara T (2018) Detection of Propagating Fast Sausage Waves through Detailed Analysis of a Zebra-pattern Fine Structure in a Solar Radio Burst. Astrophys. J. Lett. 855(2):L29, DOI 10.3847/2041-8213/aab2a5
Karlický M (2014) Solar flares: radio and X-ray signatures of magnetic reconnection processes. Research in Astronomy and Astrophysics 14(7):753-772, DOI 10.1088/1674-4527/14/7/002
Karlický M, Zlobec P, Mészárosová H (2010) Subsecond (0.1 s) Pulsations in the 11 April 2001 Radio Event. Solar Phys. 261(2):281–294, DOI 10.1007/s11207-009-9496-5
Karlický M, Mészárosová H, Jelínek P (2013) Radio fiber bursts and fast magnetoacoustic wave trains. Astron. Astrophys. 550:A1, DOI 10.1051/0004-6361/201220296, 1212.2421
Kashapova LK, Kupriyanova EG, Xu Z, Reid HAS, Kolotkov DY (2020) The origin of quasi-periodicities during circular ribbon flares. arXiv e-prints arXiv:2008.02010, 2008.02010
Katsiyannis AC, Williams DR, McAteer RTJ, Gallagher PT, Keenan FP, Murtagh F (2003) Eclipse observations of high-frequency oscillations in active region coronal loops. Astron. Astrophys. 406:709–714, DOI 10.1051/0004-6361:20030458, astro-ph/0305225
Kaufmann P, Giménez de Castro CG, Correia E, Costa JER, Raulin JP, Válio AS (2009) Rapid Pulsations in Sub-THz Solar Bursts. Astrophys. J. 697(1):420–427, DOI 10.1088/0004-637X/697/1/420, 0812.4671
Kerdraon A, Delouis JM (1997) The Nançay Radioheliograph, vol 483, p 192. DOI 10.1007/BFb0106458
Khodachenko ML, Zaitsev VV, Kislyakov AG, Rucker HO, Urpo S (2005) Low-frequency modulations in the solar microwave radiation as a possible indicator of inductive interaction of coronal magnetic loops. Astron. Astrophys. 433(2):691–699, DOI 10.1051/0004-6361:20041988
Khodachenko ML, Zaitsev VV, Kislyakov AG, Stepanov AV (2009) Equivalent Electric Circuit Models of Coronal Magnetic Loops and Related Oscillatory Phenomena on the Sun. Space Sci. Rev. 149(1-4):83–117, DOI 10.1007/s11214-009-9538-1
Kim S, Nakariakov VM, Shibasaki K (2012) Slow Magnetoacoustic Oscillations in the Microwave Emission of Solar Flares. Astrophys. J. Lett. 756(2):L36, DOI 10.1088/2041-8205/756/2/L36, 1310.2796
Kobanov NI, Chelpanov AA (2019) Oscillations Accompanying a He I 10830 Å Negative Flare in a Solar Facula II. Response of the Transition Region and Corona. Solar Phys. 294(5):58, DOI 10.1007/s11207-019-1449-z, 1904.11142
Koenigl A (1991) Disk Accretion onto Magnetic T Tauri Stars. Astrophys. J. Lett. 370:L39, DOI 10.1086/185972
Kohno M, Koyama K, Hamaguchi K (2002) Chandra Observations of High-Mass Young Stellar Objects in the Monoceros R2 Molecular Cloud. Astrophys. J. 567(1):423–433, DOI 10.1086/338381, astro-ph/0110462
Kohutova P, Verwichte E (2017) Excitation of vertical coronal loop oscillations by plasma condensations. Astron. Astrophys. 606:A120, DOI 10.1051/0004-6361/201731417
Kohutova P, Verwichte E, Froment C (2020) First direct observation of a torsional Alfvén oscillation at coronal heights. Astron. Astrophys. 633:L6, DOI 10.1051/0004-6361/201937144
Kolotkov DY, Nakariakov VM, Kupriyanova EG, Ratcliffe H, Shibasaki K (2015) Multi-mode quasi-periodic pulsations in a solar flare. Astron. Astrophys. 574:A53, DOI 10.1051/0004-6361/201424988
Kolotkov DY, Anfinogentov SA, Nakariakov VM (2016a) Empirical mode decomposition analysis of random processes in the solar atmosphere. Astron. Astrophys. 592:A153, DOI 10.1051/0004-6361/201628306
Kolotkov DY, Nakariakov VM, Rowland s G (2016b) Nonlinear oscillations of coalescing magnetic flux ropes. Phys. Rev. E 93(5):053205, DOI 10.1103/PhysRevE.93.053205
Kolotkov DY, Nisticò G, Nakariakov VM (2016c) Transverse oscillations and stability of prominences in a magnetic field dip. Astron. Astrophys. 590:A120, DOI 10.1051/0004-6361/

201628501
Kolotkov DY, Nakariakov VM, Kontar EP (2018a) Origin of the Modulation of the Radio Emission from the Solar Corona by a Fast Magnetoacoustic Wave. Astrophys. J. 861(1):33, DOI 10.3847/1538-4357/aac77e, 1805.08282
Kolotkov DY, Nisticò G, Rowland s G, Nakariakov VM (2018b) Finite amplitude transverse oscillations of a magnetic rope. Journal of Atmospheric and Solar-Terrestrial Physics 172:40–52, DOI 10.1016/j.jastp.2018.03.005, 1803.05195
Kolotkov DY, Pugh CE, Broomhall AM, Nakariakov VM (2018c) Quasi-periodic Pulsations in the Most Powerful Solar Flare of Cycle 24. Astrophys. J. Lett. 858(1):L3, DOI 10.3847/2041-8213/aabde9, 1804.04955
Kolotkov DY, Nakariakov VM, Zavershinskii DI (2019) Damping of slow magnetoacoustic oscillations by the misbalance between heating and cooling processes in the solar corona. Astron. Astrophys. 628:A133, DOI 10.1051/0004-6361/201936072, 1907.07051
Kong X, Guo F, Shen C, Chen B, Chen Y, Musset S, Glesener L, Pongkitiwanichakul P, Giacalone J (2019) The Acceleration and Confinement of Energetic Electrons by a Termination Shock in a Magnetic Trap: An Explanation for Nonthermal Loop-top Sources during Solar Flares. Astrophys. J. Lett. 887(2):L37, DOI 10.3847/2041-8213/ab5f67, 1911.08064
Kopylova YG, Melnikov AV, Stepanov AV, Tsap YT, Goldvarg TB (2007) Oscillations of coronal loops and second pulsations of solar radio emission. Astronomy Letters 33(10):706–713, DOI 10.1134/S1063773707100088
Kumar P, Nakariakov VM, Cho KS (2015) X-Ray and EUV Observations of Simultaneous Short and Long Period Oscillations in Hot Coronal Arcade Loops. Astrophys. J. 804(1):4, DOI 10.1088/0004-637X/804/1/4, 1502.07117
Kumar P, Nakariakov VM, Cho KS (2016) Observation of a Quasiperiodic Pulsation in Hard X-Ray, Radio, and Extreme-ultraviolet Wavelengths. Astrophys. J. 822(1):7, DOI 10.3847/0004-637X/822/1/7, 1603.03121
Kumar P, Nakariakov VM, Cho KS (2017) Observation of a Short Period Quasi-periodic Pulsation in Solar X-Ray, Microwave, and EUV Emissions. Astrophys. J. 836(1):121, DOI 10.3847/1538-4357/836/1/121, 1701.02159
Kupriyanova E, Kolotkov D, Nakariakov V, Kaufman A (2020) Quasi-Periodic Pulsations in Solar and Stellar Flares. Review. Solar-Terrestrial Physics 6(1):3–23, DOI 10.12737/stp-61202001
Kupriyanova EG, Ratcliffe H (2016) Minute pulsations in microwaves and X-rays during the flare on May 6, 2005. Advances in Space Research 57(7):1456–1467, DOI 10.1016/j.asr.2016.01.012
Kupriyanova EG, Melnikov VF, Shibasaki K (2013) Evolution of the Source of Quasi-Periodic Microwave Pulsations in a Single Flaring Loop. Pub. Astron. Soc. Japan 65:S3, DOI 10.1093/pasj/65.sp1.S3
Kupriyanova EG, Kashapova LK, Reid HAS, Myagkova IN (2016) Relationship of Type III Radio Bursts with Quasi-periodic Pulsations in a Solar Flare. Solar Phys. 291(11):3427–3438, DOI 10.1007/s11207-016-0958-2, 1608.00129
Kupriyanova EG, Kashapova LK, Van Doorsselaere T, Chowdhury P, Srivastava AK, Moon YJ (2019) Quasi-periodic pulsations in a solar flare with an unusual phase shift. Mon. Not. Roy. Astron. Soc. 483(4):5499–5507, DOI 10.1093/mnras/sty3480, 1812.09868
Kuznetsov SA, Zimovets IV, Morgachev AS, Struminsky AB (2016) Spatio-temporal Dynamics of Sources of Hard X-Ray Pulsations in Solar Flares. Solar Phys. 291(11):3385–3426, DOI 10.1007/s11207-016-0981-3, 1608.06594
Kuznetsov SA, Zimovets IV, Melnikov VF, Wang R (2017) Spatio-temporal Evolution of Sources of Microwave and Hard X-ray Pulsations of the Solar Flare using the NoRH, RHESSI, and AIA/SDO Observation Data. Geomagnetism and Aeronomy 57(8):1067–1072, DOI 10.1134/S001679321708014X
Laming JM (2015) The FIP and Inverse FIP Effects in Solar and Stellar Coronae. Living Reviews in Solar Physics 12(1):2, DOI 10.1007/lrsp-2015-2, 1504.08325
Lang KR, Willson RF (1986) Millisecond Radio Spikes from the Dwarf M Flare Star AD Leonis. Astrophys. J. 305:363, DOI 10.1086/164253
Lang KR, Bookbinder J, Golub L, Davis MM (1983) Bright, rapid, highly circularly polarized radio spikes from the M dwarf AD Leonis. Astrophys. J. Lett. 272:L15–L18, DOI 10.1086/184108
Ledentsov LS, Somov BV (2016) Thermal instability of the reconnecting current layer in solar flares. Astronomy Letters 42(12):841–849, DOI 10.1134/S1063773716120045

Ledentsov LS, Somov BV (2017) Thermal instability of a reconnecting current layer as a trigger for solar flares. Soviet Journal of Experimental and Theoretical Physics 125(2):347–356, DOI 10.1134/S1063776117070214

Lemen JR, Title AM, Akin DJ, Boerner PF, Chou C, Drake JF, Duncan DW, Edwards CG, Friedlaender FM, Heyman GF, Hurlburt NE, Katz NL, Kushner GD, Levay M, Lindgren RW, Mathur DP, McFeaters EL, Mitchell S, Rehse RA, Schrijver CJ, Springer LA, Stern RA, Tarbell TD, Wuelser JP, Wolfson CJ, Yanari C, Bookbinder JA, Cheimets PN, Caldwell D, Deluca EE, Gates R, Golub L, Park S, Podgorski WA, Bush RI, Scherrer PH, Gummin MA, Smith P, Auker G, Jerram P, Pool P, Soufli R, Windt DL, Beardsley S, Clapp M, Lang J, Waltham N (2012) The Atmospheric Imaging Assembly (AIA) on the Solar Dynamics Observatory (SDO). Solar Phys. 275(1-2):17–40, DOI 10.1007/s11207-011-9776-8

Li D, Ning ZJ, Zhang QM (2015) Imaging and Spectral Observations of Quasi-periodic Pulsations in a Solar Flare. Astrophys. J. 807(1):72, DOI 10.1088/0004-637X/807/1/72, 1505.03252

Li D, Ning ZJ, Huang Y, Chen NH, Zhang QM, Su YN, Su W (2017a) Doppler Shift Oscillations from a Hot Line Observed by IRIS. Astrophys. J. 849(2):113, DOI 10.3847/1538-4357/aa9073, 1709.10059

Li D, Zhang QM, Huang Y, Ning ZJ, Su YN (2017b) Quasi-periodic pulsations with periods that change depending on whether the pulsations have thermal or nonthermal components. Astron. Astrophys. 597:L4, DOI 10.1051/0004-6361/201629867, 1612.02677

Li D, Feng S, Su W, Huang Y (2020a) Preflare very long-periodic pulsations observed in Hα emission before the onset of a solar flare. Astron. Astrophys. 639:L5, DOI 10.1051/0004-6361/202038398, 2006.13423

Li D, Li Y, Lu L, Zhang Q, Ning Z, Anfinogentov S (2020b) Observations of a Quasi-periodic Pulsation in the Coronal Loop and Microwave Flux during a Solar Preflare Phase. Astrophys. J. Lett. 893(1):L17, DOI 10.3847/2041-8213/ab830c, 2003.09567

Li D, Lu L, Ning Z, Feng L, Gan W, Li H (2020c) Quasi-periodic Pulsation Detected in Lyα Emission During Solar Flares. Astrophys. J. 893(1):7, DOI 10.3847/1538-4357/ab7cd1, 2003.01877

Li T, Zhang J (2015) Quasi-periodic Slipping Magnetic Reconnection During an X-class Solar Flare Observed by the Solar Dynamics Observatory and Interface Region Imaging Spectrograph. Astrophys. J. Lett. 804(1):L8, DOI 10.1088/2041-8205/804/1/L8, 1504.01111

Lim D, Nakariakov VM, Yu DJ, Cho IH, Moon YJ (2020) Higher Radial Harmonics of Sausage Oscillations in Coronal Loops. Astrophys. J. 893(1):62, DOI 10.3847/1538-4357/ab7d3d

Lin RP, Dennis BR, Hurford GJ, Smith DM, Zehnder A, Harvey PR, Curtis DW, Pankow D, Turin P, Bester M, Csillaghy A, Lewis M, Madden N, van Beek HF, Appleby M, Raudorf T, McTiernan J, Ramaty R, Schmahl E, Schwartz R, Krucker S, Abiad R, Quinn T, Berg P, Hashii M, Sterling R, Jackson R, Pratt R, Campbell RD, Malone D, Landis D, Barrington-Leigh CP, Slassi-Sennou S, Cork C, Clark D, Amato D, Orwig L, Boyle R, Banks IS, Shirey K, Tolbert AK, Zarro D, Snow F, Thomsen K, Henneck R, McHedlishvili A, Ming P, Fivian M, Jordan J, Wanner R, Crubb J, Preble J, Matranga M, Benz A, Hudson H, Canfield RC, Holman GD, Crannell C, Kosugi T, Emslie AG, Vilmer N, Brown JC, Johns-Krull C, Aschwanden M, Metcalf T, Conway A (2002) The Reuven Ramaty High-Energy Solar Spectroscopic Imager (RHESSI). Solar Phys. 210(1):3–32, DOI 10.1023/A:1022428818870

Liu R, Alexander D, Gilbert HR (2009) Asymmetric Eruptive Filaments. Astrophys. J. 691(2):1079–1091, DOI 10.1088/0004-637X/691/2/1079

Liu W, Ofman L (2014) Advances in Observing Various Coronal EUV Waves in the SDO Era and Their Seismological Applications (Invited Review). Solar Phys. 289(9):3233–3277, DOI 10.1007/s11207-014-0528-4, 1404.0670

Liu W, Title AM, Zhao J, Ofman L, Schrijver CJ, Aschwanden MJ, De Pontieu B, Tarbell TD (2011) Direct Imaging of Quasi-periodic Fast Propagating Waves of ~2000 km s^{-1} in the Low Solar Corona by the Solar Dynamics Observatory Atmospheric Imaging Assembly. Astrophys. J. Lett. 736(1):L13, DOI 10.1088/2041-8205/736/1/L13, 1106.3150

Livingston W, Harvey JW, Malanushenko OV, Webster L (2006) Sunspots with the Strongest Magnetic Fields. Solar Phys. 239(1-2):41–68, DOI 10.1007/s11207-006-0265-4

López-Santiago J (2018) On the use of wavelets to reveal oscillatory patterns in stellar flare emission. Philosophical Transactions of the Royal Society of London Series A 376(2126):20170253, DOI 10.1098/rsta.2017.0253

López-Santiago J, Crespo-Chacón I, Flaccomio E, Sciortino S, Micela G, Reale F (2016) Star-disk interaction in classical T Tauri stars revealed using wavelet analysis. Astron. Astrophys.

590:A7, DOI 10.1051/0004-6361/201527499, 1603.06144
Loureiro NF, Schekochihin AA, Cowley SC (2007) Instability of current sheets and formation of plasmoid chains. Physics of Plasmas 14(10):100703–100703, DOI 10.1063/1.2783986, astro-ph/0703631
Lovkaya MN (2013) Analysis of the fine temporal structure of optical flares on AD Leo on February 4, 2003. Astronomy Reports 57(8):603–610, DOI 10.1134/S1063772913080040
Maehara H, Shibayama T, Notsu S, Notsu Y, Nagao T, Kusaba S, Honda S, Nogami D, Shibata K (2012) Superflares on solar-type stars. Nature 485(7399):478–481, DOI 10.1038/nature11063
Mancuso S, Barghini D, Telloni D (2020) Possible evidence of induced repetitive magnetic reconnection in a superflare from a young solar-type star. Astron. Astrophys. 636:A96, DOI 10.1051/0004-6361/201936819, 2004.01439
Mandal S, Yuan D, Fang X, Banerjee D, Pant V, Van Doorsselaere T (2016) Reflection of Propagating Slow Magneto-acoustic Waves in Hot Coronal Loops: Multi-instrument Observations and Numerical Modeling. Astrophys. J. 828(2):72, DOI 10.3847/0004-637X/828/2/72, 1604.08133
Martin DC, Fanson J, Schiminovich D, Morrissey P, Friedman PG, Barlow TA, Conrow T, Grange R, Jelinsky PN, Milliard B, Siegmund OHW, Bianchi L, Byun YI, Donas J, Forster K, Heckman TM, Lee YW, Madore BF, Malina RF, Neff SG, Rich RM, Small T, Surber F, Szalay AS, Welsh B, Wyder TK (2005) The Galaxy Evolution Explorer: A Space Ultraviolet Survey Mission. Astrophys. J. Lett. 619(1):L1–L6, DOI 10.1086/426387, astro-ph/0411302
Mathioudakis M, Seiradakis JH, Williams DR, Avgoloupis S, Bloomfield DS, McAteer RTJ (2003) White-light oscillations during a flare on II Peg. Astron. Astrophys. 403:1101–1104, DOI 10.1051/0004-6361:20030394
Mathioudakis M, Bloomfield DS, Jess DB, Dhillon VS, Marsh TR (2006) The periodic variations of a white-light flare observed with ULTRACAM. Astron. Astrophys. 456(1):323–327, DOI 10.1051/0004-6361:20054752, astro-ph/0605196
McAteer RTJ, Young CA, Ireland J, Gallagher PT (2007) The Bursty Nature of Solar Flare X-Ray Emission. Astrophys. J. 662(1):691–700, DOI 10.1086/518086
McEwan MP, Donnelly GR, Díaz AJ, Roberts B (2006) On the period ratio $P_1/2P_2$ in the oscillations of coronal loops. Astron. Astrophys. 460(3):893–899, DOI 10.1051/0004-6361:20065313
McLaughlin JA, Hood AW (2004) MHD wave propagation in the neighbourhood of a two-dimensional null point. Astron. Astrophys. 420:1129–1140, DOI 10.1051/0004-6361:20035900, 0712.1792
McLaughlin JA, De Moortel I, Hood AW, Brady CS (2009) Nonlinear fast magnetoacoustic wave propagation in the neighbourhood of a 2D magnetic X-point: oscillatory reconnection. Astron. Astrophys. 493(1):227–240, DOI 10.1051/0004-6361:200810465, 0901.1781
McLaughlin JA, Hood AW, de Moortel I (2011) Review Article: MHD Wave Propagation Near Coronal Null Points of Magnetic Fields. Space Sci. Rev. 158(2-4):205–236, DOI 10.1007/s11214-010-9654-y, 1004.5568
McLaughlin JA, Thurgood JO, MacTaggart D (2012a) On the periodicity of oscillatory reconnection. Astron. Astrophys. 548:A98, DOI 10.1051/0004-6361/201220234, 1212.1000
McLaughlin JA, Verth G, Fedun V, Erdélyi R (2012b) Generation of Quasi-periodic Waves and Flows in the Solar Atmosphere by Oscillatory Reconnection. Astrophys. J. 749(1):30, DOI 10.1088/0004-637X/749/1/30, 1203.6846
McLaughlin JA, Nakariakov VM, Dominique M, Jelínek P, Takasao S (2018) Modelling Quasi-Periodic Pulsations in Solar and Stellar Flares. Space Sci. Rev. 214(1):45, DOI 10.1007/s11214-018-0478-5, 1802.04180
Meegan C, Lichti G, Bhat PN, Bissaldi E, Briggs MS, Connaughton V, Diehl R, Fishman G, Greiner J, Hoover AS, van der Horst AeJ, von Kienlin A, Kippen RM, Kouveliotou C, McBreen S, Paciesas WS, Preece R, Steinle H, Wallace MS, Wilson RB, Wilson-Hodge C (2009) The Fermi Gamma-ray Burst Monitor. Astrophys. J. 702(1):791–804, DOI 10.1088/0004-637X/702/1/791, 0908.0450
Melnikov VF, Reznikova VE, Shibasaki K, Nakariakov VM (2005) Spatially resolved microwave pulsations of a flare loop. Astron. Astrophys. 439(2):727–736, DOI 10.1051/0004-6361:20052774
Meszarosova H, Gomory P (2020) Magnetically coupled atmosphere, fast sausage MHD waves, and forced magnetic field reconnection during the SOL2014-09-10T17:45 flare. arXiv e-prints arXiv:2010.01527, 2010.01527

Mészárosová H, Rybák J, Kashapova L, Gömöry P, Tokhchukova S, Myshyakov I (2016) Broadband microwave sub-second pulsations in an expanding coronal loop of the 2011 August 10 flare. Astron. Astrophys. 593:A80, DOI 10.1051/0004-6361/201528062, 1609.04217

Milligan RO, Fleck B, Ireland J, Fletcher L, Dennis BR (2017) Detection of Three-minute Oscillations in Full-disk Lyα Emission during a Solar Flare. Astrophys. J. Lett. 848(1):L8, DOI 10.3847/2041-8213/aa8f3a, 1709.09037

Mitra-Kraev U, Harra LK, Williams DR, Kraev E (2005) The first observed stellar X-ray flare oscillation: Constraints on the flare loop length and the magnetic field. Astron. Astrophys. 436(3):1041–1047, DOI 10.1051/0004-6361:20052834, astro-ph/0503384

Mossessian G, Fleishman GD (2012) Modeling of Gyrosynchrotron Radio Emission Pulsations Produced by Magnetohydrodynamic Loop Oscillations in Solar Flares. Astrophys. J. 748(2):140, DOI 10.1088/0004-637X/748/2/140, 1112.0609

Murawski K, Solov'ev A, Kraśkiewicz J, Srivastava AK (2015) New analytical and numerical models of a solar coronal loop. I. Application to forced vertical kink oscillations. Astron. Astrophys. 576:A22, DOI 10.1051/0004-6361/201424684, 1411.7465

Myagkova IN, Kuznetsov SN, Muravieva EA, Starostin LI (2007) Solar HXR- and [gamma]-ray emission measurements in 2005 by SONG/CORONAS-F near minimum of the last activity cycle. In: Kneer F, Puschmann KG, Wittmann AD (eds) Modern solar facilities - advanced solar science, p 281

Nakajima H, Kosugi T, Kai K, Enome S (1983) Successive electron and ion accelerations in impulsive solar flares on 7 and 21 June 1980. Nature 305(5932):292–294, DOI 10.1038/305292a0

Nakajima H, Sekiguchi H, Sawa M, Kai K, Kawashima S (1985) The radiometer and polarimeters at 80, 35, and 17 GHz for solar observations at Nobeyama. Pub. Astron. Soc. Japan 37(1):163–170

Nakajima H, Nishio M, Enome S, Shibasaki K, Takano T, Hanaoka Y, Torii C, Sekiguchi H, Bushimata T, Kawashima S, Shinohara N, Irimajiri Y, Koshiishi H, Kosugi T, Shiomi Y, Sawa M, Kai K (1994) The Nobeyama radioheliograph. IEEE Proceedings 82(5):705–713

Nakariakov VM (2007) MHD oscillations in solar and stellar coronae: Current results and perspectives. Advances in Space Research 39(12):1804–1813, DOI 10.1016/j.asr.2007.01.044

Nakariakov VM, Melnikov VF (2006) Modulation of gyrosynchrotron emission in solar and stellar flares by slow magnetoacoustic oscillations. Astron. Astrophys. 446(3):1151–1156, DOI 10.1051/0004-6361:20053944

Nakariakov VM, Melnikov VF (2009) Quasi-Periodic Pulsations in Solar Flares. Space Sci. Rev. 149(1-4):119–151, DOI 10.1007/s11214-009-9536-3

Nakariakov VM, Ofman L (2001) Determination of the coronal magnetic field by coronal loop oscillations. Astron. Astrophys. 372:L53–L56, DOI 10.1051/0004-6361:20010607

Nakariakov VM, Zimovets IV (2011) Slow Magnetoacoustic Waves in Two-ribbon Flares. Astrophys. J. Lett. 730(2):L27, DOI 10.1088/2041-8205/730/2/L27

Nakariakov VM, Ofman L, Deluca EE, Roberts B, Davila JM (1999) TRACE observation of damped coronal loop oscillations: Implications for coronal heating. Science 285:862–864, DOI 10.1126/science.285.5429.862

Nakariakov VM, Arber TD, Ault CE, Katsiyannis AC, Williams DR, Keenan FP (2004) Time signatures of impulsively generated coronal fast wave trains. Mon. Not. Roy. Astron. Soc. 349(2):705–709, DOI 10.1111/j.1365-2966.2004.07537.x

Nakariakov VM, Pascoe DJ, Arber TD (2005) Short Quasi-Periodic MHD Waves in Coronal Structures. Space Sci. Rev. 121(1-4):115–125, DOI 10.1007/s11214-006-4718-8

Nakariakov VM, Foullon C, Verwichte E, Young NP (2006) Quasi-periodic modulation of solar and stellar flaring emission by magnetohydrodynamic oscillations in a nearby loop. Astron. Astrophys. 452(1):343–346, DOI 10.1051/0004-6361:20054608

Nakariakov VM, Foullon C, Myagkova IN, Inglis AR (2010a) Quasi-Periodic Pulsations in the Gamma-Ray Emission of a Solar Flare. Astrophys. J. Lett. 708(1):L47–L51, DOI 10.1088/2041-8205/708/1/L47

Nakariakov VM, Inglis AR, Zimovets IV, Foullon C, Verwichte E, Sych R, Myagkova IN (2010b) Oscillatory processes in solar flares. Plasma Physics and Controlled Fusion 52(12):124009, DOI 10.1088/0741-3335/52/12/124009, 1010.0063

Nakariakov VM, Hornsey C, Melnikov VF (2012) Sausage Oscillations of Coronal Plasma Structures. Astrophys. J. 761(2):134, DOI 10.1088/0004-637X/761/2/134

Nakariakov VM, Anfinogentov SA, Nisticò G, Lee DH (2016a) Undamped transverse oscillations of coronal loops as a self-oscillatory process. Astron. Astrophys. 591:L5, DOI

10.1051/0004-6361/201628850
Nakariakov VM, Pilipenko V, Heilig B, Jelínek P, Karlický M, Klimushkin DY, Kolotkov DY, Lee DH, Nisticò G, Van Doorsselaere T, Verth G, Zimovets IV (2016b) Magnetohydrodynamic Oscillations in the Solar Corona and Earth's Magnetosphere: Towards Consolidated Understanding. Space Sci. Rev. 200(1-4):75–203, DOI 10.1007/s11214-015-0233-0
Nakariakov VM, Afanasyev AN, Kumar S, Moon YJ (2017) Effect of Local Thermal Equilibrium Misbalance on Long-wavelength Slow Magnetoacoustic Waves. Astrophys. J. 849(1):62, DOI 10.3847/1538-4357/aa8ea3
Nakariakov VM, Anfinogentov S, Storozhenko AA, Kurochkin EA, Bogod VM, Sharykin IN, Kaltman TI (2018) Quasi-periodic Pulsations in a Solar Microflare. Astrophys. J. 859(2):154, DOI 10.3847/1538-4357/aabfb9
Nakariakov VM, Kolotkov DY, Kupriyanova EG, Mehta T, Pugh CE, Lee DH, Broomhall AM (2019a) Non-stationary quasi-periodic pulsations in solar and stellar flares. Plasma Physics and Controlled Fusion 61(1):014024, DOI 10.1088/1361-6587/aad97c
Nakariakov VM, Kosak MK, Kolotkov DY, Anfinogentov SA, Kumar P, Moon YJ (2019b) Properties of Slow Magnetoacoustic Oscillations of Solar Coronal Loops by Multi-instrumental Observations. Astrophys. J. Lett. 874(1):L1, DOI 10.3847/2041-8213/ab0c9f
Nechaeva A, Zimovets IV, Nakariakov VM, Goddard CR (2019) Catalog of Decaying Kink Oscillations of Coronal Loops in the 24th Solar Cycle. Astrophys. J. Suppl. 241(2):31, DOI 10.3847/1538-4365/ab0e86
Nindos A, Aurass H (2007) Pulsating Solar Radio Emission, vol 725, p 251
Nishizuka N, Asai A, Takasaki H, Kurokawa H, Shibata K (2009) The Power-Law Distribution of Flare Kernels and Fractal Current Sheets in a Solar Flare. Astrophys. J. Lett. 694(1):L74–L78, DOI 10.1088/0004-637X/694/1/L74, 1301.6244
Nisticò G, Pascoe DJ, Nakariakov VM (2014) Observation of a high-quality quasi-periodic rapidly propagating wave train using SDO/AIA. Astron. Astrophys. 569:A12, DOI 10.1051/0004-6361/201423763
Ofman L, Wang T (2002) Hot Coronal Loop Oscillations Observed by SUMER: Slow Magnetosonic Wave Damping by Thermal Conduction. Astrophys. J. Lett. 580(1):L85–L88, DOI 10.1086/345548
Ofman L, Liu W, Title A, Aschwanden M (2011) Modeling Super-fast Magnetosonic Waves Observed by SDO in Active Region Funnels. Astrophys. J. Lett. 740(2):L33, DOI 10.1088/2041-8205/740/2/L33
Orlando S, Reale F, Peres G, Mignone A (2011) Mass accretion to young stars triggered by flaring activity in circumstellar discs. Mon. Not. Roy. Astron. Soc. 415(4):3380–3392, DOI 10.1111/j.1365-2966.2011.18954.x, 1104.5107
Osten RA, Bastian TS (2006) Wide-Band Spectroscopy of Two Radio Bursts on AD Leonis. Astrophys. J. 637(2):1016–1024, DOI 10.1086/498410, astro-ph/0509815
Osten RA, Bastian TS (2008) Ultrahigh Time Resolution Observations of Radio Bursts on AD Leonis. Astrophys. J. 674(2):1078–1085, DOI 10.1086/525013, 0710.5881
Osten RA, Hawley SL, Allred JC, Johns-Krull CM, Roark C (2005) From Radio to X-Ray: Flares on the dMe Flare Star EV Lacertae. Astrophys. J. 621(1):398–416, DOI 10.1086/427275, astro-ph/0411236
Pal'shin VD, Charikov YE, Aptekar RL, Golenetskii SV, Kokomov AA, Svinkin DS, Sokolova ZY, Ulanov MV, Frederiks DD, Tsvetkova AE (2014) Konus- Wind and Helicon- Coronas-F observations of solar flares. Geomagnetism and Aeronomy 54(7):943–948, DOI 10.1134/S0016793214070093, 1412.2015
Pandey JC, Srivastava AK (2009) Observations of X-Ray Oscillations in ξ Boo: Evidence of a Fast-Kink Mode in the Stellar Loops. Astrophys. J. Lett. 697(2):L153–L157, DOI 10.1088/0004-637X/697/2/L153, 0904.4084
Parks GK, Winckler JR (1969) Sixteen-Second Periodic Pulsations Observed in the Correlated Microwave and Energetic X-Ray Emission from a Solar Flare. Astrophys. J. Lett. 155:L117, DOI 10.1086/180315
Pascoe DJ, Hood AW, de Moortel I, Wright AN (2012) Spatial damping of propagating kink waves due to mode coupling. Astron. Astrophys. 539:A37, DOI 10.1051/0004-6361/201117979
Pascoe DJ, Hood AW, De Moortel I, Wright AN (2013a) Damping of kink waves by mode coupling. II. Parametric study and seismology. Astron. Astrophys. 551:A40, DOI 10.1051/0004-6361/201220620
Pascoe DJ, Nakariakov VM, Kupriyanova EG (2013b) Fast magnetoacoustic wave trains in

magnetic funnels of the solar corona. Astron. Astrophys. 560:A97, DOI 10.1051/0004-6361/201322678
Pascoe DJ, Nakariakov VM, Kupriyanova EG (2014) Fast magnetoacoustic wave trains in coronal holes. Astron. Astrophys. 568:A20, DOI 10.1051/0004-6361/201423931
Pascoe DJ, Goddard CR, Nakariakov VM (2016a) Spatially resolved observation of the fundamental and second harmonic standing kink modes using SDO/AIA. Astron. Astrophys. 593:A53, DOI 10.1051/0004-6361/201628784
Pascoe DJ, Goddard CR, Nisticò G, Anfinogentov S, Nakariakov VM (2016b) Coronal loop seismology using damping of standing kink oscillations by mode coupling. Astron. Astrophys. 589:A136, DOI 10.1051/0004-6361/201628255
Pascoe DJ, Goddard CR, Nisticò G, Anfinogentov S, Nakariakov VM (2016c) Damping profile of standing kink oscillations observed by SDO/AIA. Astron. Astrophys. 585:L6, DOI 10.1051/0004-6361/201527835
Pascoe DJ, Anfinogentov S, Nisticò G, Goddard CR, Nakariakov VM (2017a) Coronal loop seismology using damping of standing kink oscillations by mode coupling. II. additional physical effects and Bayesian analysis. Astron. Astrophys. 600:A78, DOI 10.1051/0004-6361/201629702
Pascoe DJ, Goddard CR, Nakariakov VM (2017b) Dispersive Evolution of Nonlinear Fast Magnetoacoustic Wave Trains. Astrophys. J. Lett. 847(2):L21, DOI 10.3847/2041-8213/aa8db8
Pascoe DJ, Russell AJB, Anfinogentov SA, Simões PJA, Goddard CR, Nakariakov VM, Fletcher L (2017c) Seismology of contracting and expanding coronal loops using damping of kink oscillations by mode coupling. Astron. Astrophys. 607:A8, DOI 10.1051/0004-6361/201730915
Paudel RR, Gizis JE, Mullan DJ, Schmidt SJ, Burgasser AJ, Williams PKG, Berger E (2018) K 2 Ultracool Dwarfs Survey. IV. Monster Flares Observed on the Young Brown Dwarf CFHT-BD-Tau 4. Astrophys. J. 861(2):76, DOI 10.3847/1538-4357/aac8e0, 1805.11185
Pedersen MG, Antoci V, Korhonen H, White TR, Jessen-Hansen J, Lehtinen J, Nikbakhsh S, Viuho J (2017) Do A-type stars flare? Mon. Not. Roy. Astron. Soc. 466(3):3060–3076, DOI 10.1093/mnras/stw3226, 1612.04575
Pettersen BR (1989) A Review of Stellar Flares and Their Characteristics. Solar Phys. 121(1-2):299–312, DOI 10.1007/BF00161702
Pillitteri I, Wolk SJ, Goodman A, Sciortino S (2014) Smooth X-ray variability from ρ Ophiuchi A+B. A strongly magnetized primary B2 star? Astron. Astrophys. 567:L4, DOI 10.1051/0004-6361/201424243, 1406.5049
Pillitteri I, Wolk SJ, Reale F, Oskinova L (2017) The early B-type star Rho Ophiuchi A is an X-ray lighthouse. Astron. Astrophys. 602:A92, DOI 10.1051/0004-6361/201630070, 1703.04686
Pizzocaro D, Stelzer B, Poretti E, Raetz S, Micela G, Belfiore A, Marelli M, Salvetti D, De Luca A (2019) Activity and rotation of the X-ray emitting Kepler stars. Astron. Astrophys. 628:A41, DOI 10.1051/0004-6361/201731674, 1906.05587
Preibisch T, Zinnecker H (2002) X-Ray Properties of the Young Stellar and Substellar Objects in the IC 348 Cluster: The Chandra View. Astron. J. 123(3):1613–1628, DOI 10.1086/338851
Preibisch T, Kim YC, Favata F, Feigelson ED, Flaccomio E, Getman K, Micela G, Sciortino S, Stassun K, Stelzer B, Zinnecker H (2005) The Origin of T Tauri X-Ray Emission: New Insights from the Chandra Orion Ultradeep Project. Astrophys. J. Suppl. 160(2):401–422, DOI 10.1086/432891, astro-ph/0506526
Priest ER, Forbes TG (2002) The magnetic nature of solar flares. Astron. Astrophys. Rev. 10(4):313–377, DOI 10.1007/s001590100013
Pugh CE, Nakariakov VM, Broomhall AM (2015) A Multi-period Oscillation in a Stellar Superflare. Astrophys. J. Lett. 813(1):L5, DOI 10.1088/2041-8205/813/1/L5, 1510.03613
Pugh CE, Armstrong DJ, Nakariakov VM, Broomhall AM (2016) Statistical properties of quasi-periodic pulsations in white-light flares observed with Kepler. Mon. Not. Roy. Astron. Soc. 459(4):3659–3676, DOI 10.1093/mnras/stw850, 1604.03018
Pugh CE, Broomhall AM, Nakariakov VM (2017a) Significance testing for quasi-periodic pulsations in solar and stellar flares. Astron. Astrophys. 602:A47, DOI 10.1051/0004-6361/201730595, 1703.07294
Pugh CE, Nakariakov VM, Broomhall AM, Bogomolov AV, Myagkova IN (2017b) Properties of quasi-periodic pulsations in solar flares from a single active region. Astron. Astrophys.

608:A101, DOI 10.1051/0004-6361/201731636, 1709.09472
Pugh CE, Broomhall AM, Nakariakov VM (2019) Scaling laws of quasi-periodic pulsations in solar flares. Astron. Astrophys. 624:A65, DOI 10.1051/0004-6361/201834455, 1902.09627
Qian SB, Zhang J, Zhu LY, Liu L, Liao WP, Zhao EG, He JJ, Li LJ, Li K, Dai ZB (2012) Optical flares and flaring oscillations on the M-type eclipsing binary CU Cancri. Mon. Not. Roy. Astron. Soc. 423(4):3646–3651, DOI 10.1111/j.1365-2966.2012.21157.x
Qiu J, Liu W, Hill N, Kazachenko M (2010) Reconnection and Energetics in Two-ribbon Flares: A Revisit of the Bastille-day Flare. Astrophys. J. 725(1):319–330, DOI 10.1088/0004-637X/725/1/319
Qiu J, Longcope DW, Cassak PA, Priest ER (2017) Elongation of Flare Ribbons. Astrophys. J. 838(1):17, DOI 10.3847/1538-4357/aa6341, 1707.02478
Reale F (2007) Diagnostics of stellar flares from X-ray observations: from the decay to the rise phase. Astron. Astrophys. 471(1):271–279, DOI 10.1051/0004-6361:20077223, 0705.3254
Reale F (2014) Coronal Loops: Observations and Modeling of Confined Plasma. Living Reviews in Solar Physics 11(1):4, DOI 10.12942/lrsp-2014-4
Reale F (2016) Plasma Sloshing in Pulse-heated Solar and Stellar Coronal Loops. Astrophys. J. Lett. 826(2):L20, DOI 10.3847/2041-8205/826/2/L20, 1607.01329
Reale F, Peres G, Serio S, Rosner R, Schmitt JHMM (1988) Hydrodynamic Modeling of an X-Ray Flare on Proxima Centauri Observed by the Einstein Telescope. Astrophys. J. 328:256, DOI 10.1086/166288
Reale F, Betta R, Peres G, Serio S, McTiernan J (1997) Determination of the length of coronal loops from the decay of X-ray flares I. Solar flares observed with YOHKOH SXT. Astron. Astrophys. 325:782–790
Reale F, Lopez-Santiago J, Flaccomio E, Petralia A, Sciortino S (2018) X-Ray Flare Oscillations Track Plasma Sloshing along Star-disk Magnetic Tubes in the Orion Star-forming Region. Astrophys. J. 856(1):51, DOI 10.3847/1538-4357/aaaf1f, 1802.05093
Reale F, Testa P, Petralia A, Kolotkov DY (2019) Large-amplitude Quasiperiodic Pulsations as Evidence of Impulsive Heating in Hot Transient Loop Systems Detected in the EUV with SDO/AIA. Astrophys. J. 884(2):131, DOI 10.3847/1538-4357/ab4270, 1909.02847
Reid HAS, Vilmer N, Kontar EP (2011) Characteristics of the flare acceleration region derived from simultaneous hard X-ray and radio observations. Astron. Astrophys. 529:A66, DOI 10.1051/0004-6361/201016181, 1102.2342
Reva A, Shestov S, Zimovets I, Bogachev S, Kuzin S (2015) Wave-like Formation of Hot Loop Arcades. Solar Phys. 290(10):2909–2921, DOI 10.1007/s11207-015-0769-x, 1510.02319
Reznikova VE, Shibasaki K (2011) Flare quasi-periodic pulsations with growing periodicity. Astron. Astrophys. 525:A112, DOI 10.1051/0004-6361/201015600
Ricker GR, Winn JN, Vanderspek R, Latham DW, Bakos GÁ, Bean JL, Berta-Thompson ZK, Brown TM, Buchhave L, Butler NR, Butler RP, Chaplin WJ, Charbonneau D, Christensen-Dalsgaard J, Clampin M, Deming D, Doty J, De Lee N, Dressing C, Dunham EW, Endl M, Fressin F, Ge J, Henning T, Holman MJ, Howard AW, Ida S, Jenkins J, Jernigan G, Johnson JA, Kaltenegger L, Kawai N, Kjeldsen H, Laughlin G, Levine AM, Lin D, Lissauer JJ, MacQueen P, Marcy G, McCullough PR, Morton TD, Narita N, Paegert M, Palle E, Pepe F, Pepper J, Quirrenbach A, Rinehart SA, Sasselov D, Sato B, Seager S, Sozzetti A, Stassun KG, Sullivan P, Szentgyorgyi A, Torres G, Udry S, Villasenor J (2014) Transiting Exoplanet Survey Satellite (TESS). In: Oschmann J Jacobus M, Clampin M, Fazio GG, MacEwen HA (eds) Space Telescopes and Instrumentation 2014: Optical, Infrared, and Millimeter Wave, Society of Photo-Optical Instrumentation Engineers (SPIE) Conference Series, vol 9143, p 914320, DOI 10.1117/12.2063489, 1406.0151
Roberts B, Edwin PM, Benz AO (1984) On coronal oscillations. Astrophys. J. 279:857–865, DOI 10.1086/161956
Rodono M (1974) Short-lived Flare Activity of the Hyades Flare Star H XI 2411. Astron. Astrophys. 32:337
Romanova MM, Ustyugova GV, Koldoba AV, Lovelace RVE (2002) Magnetohydrodynamic Simulations of Disk-Magnetized Star Interactions in the Quiescent Regime: Funnel Flows and Angular Momentum Transport. Astrophys. J. 578(1):420–438, DOI 10.1086/342464, astro-ph/0209426
Ruan W, Xia C, Keppens R (2018) Solar flares and Kelvin-Helmholtz instabilities: A parameter survey. Astron. Astrophys. 618:A135, DOI 10.1051/0004-6361/201833362, 1809.02410
Ruan W, Xia C, Keppens R (2019) Extreme-ultraviolet and X-Ray Emission of Turbulent Solar Flare Loops. Astrophys. J. Lett. 877(1):L11, DOI 10.3847/2041-8213/ab1f78

Ruan W, Xia C, Keppens R (2020) A Fully Self-consistent Model for Solar Flares. Astrophys. J. 896(2):97, DOI 10.3847/1538-4357/ab93db, 2005.08578
Ruderman MS, Terradas J (2013) Damping of coronal loop kink oscillations due to mode conversion. Astron. Astrophys. 555:A27, DOI 10.1051/0004-6361/201220195
Schrijver CJ (2007) Braiding-induced Interchange Reconnection of the Magnetic Field and the Width of Solar Coronal Loops. Astrophys. J. Lett. 662(2):L119–L122, DOI 10.1086/519455
Selwa M, Murawski K, Solanki SK (2005) Excitation and damping of slow magnetosonic standing waves in a solar coronal loop. Astron. Astrophys. 436(2):701–709, DOI 10.1051/0004-6361:20042319
Sharykin IN, Zimovets IV, Myshyakov II, Meshalkina NS (2018) Flare Energy Release at the Magnetic Field Polarity Inversion Line during the M1.2 Solar Flare of 2015 March 15. I. Onset of Plasma Heating and Electron Acceleration. Astrophys. J. 864(2):156, DOI 10.3847/1538-4357/aada15, 1805.05792
Sharykin IN, Zimovets IV, Myshyakov II (2020) Flare Energy Release at the Magnetic Field Polarity Inversion Line during the M1.2 Solar Flare of 2015 March 15. II. Investigation of Photospheric Electric Current and Magnetic Field Variations Using HMI 135 s Vector Magnetograms. Astrophys. J. 893(2):159, DOI 10.3847/1538-4357/ab84ef, 1905.03352
Shen Y, Liu Y (2012) Observational Study of the Quasi-periodic Fast-propagating Magnetosonic Waves and the Associated Flare on 2011 May 30. Astrophys. J. 753(1):53, DOI 10.1088/0004-637X/753/1/53, 1204.6649
Shi M, Li B, Huang Z, Chen SX (2019) Synthetic Emissions of the Fe XXI 1354 Å Line from Flare Loops Experiencing Fundamental Fast Sausage Oscillations. Astrophys. J. 874(1):87, DOI 10.3847/1538-4357/ab07b8, 1902.06087
Shibasaki K, Ishiguro M, Enome S (1979) Solar Radio Acquisition and Communication System /SORDACS/ of Toyokawa Observatory. Proceedings of the Research Institute of Atmospherics, Nagoya University 26:117–127
Shibata K, Magara T (2011) Solar Flares: Magnetohydrodynamic Processes. Living Reviews in Solar Physics 8(1):6, DOI 10.12942/lrsp-2011-6
Shibata K, Tanuma S (2001) Plasmoid-induced-reconnection and fractal reconnection. Earth, Planets, and Space 53:473–482, DOI 10.1186/BF03353258, astro-ph/0101008
Shibata K, Yokoyama T (1999) Origin of the Universal Correlation between the Flare Temperature and the Emission Measure for Solar and Stellar Flares. Astrophys. J. Lett. 526(1):L49–L52, DOI 10.1086/312354
Shibata K, Yokoyama T (2002) A Hertzsprung-Russell-like Diagram for Solar/Stellar Flares and Corona: Emission Measure versus Temperature Diagram. Astrophys. J. 577(1):422–432, DOI 10.1086/342141, astro-ph/0206016
Shibata K, Isobe H, Hillier A, Choudhuri AR, Maehara H, Ishii TT, Shibayama T, Notsu S, Notsu Y, Nagao T, Honda S, Nogami D (2013) Can Superflares Occur on Our Sun? Pub. Astron. Soc. Japan 65:49, DOI 10.1093/pasj/65.3.49, 1212.1361
Simões PJA, Hudson HS, Fletcher L (2015) Soft X-Ray Pulsations in Solar Flares. Solar Phys. 290(12):3625–3639, DOI 10.1007/s11207-015-0691-2, 1412.3045
Somov BV (2013) Plasma Astrophysics, Part II, vol 392. DOI 10.1007/978-1-4614-4295-0
Srivastava AK, Dwivedi BN (2010) Signature of slow acoustic oscillations in a non-flaring loop observed by EIS/Hinode. New Astron. 15(1):8–15, DOI 10.1016/j.newast.2009.05.006
Srivastava AK, Lalitha S (2013) MHD seismology as a tool to diagnose the coronae of X-ray active sun-like flaring stars. In: Astronomical Society of India Conference Series, Astronomical Society of India Conference Series, vol 10, pp 59–66, 1308.4489
Srivastava AK, Lalitha S, Pandey JC (2013) Evidence of Multiple Slow Acoustic Oscillations in the Stellar Flaring Loops of Proxima Centauri. Astrophys. J. Lett. 778(2):L28, DOI 10.1088/2041-8205/778/2/L28, 1310.6835
Srivastava AK, Mishra SK, Jelínek P, Samanta T, Tian H, Pant V, Kayshap P, Banerjee D, Doyle JG, Dwivedi BN (2019) On the Observations of Rapid Forced Reconnection in the Solar Corona. Astrophys. J. 887(2):137, DOI 10.3847/1538-4357/ab4a0c, 1901.07971
Stelzer B, Neuhäuser R, Casanova S, Montmerle T (1999) Rotational modulation of X-ray flares on late-type stars: T Tauri stars and Algol. Astron. Astrophys. 344:154–162, astro-ph/9901317
Stelzer B, Damasso M, Scholz A, Matt SP (2016) A path towards understanding the rotation-activity relation of M dwarfs with K2 mission, X-ray and UV data. Mon. Not. Roy. Astron. Soc. 463(2):1844–1864, DOI 10.1093/mnras/stw1936, 1608.00772
Stepanov AV, Kliem B, Zaitsev VV, Fürst E, Jessner A, Krüger A, Hildebrand t J, Schmitt

JHMM (2001) Microwave plasma emission of a flare on AD Leo. Astron. Astrophys. 374:1072–1084, DOI 10.1051/0004-6361:20010518, astro-ph/0106369
Stepanov AV, Kopylova YG, Tsap YT, Kupriyanova EG (2005) Oscillations of Optical Emission from Flare Stars and Coronal Loop Diagnostics. Astronomy Letters 31(9):612–619, DOI 10.1134/1.2039972
Stepanov AV, Tsap YT, Kopylova YG (2006) Soft X-ray oscillations from AT Mic: Flare plasma diagnostics. Astronomy Letters 32(8):569–573, DOI 10.1134/S1063773706080081
Stepanov AV, Tsap YT, Kopylova YG (2010) Stellar flare diagnostics from multi-wavelength observations. In: Kosovichev AG, Andrei AH, Rozelot JP (eds) Solar and Stellar Variability: Impact on Earth and Planets, vol 264, pp 288–291, DOI 10.1017/S174392130999281X
Stepanov AV, Zaitsev VV, Nakariakov VM (2012) Coronal Seismology: Waves and Oscillations in Stellar Coronae Flare Plasma. DOI 10.1002/9783527645985
Sych R, Nakariakov VM, Karlicky M, Anfinogentov S (2009) Relationship between wave processes in sunspots and quasi-periodic pulsations in active region flares. Astron. Astrophys. 505(2):791–799, DOI 10.1051/0004-6361/200912132, 1005.3594
Tajima T, Shibata K (2002) Plasma astrophysics
Tajima T, Sakai J, Nakajima H, Kosugi T, Brunel F, Kundu MR (1987) Current Loop Coalescence Model of Solar Flares. Astrophys. J. 321:1031, DOI 10.1086/165694
Takahashi T, Qiu J, Shibata K (2017) Quasi-periodic Oscillations in Flares and Coronal Mass Ejections Associated with Magnetic Reconnection. Astrophys. J. 848(2):102, DOI 10.3847/1538-4357/aa8f97, 1709.05234
Takakura T, Kaufmann P, Costa JER, Degaonkar SS, Ohki K, Nitta N (1983) Sub-second pulsations simultaneously observed at microwaves and hard X rays in a solar burst. Nature 302(5906):317–319, DOI 10.1038/302317a0
Takasao S, Shibata K (2016) Above-the-loop-top Oscillation and Quasi-periodic Coronal Wave Generation in Solar Flares. Astrophys. J. 823(2):150, DOI 10.3847/0004-637X/823/2/150, 1606.09354
Takasao S, Asai A, Isobe H, Shibata K (2012) Simultaneous Observation of Reconnection Inflow and Outflow Associated with the 2010 August 18 Solar Flare. Astrophys. J. Lett. 745(1):L6, DOI 10.1088/2041-8205/745/1/L6, 1112.1398
Takasao S, Matsumoto T, Nakamura N, Shibata K (2015) Magnetohydrodynamic Shocks in and above Post-flare Loops: Two-dimensional Simulation and a Simplified Model. Astrophys. J. 805(2):135, DOI 10.1088/0004-637X/805/2/135, 1504.05700
Takasao S, Asai A, Isobe H, Shibata K (2016) Observational Evidence of Particle Acceleration Associated with Plasmoid Motions. Astrophys. J. 828(2):103, DOI 10.3847/0004-637X/828/2/103, 1611.00108
Takeshige S, Takasao S, Shibata K (2015) A Theoretical Model of a Thinning Current Sheet in the Low-β Plasmas. Astrophys. J. 807(2):159, DOI 10.1088/0004-637X/807/2/159, 1504.05677
Tan B, Tan C (2012) Microwave Quasi-periodic Pulsation with Millisecond Bursts in a Solar Flare on 2011 August 9. Astrophys. J. 749(1):28, DOI 10.1088/0004-637X/749/1/28, 1202.1578
Tan B, Yu Z, Huang J, Tan C, Zhang Y (2016) Very Long-period Pulsations before the Onset of Solar Flares. Astrophys. J. 833(2):206, DOI 10.3847/1538-4357/833/2/206, 1610.09291
Telleschi A, Güdel M, Briggs KR, Audard M, Palla F (2007) X-ray emission from T Tauri stars and the role of accretion: inferences from the XMM-Newton extended survey of the Taurus molecular cloud. Astron. Astrophys. 468(2):425–442, DOI 10.1051/0004-6361:20066565, astro-ph/0612338
Testa P, Saar SH, Drake JJ (2015) Stellar activity and coronal heating: an overview of recent results. Philosophical Transactions of the Royal Society of London Series A 373(2042):20140259–20140259, DOI 10.1098/rsta.2014.0259, 1502.07401
Thompson AR, Maxwell A (1962) Spectral Observations of Solar Radio Bursts. III. Continuum Bursts. Astrophys. J. 136:546, DOI 10.1086/147406
Thurgood JO, McLaughlin JA (2012) Linear and nonlinear MHD mode coupling of the fast magnetoacoustic wave about a 3D magnetic null point. Astron. Astrophys. 545:A9, DOI 10.1051/0004-6361/201219850, 1208.5885
Thurgood JO, Pontin DI, McLaughlin JA (2017) Three-dimensional Oscillatory Magnetic Reconnection. Astrophys. J. 844(1):2, DOI 10.3847/1538-4357/aa79fa, 1706.09662
Thurgood JO, Pontin DI, McLaughlin JA (2018) Implosive Collapse about Magnetic Null Points: A Quantitative Comparison between 2D and 3D Nulls. Astrophys. J. 855(1):50,

DOI 10.3847/1538-4357/aab0a0, 1802.07076
Thurgood JO, Pontin DI, McLaughlin JA (2019) On the periodicity of linear and nonlinear oscillatory reconnection. Astron. Astrophys. 621:A106, DOI 10.1051/0004-6361/201834369, 1811.08831
Tian H (2017) Probing the solar transition region: current status and future perspectives. Research in Astronomy and Astrophysics 17(11):110, DOI 10.1088/1674-4527/17/11/110
Tian H, Young PR, Reeves KK, Wang T, Antolin P, Chen B, He J (2016) Global Sausage Oscillation of Solar Flare Loops Detected by the Interface Region Imaging Spectrograph. Astrophys. J. Lett. 823(1):L16, DOI 10.3847/2041-8205/823/1/L16, 1605.01963
Torii C, Tsukiji Y, Kobayashi S, Yoshimi N, Tanaka H, Enome S (1979) Full-automatic radiopolarimeters for solar patrol at microwave frequencies. Proceedings of the Research Institute of Atmospherics, Nagoya University 26:129–132
Torrence C, Compo GP (1998) A Practical Guide to Wavelet Analysis. Bulletin of the American Meteorological Society 79(1):61–78, DOI 10.1175/1520-0477(1998)079⟨0061:APGTWA⟩2.0.CO;2
Trigilio C, Leto P, Leone F, Umana G, Buemi C (2000) Coherent radio emission from the magnetic chemically peculiar star CU Virginis. Astron. Astrophys. 362:281–288, astro-ph/0007097
Tsang BTH, Pun CSJ, Di Stefano R, Li KL, Kong AKH (2012) The Discovery of an X-Ray/UV Stellar Flare from the Late-K/Early-M Dwarf LMC 335. Astrophys. J. 754(2):107, DOI 10.1088/0004-637X/754/2/107, 1205.6021
Tsap YT, Stepanov AV, Kopylova YG, Zhilyaev BE (2011) Diagnostics of a flare on EQ Peg B from optical pulsations. Astronomy Letters 37(1):49–54, DOI 10.1134/S1063773710101032
Tsikoudi V, Kellett BJ (2000) ROSAT All-Sky Survey X-ray and EUV observations of YY Gem and AU Mic. Mon. Not. Roy. Astron. Soc. 319(4):1147–1153, DOI 10.1046/j.1365-8711.2000.03905.x
Tsuboi Y, Imanishi K, Koyama K, Grosso N, Montmerle T (2000) Quasi-periodic X-Ray Flares from the Protostar YLW 15. Astrophys. J. 532(2):1089–1096, DOI 10.1086/308591, astro-ph/9911373
Tsuboi Y, Yamazaki K, Sugawara Y, Kawagoe A, Kaneto S, Iizuka R, Matsumura T, Nakahira S, Higa M, Matsuoka M, Sugizaki M, Ueda Y, Kawai N, Morii M, Serino M, Mihara T, Tomida H, Ueno S, Negoro H, Daikyuji A, Ebisawa K, Eguchi S, Hiroi K, Ishikawa M, Isobe N, Kawasaki K, Kimura M, Kitayama H, Kohama M, Kotani T, Nakagawa YE, Nakajima M, Ozawa H, Shidatsu M, Sootome T, Sugimori K, Suwa F, Tsunemi H, Usui R, Yamamoto T, Yamaoka K, Yoshida A (2016) Large X-ray flares on stars detected with MAXI/GSC: A universal correlation between the duration of a flare and its X-ray luminosity. Pub. Astron. Soc. Japan 68(5):90, DOI 10.1093/pasj/psw081, 1609.01925
Tsuneta S, Naito T (1998) Fermi Acceleration at the Fast Shock in a Solar Flare and the Impulsive Loop-Top Hard X-Ray Source. Astrophys. J. Lett. 495(1):L67–L70, DOI 10.1086/311207, astro-ph/9801109
Tuomi M, Jones HRA, Barnes JR, Anglada-Escudé G, Butler RP, Kiraga M, Vogt SS (2018) AD Leonis: Radial Velocity Signal of Stellar Rotation or Spin-Orbit Resonance? Astron. J. 155(5):192, DOI 10.3847/1538-3881/aab09c, 1802.06064
van der Klis M (2006) Rapid X-ray Variability, vol 39, pp 39–112
Van Doorsselaere T, Kupriyanova EG, Yuan D (2016) Quasi-periodic Pulsations in Solar and Stellar Flares: An Overview of Recent Results (Invited Review). Solar Phys. 291(11):3143–3164, DOI 10.1007/s11207-016-0977-z, 1609.02689
Vander Haagen G (2019) High Occurrence Optical Spikes and Quasi-Periodic Pulses (QPPs) on X-ray Star 47 Cassiopeiae. Journal of the American Association of Variable Star Observers (JAAVSO) 47(2):141
Veronig A, Vršnak B, Dennis BR, Temmer M, Hanslmeier A, Magdalenić J (2002) Investigation of the Neupert effect in solar flares. I. Statistical properties and the evaporation model. Astron. Astrophys. 392:699–712, DOI 10.1051/0004-6361:20020947, astro-ph/0207217
Vida K, Oláh K, Kővári Z, van Driel-Gesztelyi L, Moór A, Pál A (2019) Flaring Activity of Proxima Centauri from TESS Observations: Quasiperiodic Oscillations during Flare Decay and Inferences on the Habitability of Proxima b. Astrophys. J. 884(2):160, DOI 10.3847/1538-4357/ab41f5, 1907.12580
Vorpahl JA (1976) The triggering and subsequent development of a solar flare. Astrophys. J. 205:868–873, DOI 10.1086/154343
Wang T (2011) Standing Slow-Mode Waves in Hot Coronal Loops: Observations, Modeling, and

Coronal Seismology. Space Sci. Rev. 158(2-4):397–419, DOI 10.1007/s11214-010-9716-1, 1011.2483

Waterfall COG, Browning PK, Fuller GA, Gordovskyy M (2019) Modelling the radio and X-ray emission from T-Tauri flares. Mon. Not. Roy. Astron. Soc. 483(1):917–930, DOI 10.1093/mnras/sty2875

Welsh BY, Wheatley J, Browne SE, Siegmund OHW, Doyle JG, O'Shea E, Antonova A, Forster K, Seibert M, Morrissey P, Taroyan Y (2006) GALEX high time-resolution ultraviolet observations of dMe flare events. Astron. Astrophys. 458(3):921–930, DOI 10.1051/0004-6361:20065304, astro-ph/0608254

Weltman A, Bull P, Camera S, Kelley K, Padmanabhan H, Pritchard J, Raccanelli A, Riemer-Sørensen S, Shao L, Andrianomena S, Athanassoula E, Bacon D, Barkana R, Bertone G, Bœhm C, Bonvin C, Bosma A, Brüggen M, Burigana C, Calore F, Cembranos JAR, Clarkson C, Connors RMT, Cruz-Dombriz Ádl, Dunsby PKS, Fonseca J, Fornengo N, Gaggero D, Harrison I, Larena J, Ma YZ, Maartens R, Méndez-Isla M, Mohanty SD, Murray S, Parkinson D, Pourtsidou A, Quinn PJ, Regis M, Saha P, Sahlén M, Sakellariadou M, Silk J, Trombetti T, Vazza F, Venumadhav T, Vidotto F, Villaescusa-Navarro F, Wang Y, Weniger C, Wolz L, Zhang F, Gaensler BM (2020) Fundamental physics with the Square Kilometre Array. Pub. Astron. Soc. Australia 37:e002, DOI 10.1017/pasa.2019.42, 1810.02680

Williams PKG, Cook BA, Berger E (2014) Trends in Ultracool Dwarf Magnetism. I. X-Ray Suppression and Radio Enhancement. Astrophys. J. 785(1):9, DOI 10.1088/0004-637X/785/1/9, 1310.6757

Wright NJ, Drake JJ (2016) Solar-type dynamo behaviour in fully convective stars without a tachocline. Nature 535(7613):526–528, DOI 10.1038/nature18638, 1607.07870

Yan Y, Zhang J, Wang W, Liu F, Chen Z, Ji G (2009) The Chinese Spectral Radioheliograph—CSRH. Earth Moon and Planets 104(1-4):97–100, DOI 10.1007/s11038-008-9254-y

Yan Y, Chen L, Yu S (2016) First radio burst imaging observation from Mingantu Ultrawide Spectral Radioheliograph. In: Kosovichev AG, Hawley SL, Heinzel P (eds) Solar and Stellar Flares and their Effects on Planets, IAU Symposium, vol 320, pp 427–435, DOI 10.1017/S174392131600051X

Yu H, Li B, Chen SX, Xiong M, Guo MZ (2017) Impulsively Generated Wave Trains in Coronal Structures. I. Effects of Transverse Structuring on Sausage Waves in Pressureless Tubes. Astrophys. J. 836(1):1, DOI 10.3847/1538-4357/836/1/1, 1612.09479

Yu S, Chen B, Reeves KK, Gary DE, Musset S, Fleishman GD, Nita GM, Glesener L (2020) Magnetic Reconnection during the Post-impulsive Phase of a Long-duration Solar Flare: Bidirectional Outflows as a Cause of Microwave and X-Ray Bursts. Astrophys. J. 900(1):17, DOI 10.3847/1538-4357/aba8a6, 2007.10443

Yuan D, Shen Y, Liu Y, Nakariakov VM, Tan B, Huang J (2013) Distinct propagating fast wave trains associated with flaring energy releases. Astron. Astrophys. 554:A144, DOI 10.1051/0004-6361/201321435

Yuan D, Van Doorsselaere T, Banerjee D, Antolin P (2015) Forward Modeling of Standing Slow Modes in Flaring Coronal Loops. Astrophys. J. 807(1):98, DOI 10.1088/0004-637X/807/1/98, 1504.07475

Yuan D, Feng S, Li D, Ning Z, Tan B (2019) A Compact Source for Quasi-periodic Pulsation in an M-class Solar Flare. Astrophys. J. Lett. 886(2):L25, DOI 10.3847/2041-8213/ab5648, 1911.05217

Zaitsev VV, Stepanov AV (1982) On the Origin of the Hard X-Ray Pulsations during Solar Flares. Soviet Astronomy Letters 8:132–134

Zaitsev VV, Stepanov AV (1989) Elementary Flare Bursts and the Properties of Eruptive Solar Plasma. Soviet Astronomy Letters 15:66

Zaitsev VV, Stepanov AV (2008) REVIEWS OF TOPICAL PROBLEMS: Coronal magnetic loops. Physics Uspekhi 51(11):1123–1160, DOI 10.1070/PU2008v051n11ABEH006657

Zaitsev VV, Stepanov AV (2018) Prominence activation by increase in electric current. Journal of Atmospheric and Solar-Terrestrial Physics 179:149–153, DOI 10.1016/j.jastp.2018.06.004

Zaitsev VV, Stepanov AV, Urpo S, Pohjolainen S (1998) LRC-circuit analog of current-carrying magnetic loop: diagnostics of electric parameters. Astron. Astrophys. 337:887–896

Zaitsev VV, Kislyakov AG, Stepanov AV, Kliem B, Furst E (2004) Pulsating Microwave Emission from the Star AD Leo. Astronomy Letters 30:319–324, DOI 10.1134/1.1738154

Zaitsev VV, Stepanov AV, Kaufmann P (2014) On the Origin of Pulsations of Sub-THz Emission from Solar Flares. Solar Phys. 289(8):3017–3032, DOI 10.1007/s11207-014-0515-9

Zajtsev VV, Stepanov AV (1975) On the origin of pulsations of type IV solar radio emission.

Plasma cylinder oscillations (I). Issledovaniia Geomagnetizmu Aeronomii i Fizike Solntsa 37:3–10
Zaqarashvili TV, Melnik VN, Brazhenko AI, Panchenko M, Konovalenko AA, Franzuzenko AV, Dorovskyy VV, Rucker HO (2013) Radio seismology of the outer solar corona. Astron. Astrophys. 555:A55, DOI 10.1051/0004-6361/201321548, 1305.2287
Zavershinskii DI, Kolotkov DY, Nakariakov VM, Molevich NE, Ryashchikov DS (2019) Formation of quasi-periodic slow magnetoacoustic wave trains by the heating/cooling misbalance. Physics of Plasmas 26(8):082113, DOI 10.1063/1.5115224, 1907.08168
Zhang QM, Li D, Ning ZJ (2016) Chromospheric Condensation and Quasi-periodic Pulsations in a Circular-ribbon Flare. Astrophys. J. 832(1):65, DOI 10.3847/0004-637X/832/1/65, 1609.03165
Zhang QM, Dai J, Xu Z, Li D, Lu L, Tam KV, Xu AA (2020) Transverse coronal loop oscillations excited by homologous circular-ribbon flares. Astron. Astrophys. 638:A32, DOI 10.1051/0004-6361/202038233, 2005.02067
Zhao X, Xia C, Van Doorsselaere T, Keppens R, Gan W (2019) Forward Modeling of SDO/AIA and X-Ray Emission from a Simulated Flux Rope Ejection. Astrophys. J. 872(2):190, DOI 10.3847/1538-4357/ab0284, 1904.09965
Zharkova VV, Arzner K, Benz AO, Browning P, Dauphin C, Emslie AG, Fletcher L, Kontar EP, Mann G, Onofri M, Petrosian V, Turkmani R, Vilmer N, Vlahos L (2011) Recent Advances in Understanding Particle Acceleration Processes in Solar Flares. Space Sci. Rev. 159(1-4):357–420, DOI 10.1007/s11214-011-9803-y, 1110.2359
Zhilyaev BE, Romanyuk YO, Verlyuk IA, Svyatogorov OA, Khalack VR, Sergeev AV, Konstantinova-Antova RK, Antov AP, Bachev RS, Alekseev IY, Chalenko VE, Shakhovskoy DN, Contadakis ME, Avgoloupis SJ (2000) Detection of high-frequency optical oscillations on the flare star EV Lacertae. Astron. Astrophys. 364:641–645
Zhilyaev BE, Romanyuk YO, Svyatogorov OA, Verlyuk IA, Kaminsky B, Andreev M, Sergeev AV, Gershberg RE, Lovkaya MN, Avgoloupis SJ, Seiradakis JH, Contadakis ME, Antov AP, Konstantinova-Antova RK, Bogdanovski R (2007) Fast colorimetry of the flare star EV Lacertae from UBVRI observations in 2004. Astron. Astrophys. 465(1):235–240, DOI 10.1051/0004-6361:20065632
Zhilyaev BE, Tsap YT, Andreev MV, Stepanov AV, Kopylova YG, Gershberg RE, Lovkaya MN, Sergeev AV, Verlyuk IA, Stetsenko KO (2011) Pulsations of optical radiation during the flare of YZ CMi occurred on February 9, 2008. Kinematics and Physics of Celestial Bodies 27(3):154–159, DOI 10.3103/S088459131103007X
Zic A, Stewart A, Lenc E, Murphy T, Lynch C, Kaplan DL, Hotan A, Anderson C, Bunton JD, Chippendale A, Mader S, Phillips C (2019) ASKAP detection of periodic and elliptically polarized radio pulses from UV Ceti. Mon. Not. Roy. Astron. Soc. 488(1):559–571, DOI 10.1093/mnras/stz1684, 1906.06570
Zimovets I, Struminsky A (2012) Non-thermal "Burst-on-Tail" of Long-Duration Solar Event on 26 October 2003. Solar Phys. 281(2):749–763, DOI 10.1007/s11207-012-0112-8, 1205.3719
Zimovets IV, Nakariakov VM (2015) Excitation of kink oscillations of coronal loops: statistical study. Astron. Astrophys. 577:A4, DOI 10.1051/0004-6361/201424960
Zimovets IV, Struminsky AB (2009) Imaging Observations of Quasi-Periodic Pulsatory Nonthermal Emission in Two-Ribbon Solar Flares. Solar Phys. 258(1):69–88, DOI 10.1007/s11207-009-9394-x, 0809.0138
Zimovets IV, Struminsky AB (2010) Observations of Double-Periodic X-Ray Emission in Interacting Systems of Solar Flare Loops. Solar Phys. 263(1-2):163–174, DOI 10.1007/s11207-010-9518-3, 0910.0216
Zimovets IV, Kuznetsov SA, Struminsky AB (2013) Fine structure of the sources of quasi-periodic pulsations in "single-loop" solar flares. Astronomy Letters 39(4):267–278, DOI 10.1134/S1063773713040063
Zimovets IV, Wang R, Liu YD, Wang C, Kuznetsov SA, Sharykin IN, Struminsky AB, Nakariakov VM (2018) Magnetic structure of solar flare regions producing hard X-ray pulsations. Journal of Atmospheric and Solar-Terrestrial Physics 174:17–27, DOI 10.1016/j.jastp.2018.04.017, 1708.01869
Zimovets IV, Sharykin IN, Gan WQ (2020) Relationships between Photospheric Vertical Electric Currents and Hard X-Ray Sources in Solar Flares: Statistical Study. Astrophys. J. 891(2):138, DOI 10.3847/1538-4357/ab75be, 2002.06646
Zweibel EG, Yamada M (2009) Magnetic Reconnection in Astrophysical and Lab-

3948 oratory Plasmas. Annu. Rev. Astron. Astrophys. 47(1):291–332, DOI 10.1146/
3949 annurev-astro-082708-101726